

Shock and Turbulence in Galaxy Clusters and the Large-Scale Structure



Takuya Akahori^{1,2}

¹Korea Astronomy and Space Science Institute (KASI)

²Research Fellow for Young Scientist,
Korea Research Council of Fundamental Science and
Technology (KRCF)



1. Introduction

2. Shock

2.1 As a heating mechanism of ICM/WHIM

2.2 Non-equilibrium plasma (TA & Yoshikawa 2010; 2012)

2.3 Sunyaev-Zel'dovich effect (Prokhorov, TA, et al. 2011abc)

3. Turbulence

3.1 As a driving mechanism of IGMF

3.2 Faraday rotation measure (TA & Ryu 2010; 2011)

3.3 Galactic foreground (TA, Kim, Ryu, Gaensler in prep.)

4. Future Observations

1. Introduction of Galaxy Clusters and the Large-Scale Structure

1. Cosmological Structure Formation

4/53

ΛCDM cosmology

Primordial perturbation

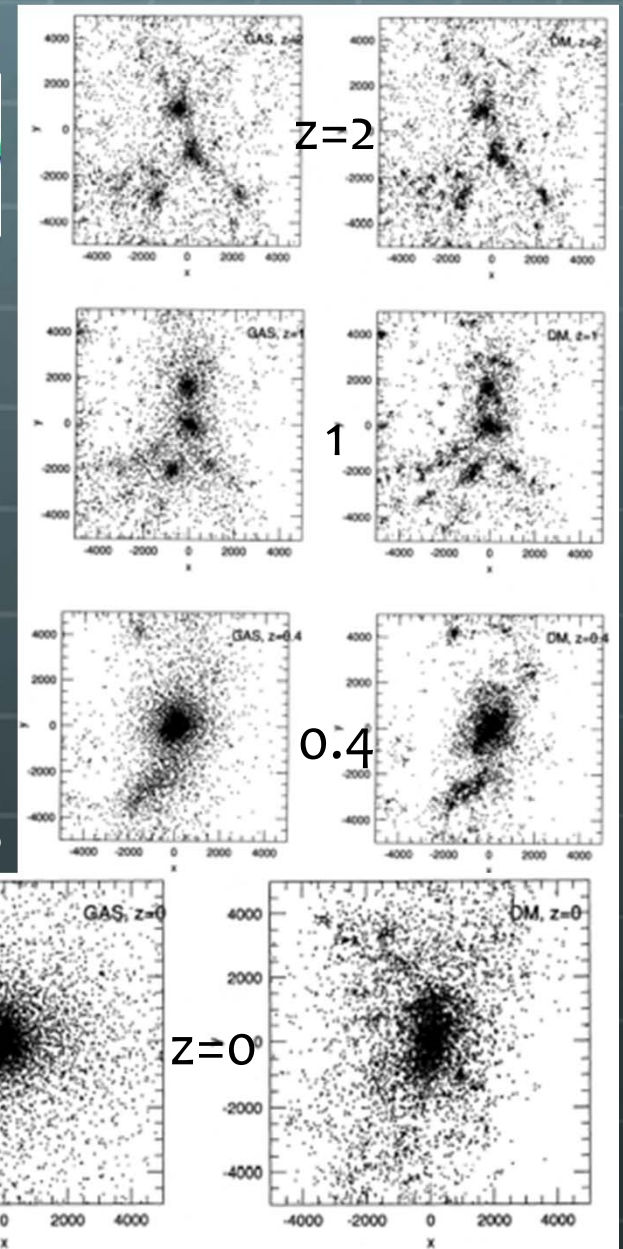
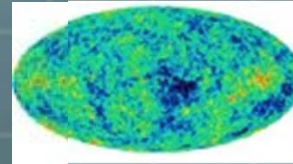
Jeans instability

Sheet/filament structures

Mergers of smaller objects

Intersections → Galaxy clusters

3K CMB (WMAP)



Navarro+ 95

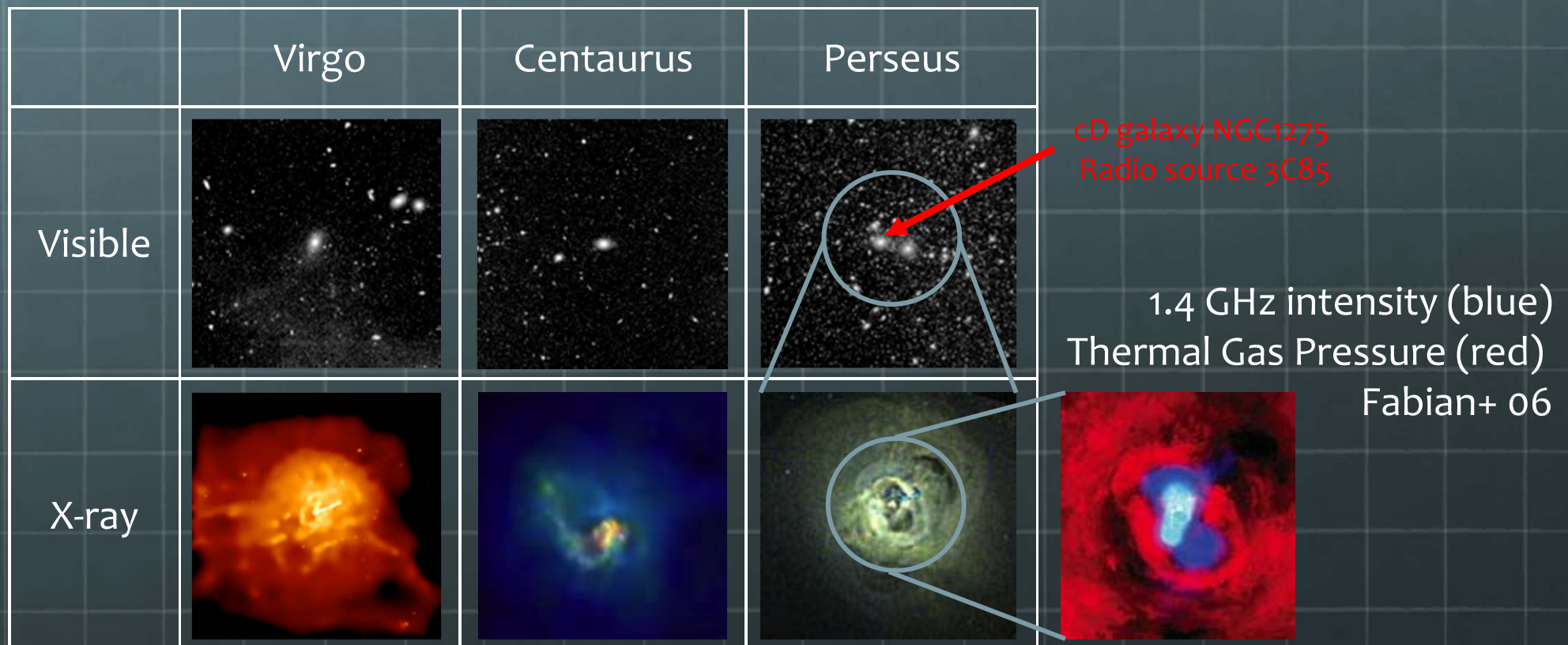
73%

1. Galaxy Clusters

5/53

Galaxy cluster consists of

- Galaxies (1) – Radio, IR, visible, UV, (X-ray, γ -ray)
- Intracluster medium (ICM) (5) – X-ray
- Dark matter (30) – indirect evidences (σ_{gal} , T_{ICM})

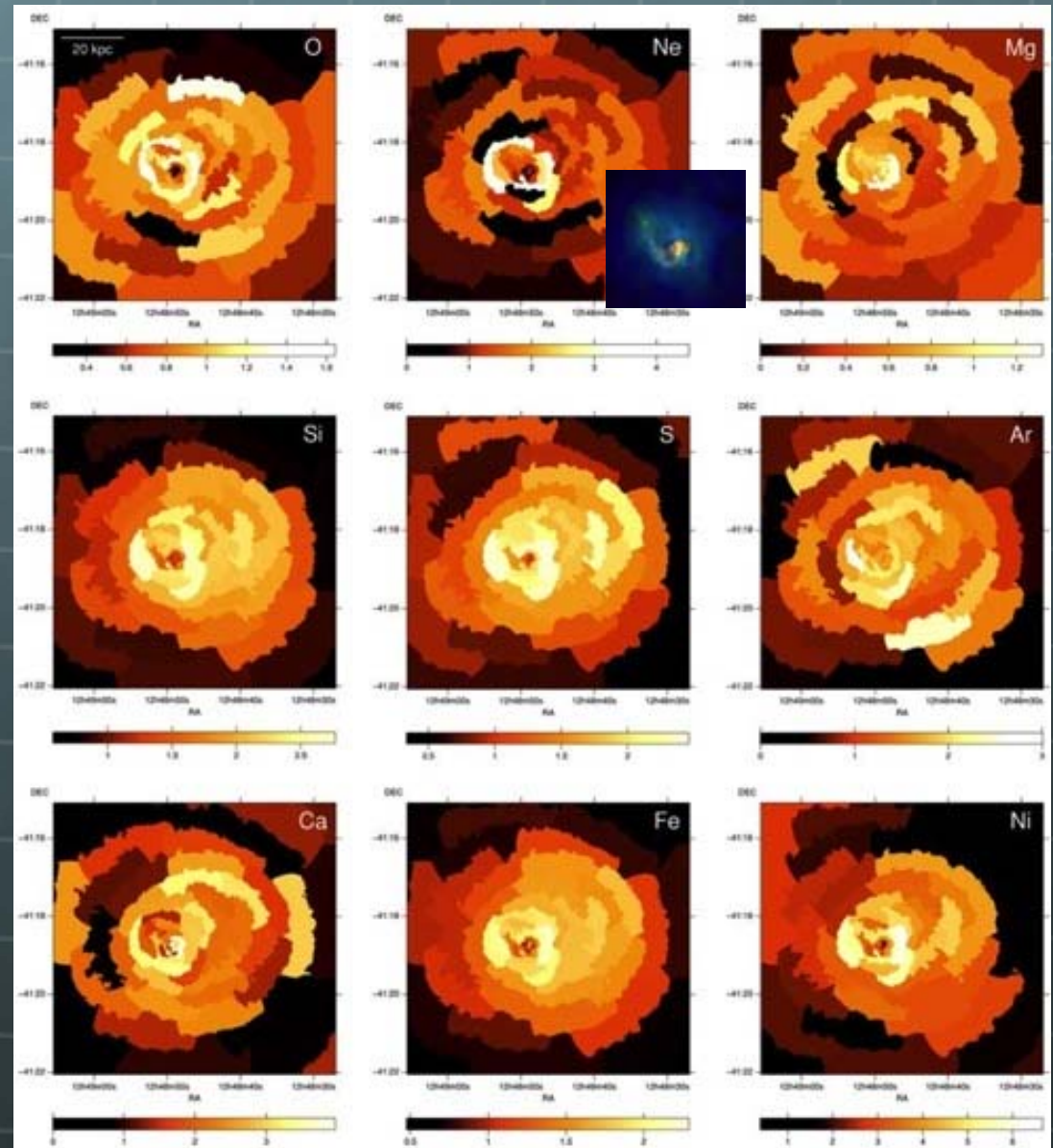
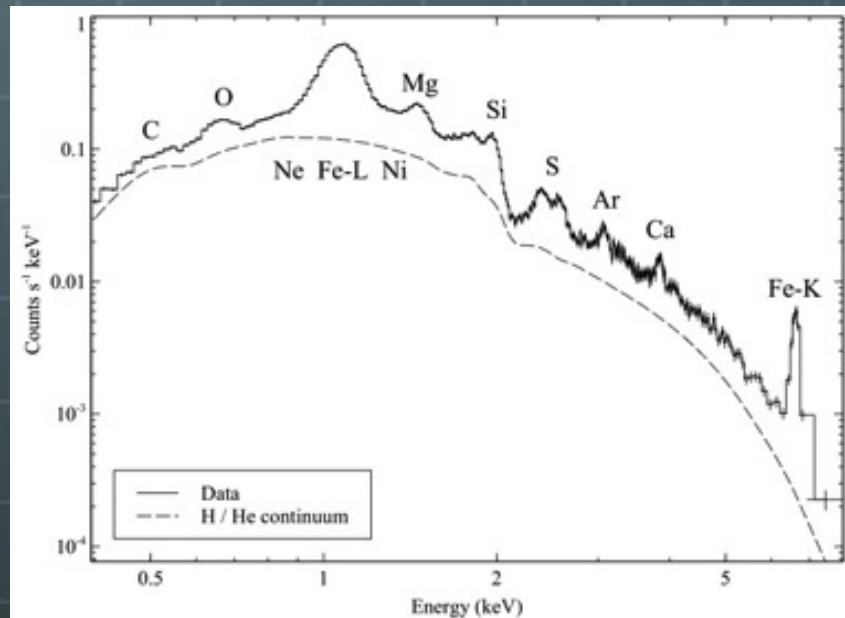


1. Intracluster Medium (ICM)

6/53

X-ray emissions

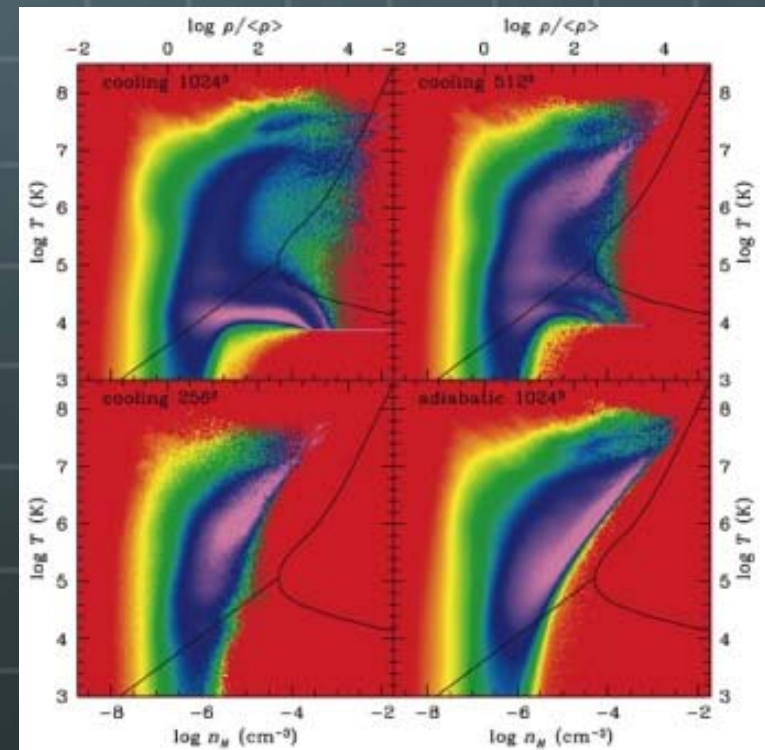
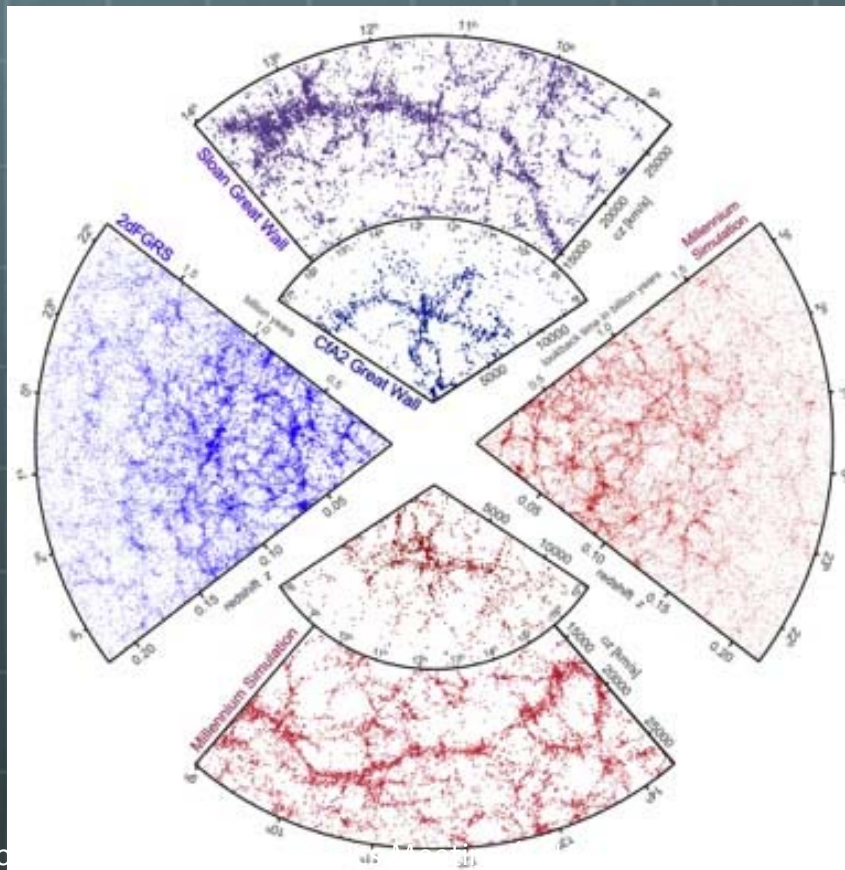
- Bremsstrahlung
- Lines (O, Si, Fe, ...)
- $T \sim 10^7 - 10^8$ K
- $Z \sim 0.1 - 1.0 Z_{\text{sun}}$



1. Large-Scale Structure

7/53

- 🌐 The large-scale structure consists of
 - 🌐 **Galaxies** – Radio, IR, visible, UV, (X-ray, γ -ray)
 - 🌐 **Warm-Hot Intergalactic medium (WHIM)** – UV, X-ray
 - 🌐 **Dark matter** – (theoretically predicted)



Virgo consortium

<http://www.mpa-garching.mpg.de/millennium/>

Kang+ 05

2011.11.25

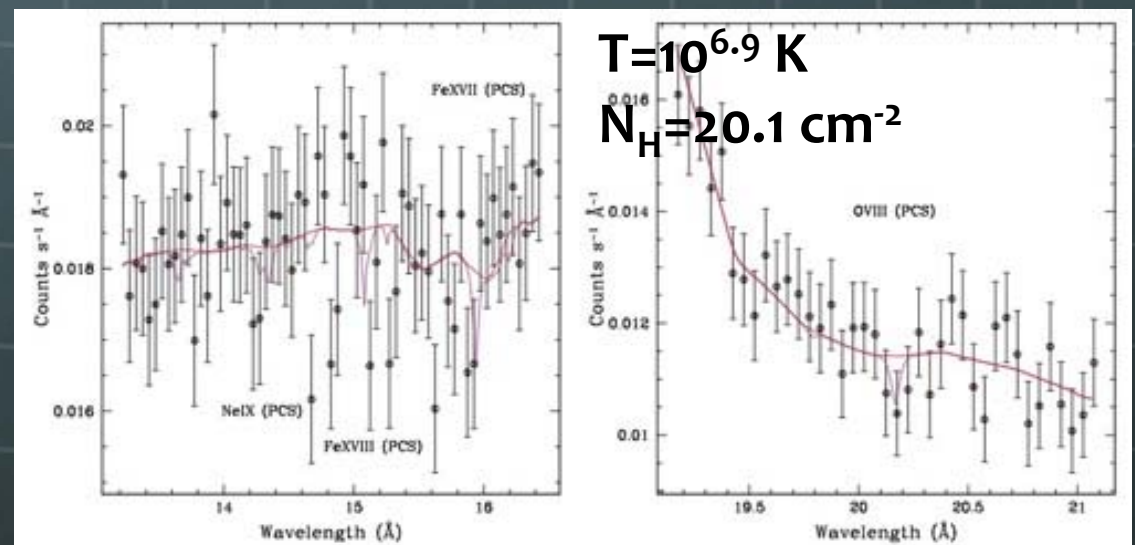
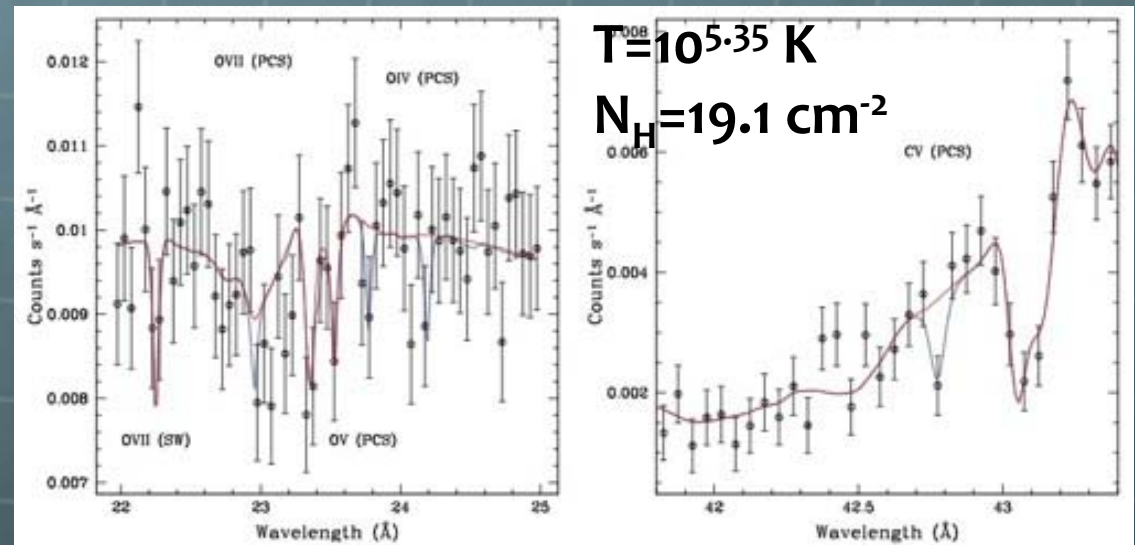
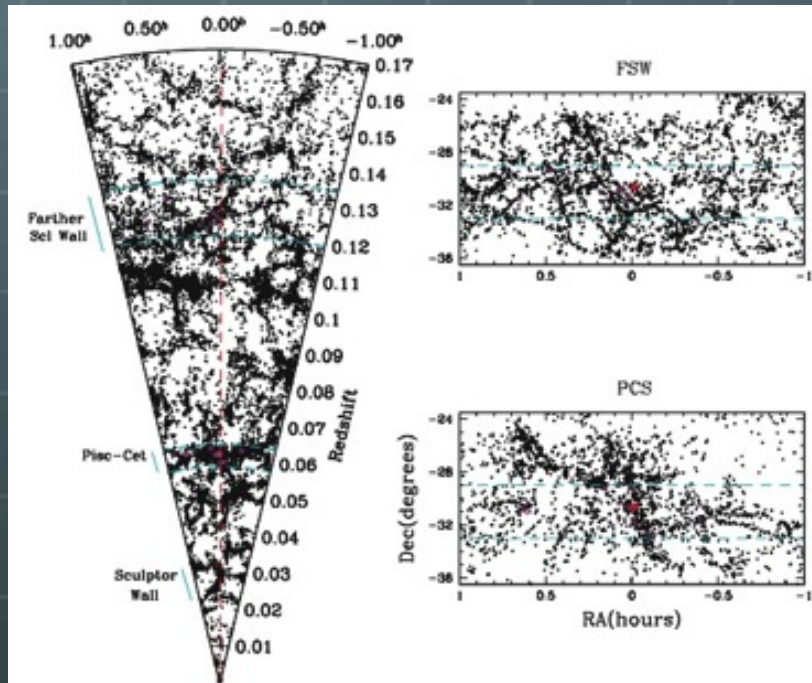
1. Warm-Hot Intergalactic Medium (WHIM) 8/53

X-ray emissions

detection?

Absorption Lines

Some “detections”



500 ksec Chandra obs. of Blazar
H2356-309 (Zappacosta+ 10)

2. Shock

2.1 As a Heating Mechanism

2.2 Non-Equilibrium Plasma

2.3 Sunyaev-Zel'dovich effect

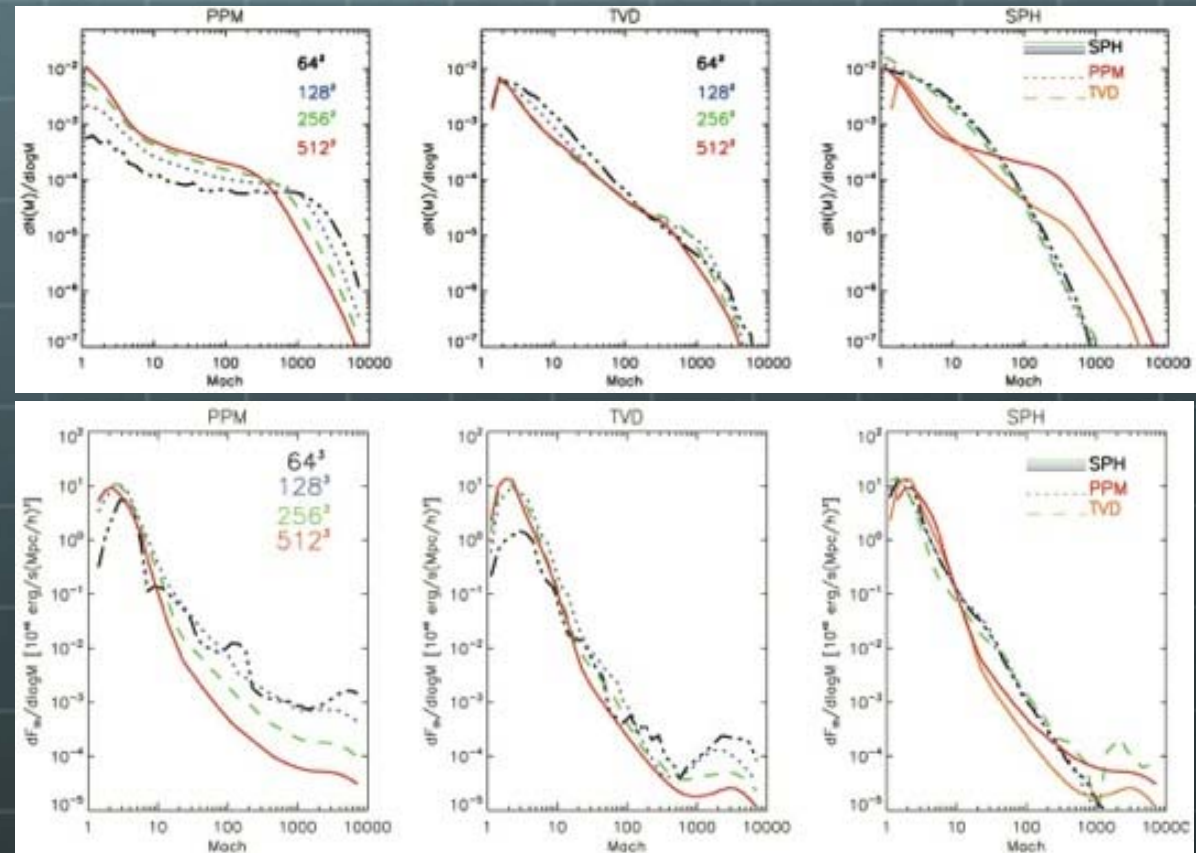
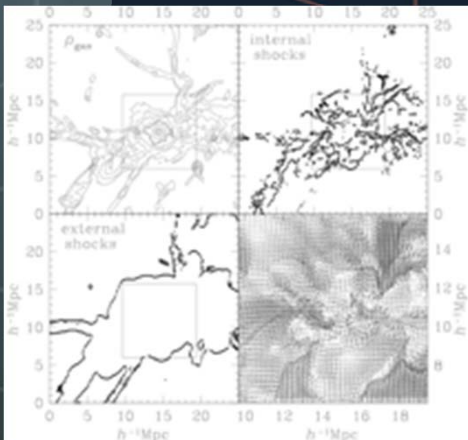
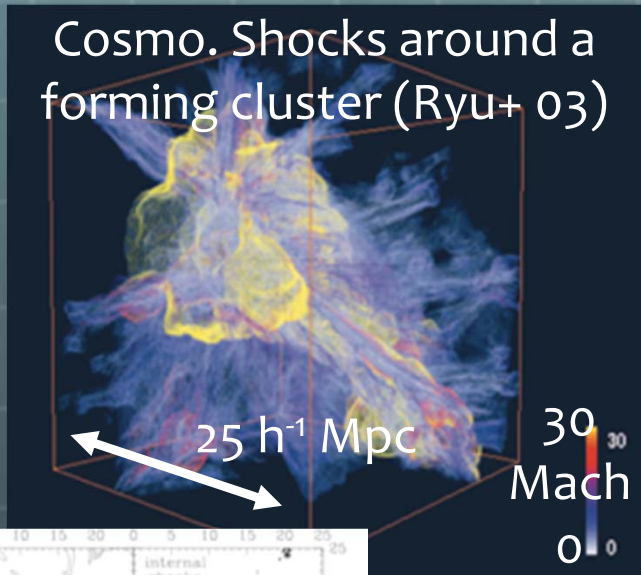
2.1 Shocks as Heating Mechanism

10/53

Shocks are ubiquitous

Usually, $V_{\text{infall}} > V_{\text{sound}}$

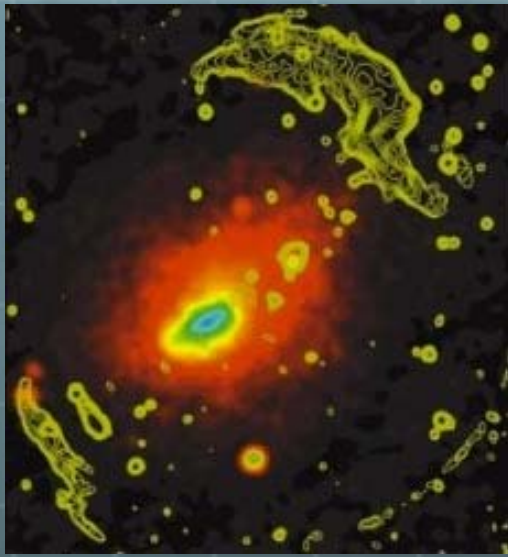
	Clusters	Filaments
Temperature	$10^7 - 10^8$ K	$10^5 - 10^7$ K
Mach number	a few	10 - 100



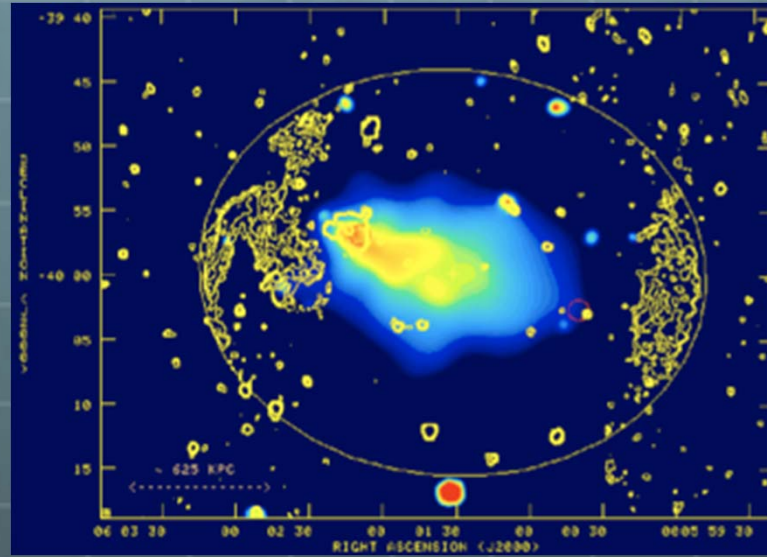
Volume-weighted number distribution of shocks and thermalized energy flux through shocks (Vazza+ 11)

2.1 Clues for Shocks (Radio)

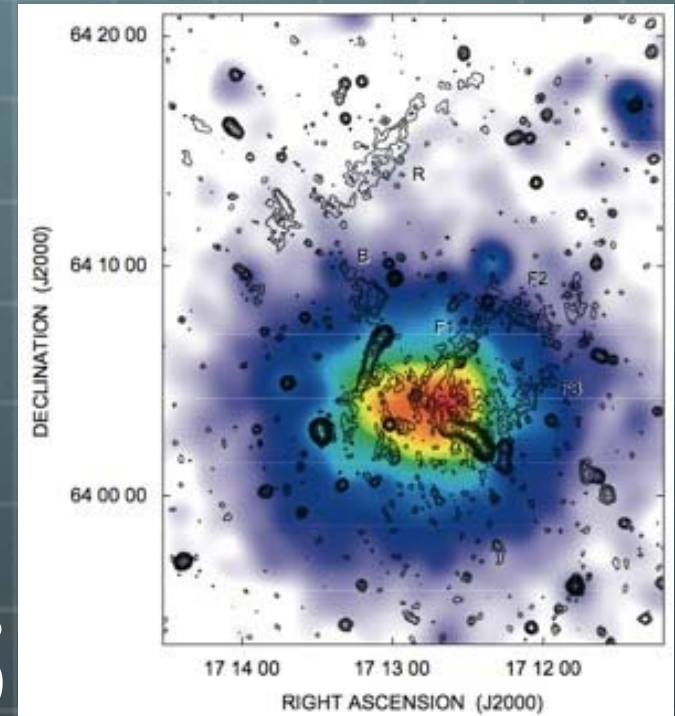
11/53



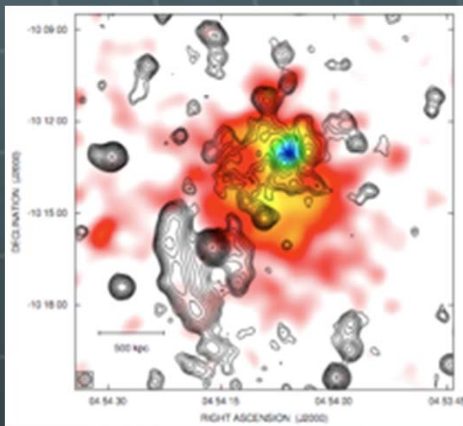
Abell 3667
(Roettiger+ 99)



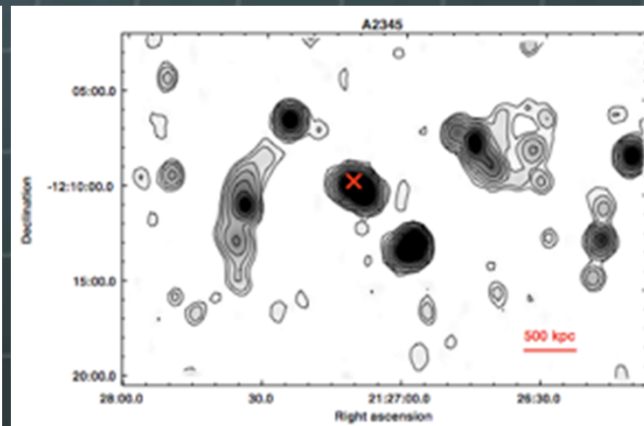
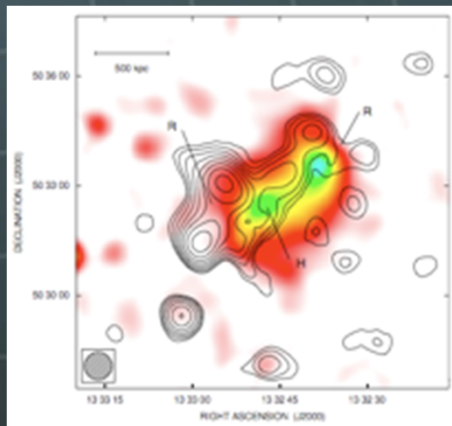
Abell 3376
(Bagchi+ 06)



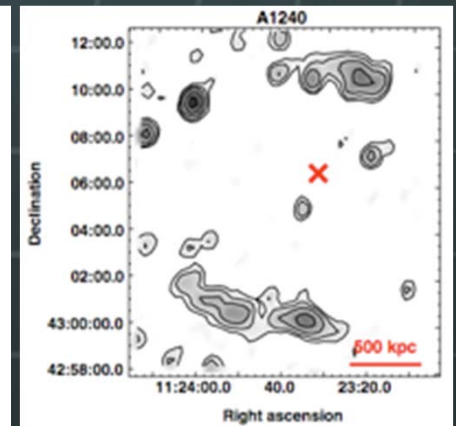
Abell 2255
(Govoni+ 05)



A521, A1758 (Giovanini+ 09)

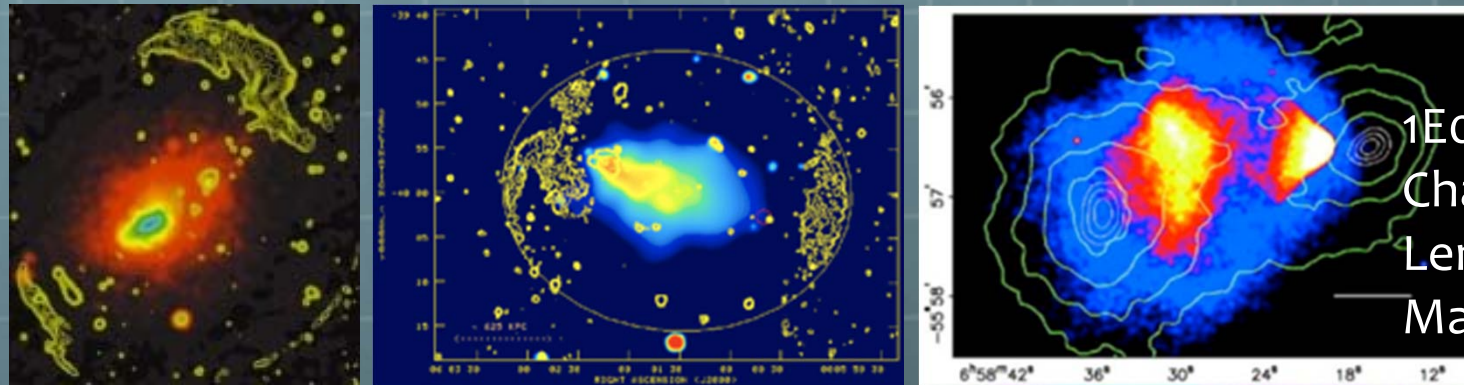


A2345, A1240 (Bonafede+ 09)
X=X-ray peak

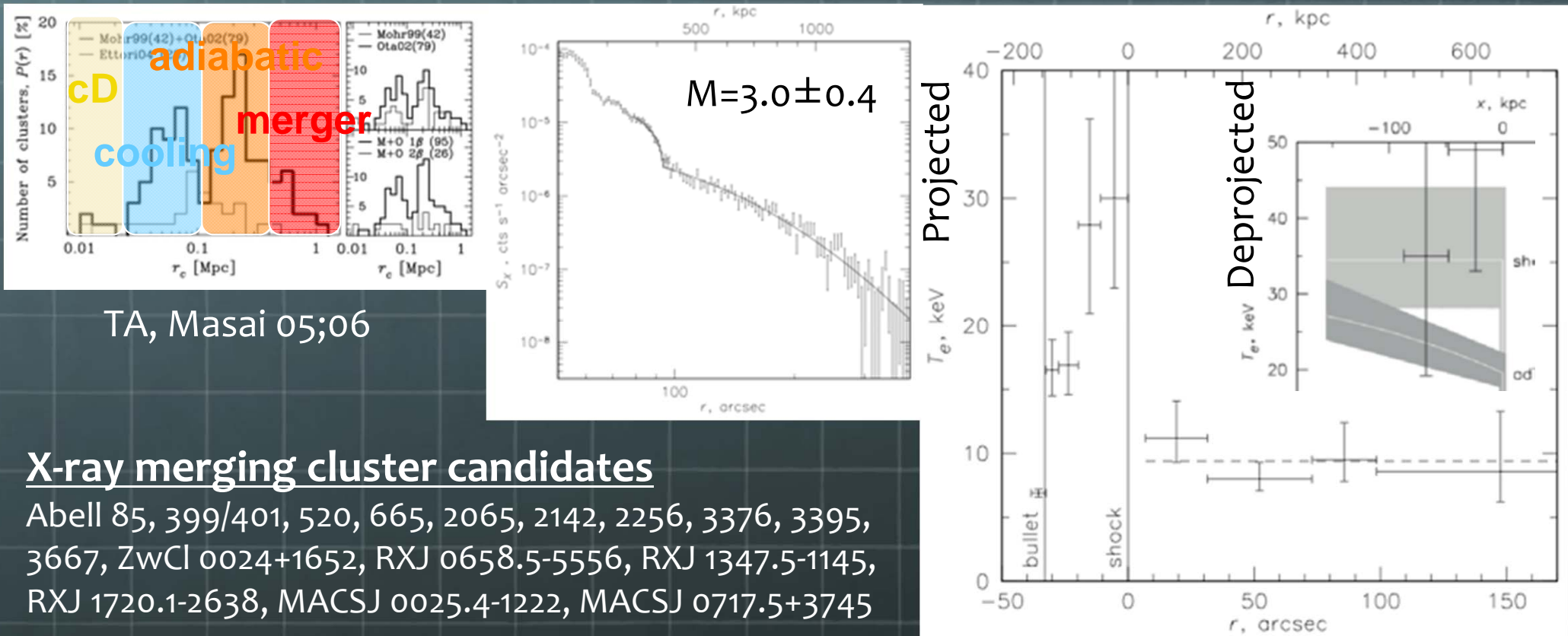


2.1 Clues for Shocks (X-ray)

12/53



1E0657-56
Chandra 0.8-4.0 keV (color)
Lensing mass (contour)
Markevitch 06; Clowe+ 06



TA, Masai 05;06

X-ray merging cluster candidates

Abell 85, 399/401, 520, 665, 2065, 2142, 2256, 3376, 3395, 3667, ZwCl 0024+1652, RXJ 0658.5-5556, RXJ 1347.5-1145, RXJ 1720.1-2638, MACSJ 0025.4-1222, MACSJ 0717.5+3745

2.2 Non-Equilibrium Plasma

How the ICM/WHIM is heated by the shock?

- Particle acceleration (non thermal)

- Non-thermal emissions

- Thermalization ($T_i \geq T_e > T_{ionize}$)

- Thermal but non-equilibrium emissions

- Equilibration ($T_i = T_e = T_{ionize}$)

- Thermal emissions

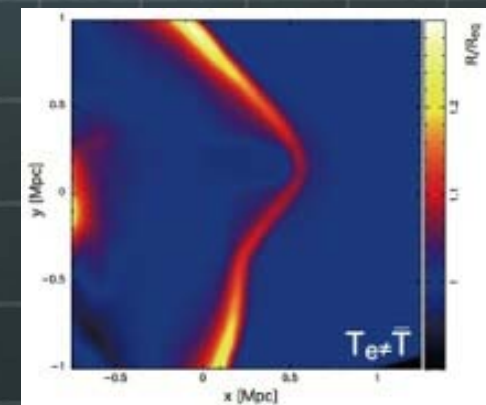
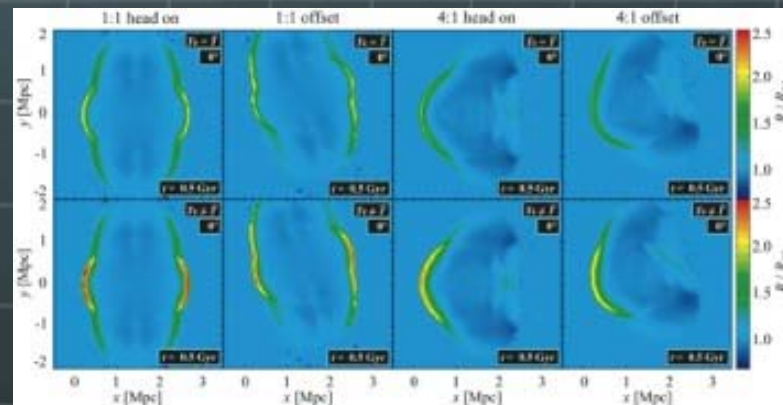
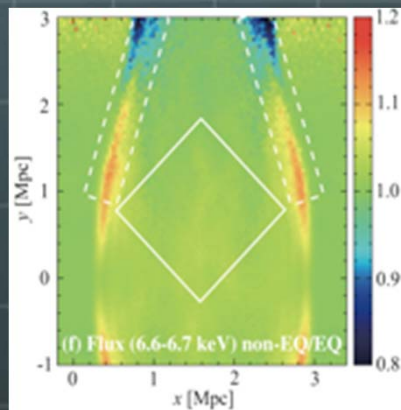
Importance

2T: for discussing T & M

NEI: for discussing T & Z

$$t_{el} \sim 2 \text{ Gyr } (n_e^{-4} \text{cm}^{-3})^{-1} (T_e^8 \text{K})^{3/2}$$

$$t_{CIE} \sim 3 \text{ Gyr } (n_e^{-4} \text{cm}^{-3})^{-1}$$



TA, Yoshikawa 08; 10; 12

2.2 Electron-Ion Two Temperatures

14/53

🌐 Thermal relaxation at the post-shock

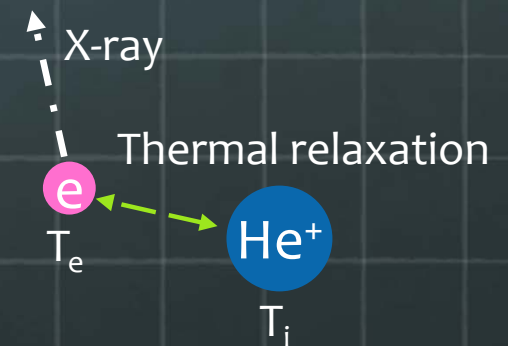
- I. Typically, $E_e \sim m_e V_s^2$, $E_p \sim m_i V_s^2$ at the post shock (V_s the shock velocity)
- II. Since $m_i \sim 1830 m_e$, ions mainly get the energy ($T_i \gg T_e$)
- III. Electrons get energy from ions through Coulomb collisions, where $t_{ei} \sim 43 t_{ii} \sim 1830 t_{ee}$

$$\frac{dT_e}{dt} = \frac{T_i - T_e}{t_{eq,ei}}$$



$$t_{eq,ei} = 7.97 \times 10^9 \text{ yr} \frac{(T_e/10^8 \text{ K})^{3/2}}{(n_i/10^{-3} \text{ cm}^{-3}) \ln \Lambda}$$

~40

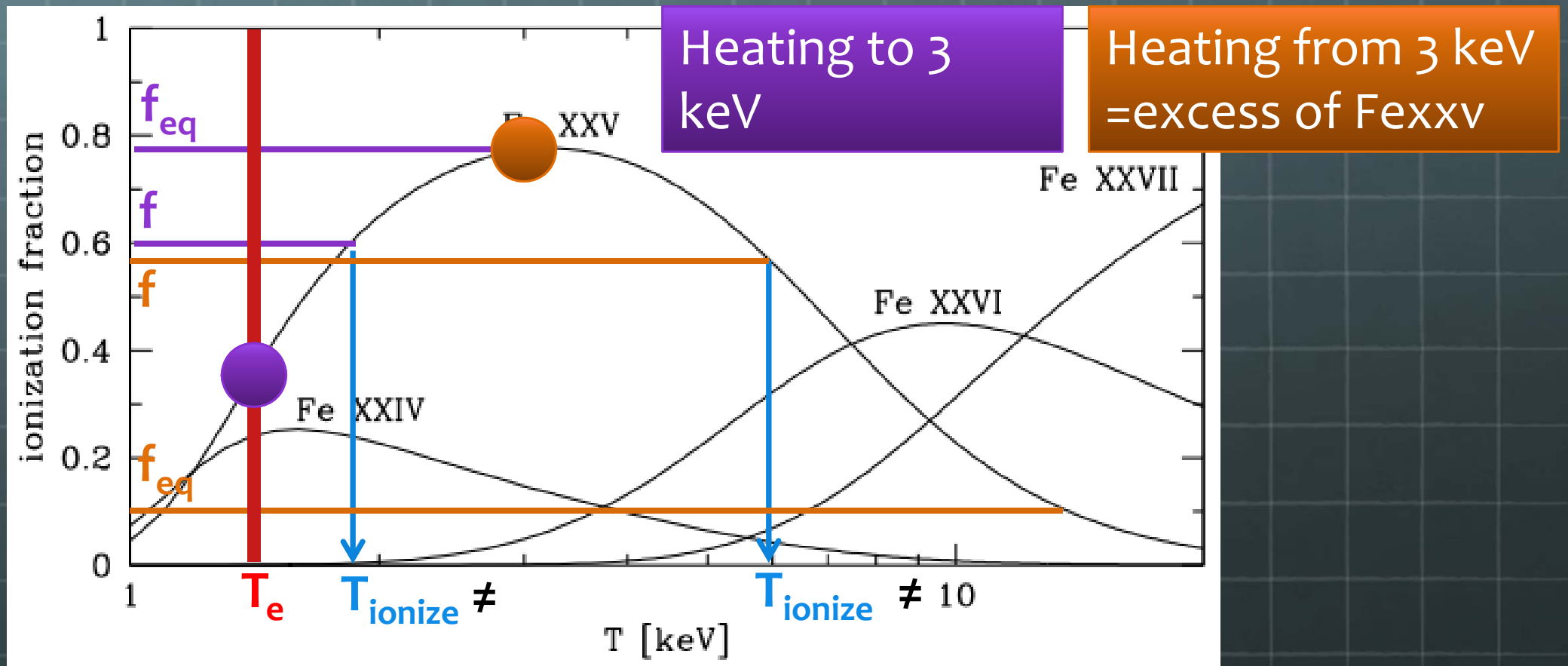


2.2 Non-Equilibrium Ionization (NEI)

15/53

- Actual ionization state with the temperature T differs from the state of the CIE with T

Ionization fraction of Fe in the CIE



2.2 Abell 399/ Abell 401 Linked Region 16/53

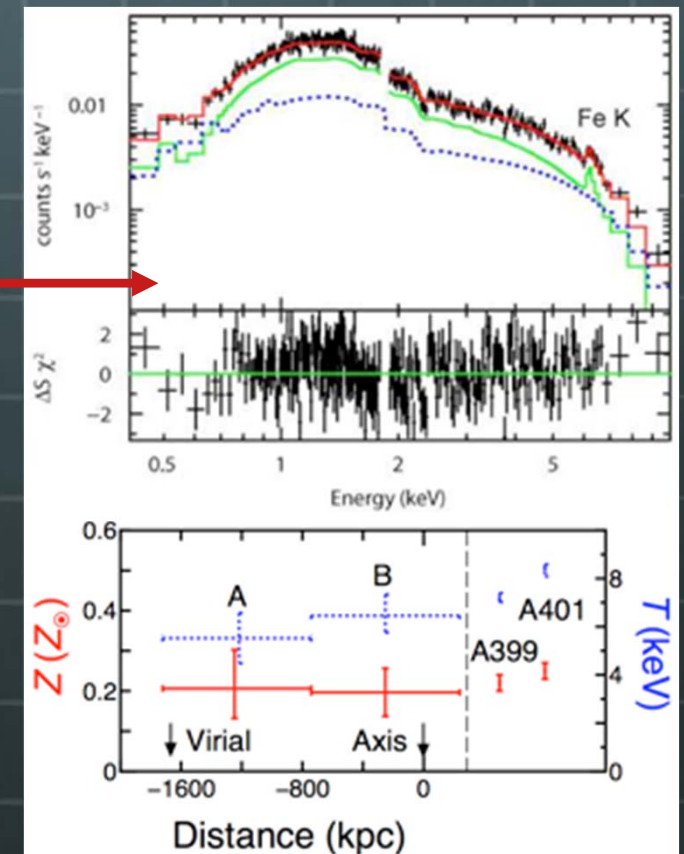
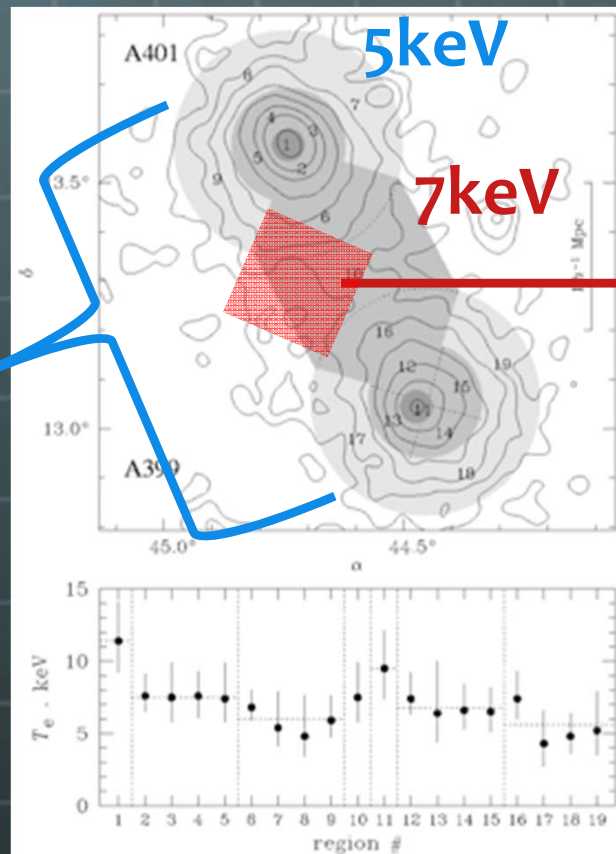
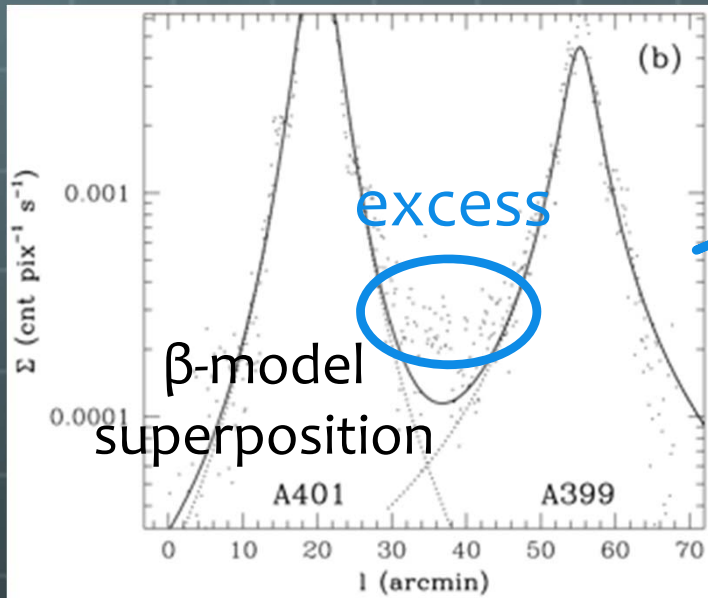
🌍 Compression makes the outskirts visible!

🌍 Metallicity $\sim 0.2 Z_{\text{sun}}$... **Is it real?**

ASCA: Temperature
(Markevitch+ 98)

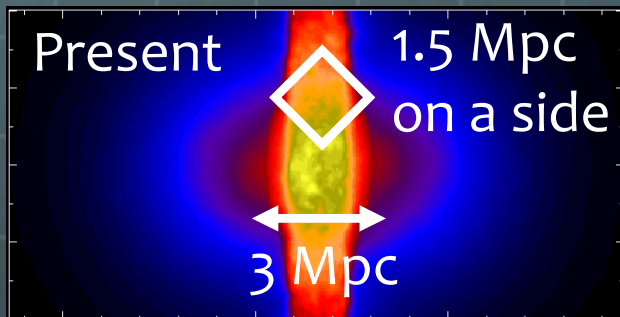
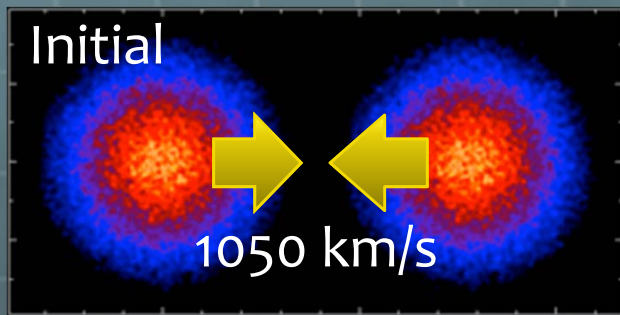
Suzaku: Metallicity
(Fujita+ 08)

XMM-Newton: Brightness
(Sakelliou, Ponman 04)

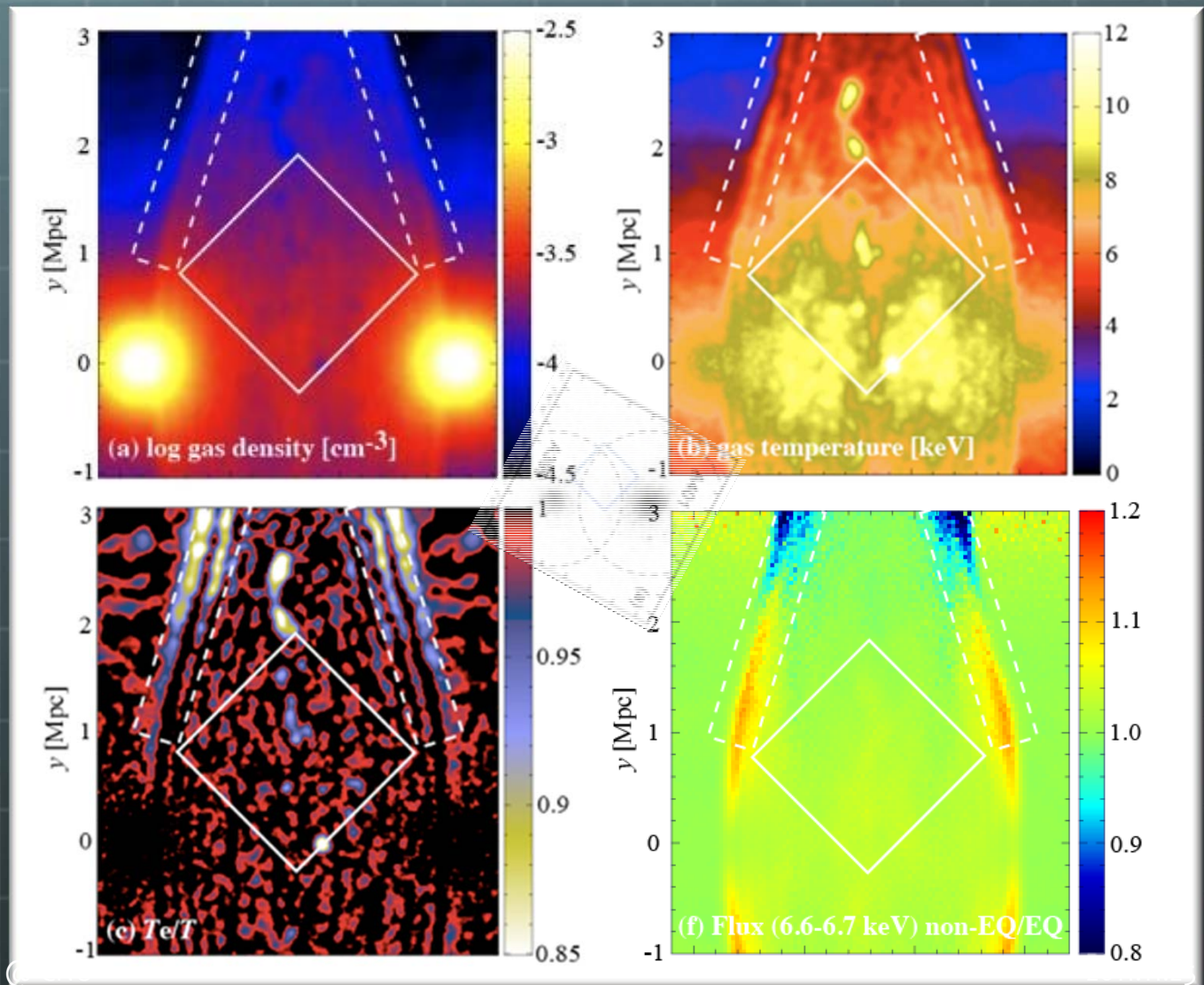


2.2 Abell 399/ Abell 401 Linked Region 17/53

- 🌐 Suzaku region already have relaxed \rightarrow CIE/1T OK.
- 🌐 Shock layers are newly predicted \rightarrow NEI/2T



TA, Yoshikawa o8

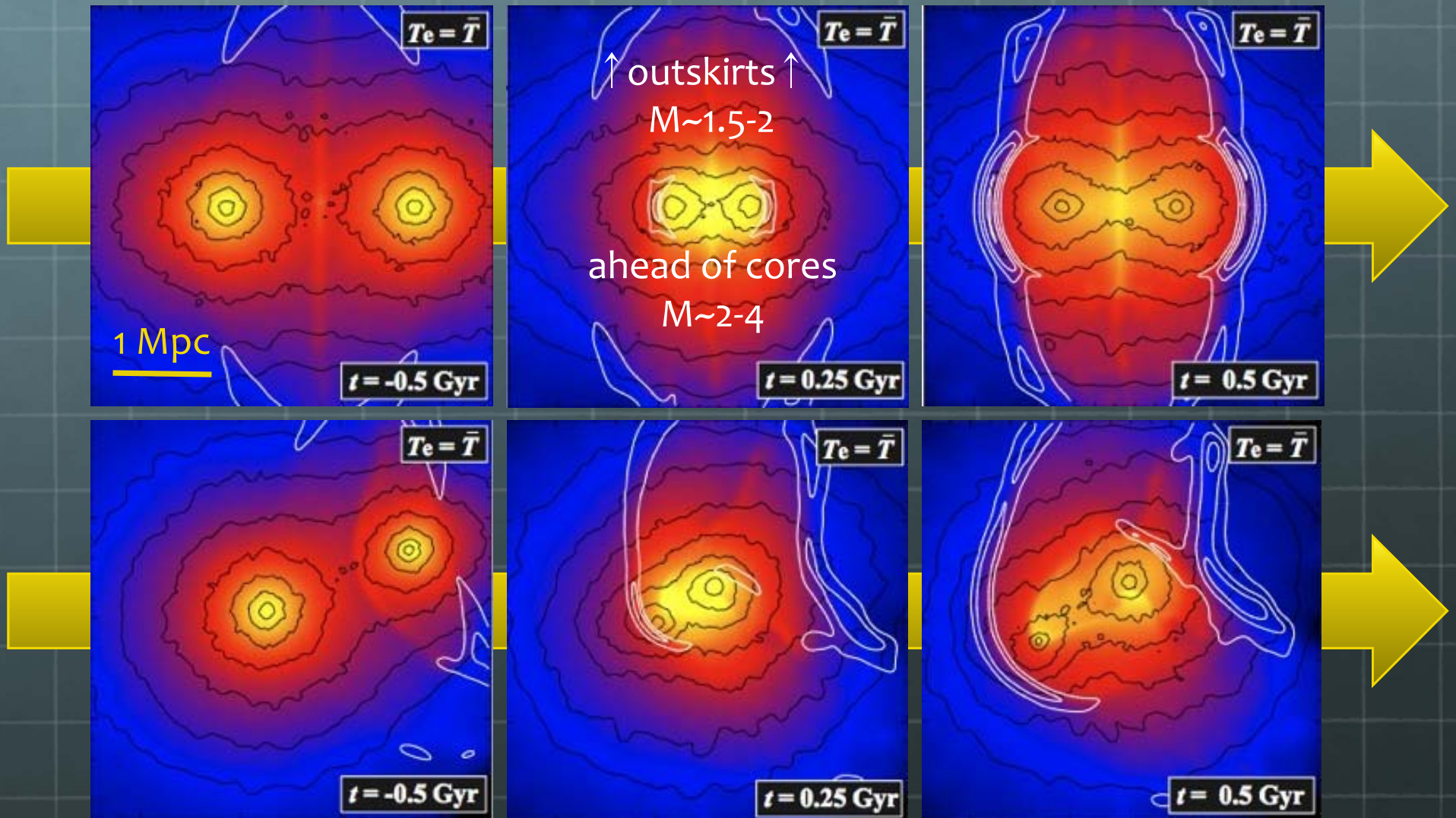


2.2 Merging Cluster Simulations

18/53

Shocks in merging clusters

White contour :
Mach number (1.4, 2.0, 2.6,...)

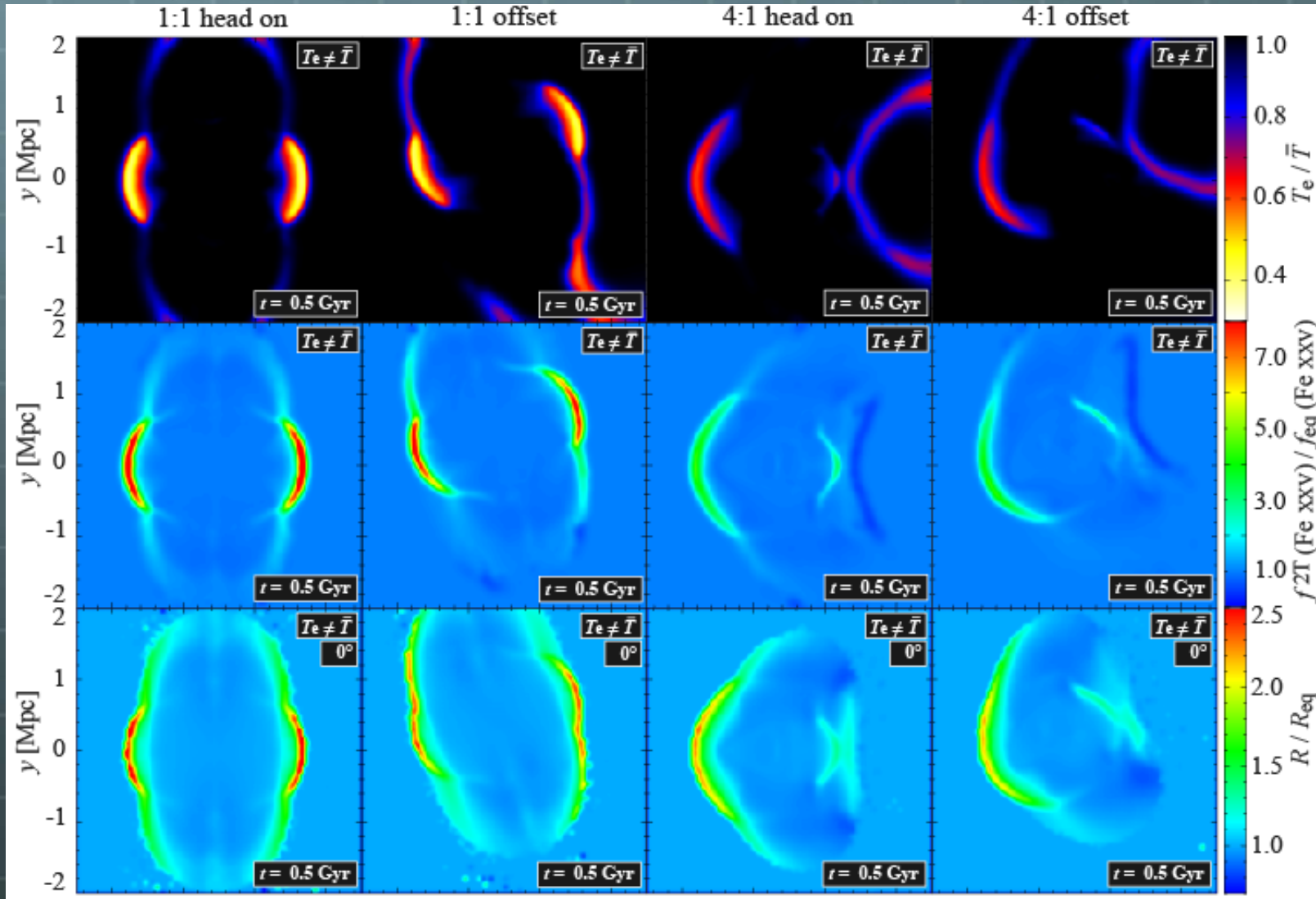


2.2 Merging Galaxy Clusters

19/53

🌐 Behind the shock layers → NEI/2T

$$\frac{R}{R_{eq}} = \frac{[I_{6.6-6.7}/I_{6.9-7.0}]}{[I_{6.6-6.7}/I_{6.9-7.0}]_{eq}}$$



T_e/T

0.8-0.9 (outskirts)
0.5-0.8 (core)

f/f_{eq} Fe xxv

2-4 (outskirts)
3-8 (core)

R/R_{eq}

1.2-1.4 (outskirts)
1.6-2.2 (core)

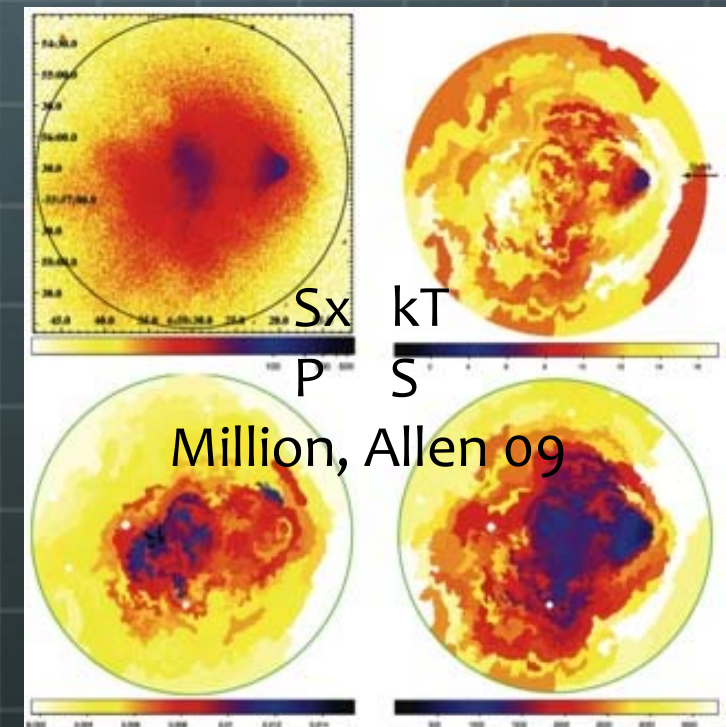
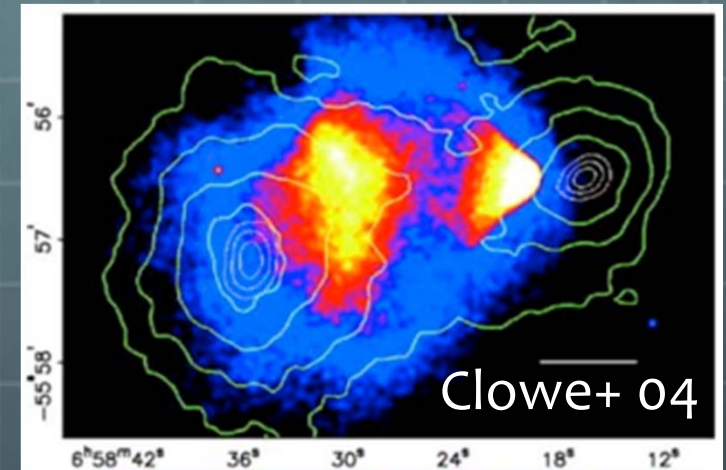
2.2 The Bullet Cluster 1E0657-56

20/53

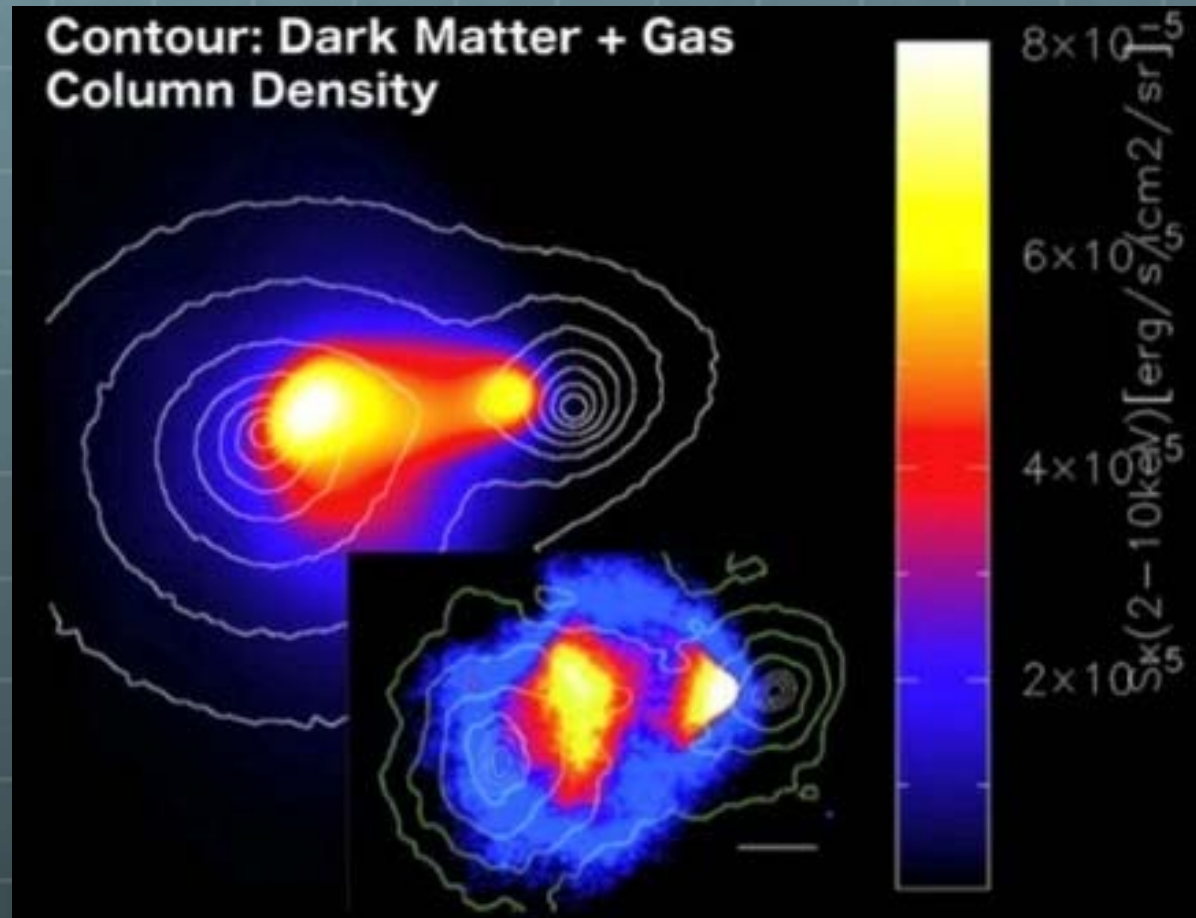
Textbook of cluster merger

- Two distinct peaks → evidence of merger
- Offset of weak lensing → evidence of dark matter (pressure-less matter)
- Very-high average temperature → evidence of shock heating to the ICM
- Brightness jump → evidence of the shock with $M \sim 3.0 \pm 0.4$

1E0657-56 is suited to “test” standard cosmology and plasma relaxation processes



2.2 Simulating Bullet Cluster 1E0657-56 21/53

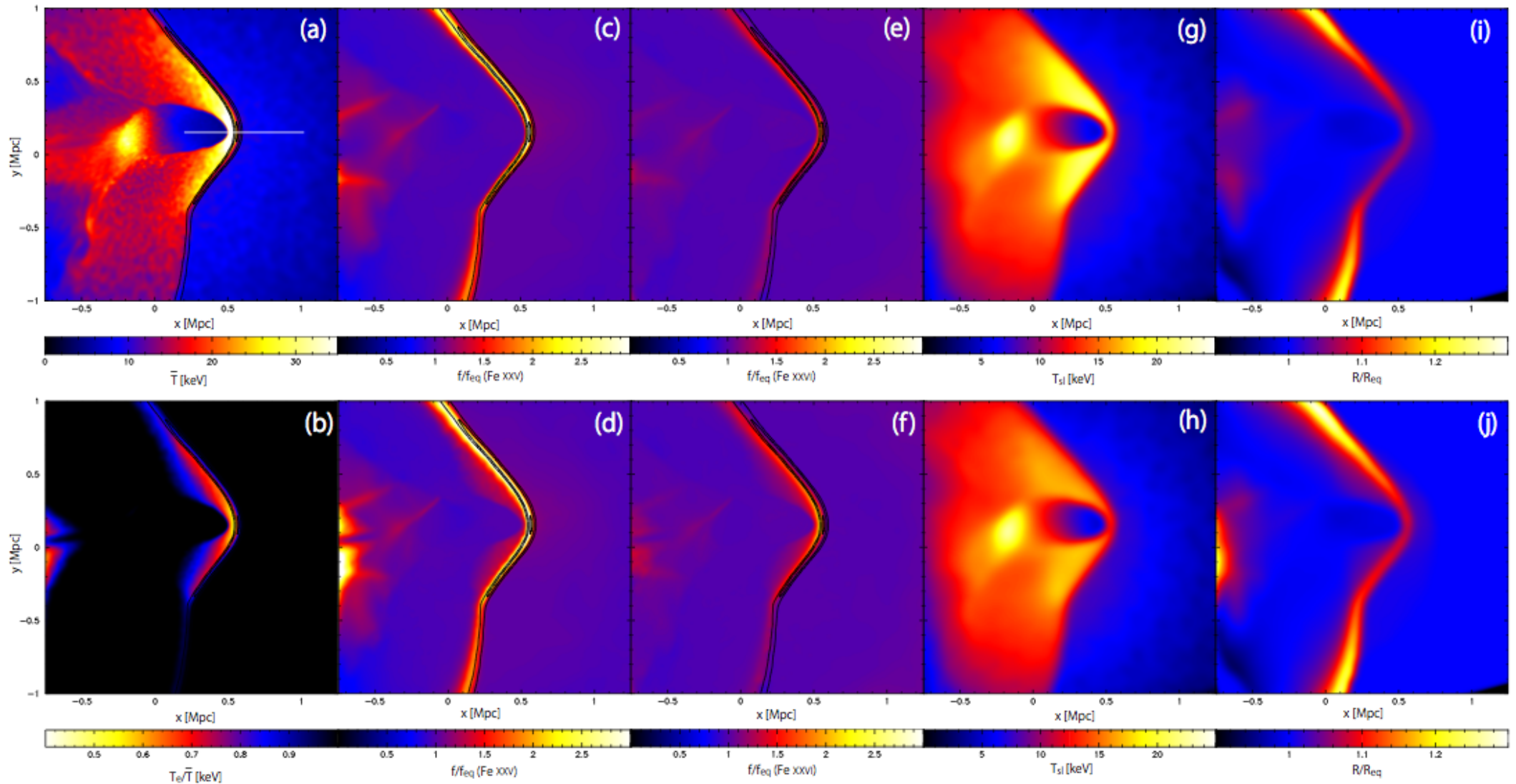


Simulation Movie

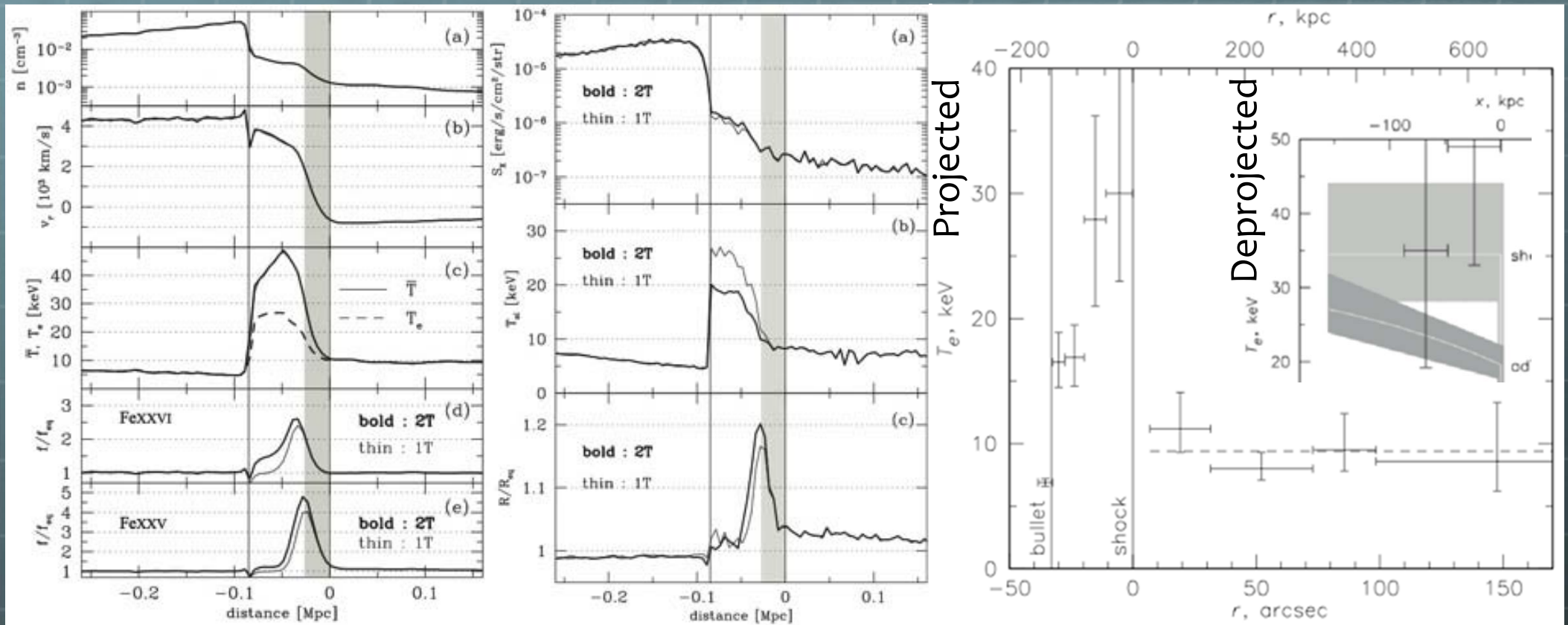
Please visit <http://canopus.cnu.ac.kr/akataku/Activity.html>

2.2 Simulating Bullet Cluster 1E0657-56 22/53

NEI/2T appear behind the shock front



2.2 Simulating Bullet Cluster 1E0657-56 23/53

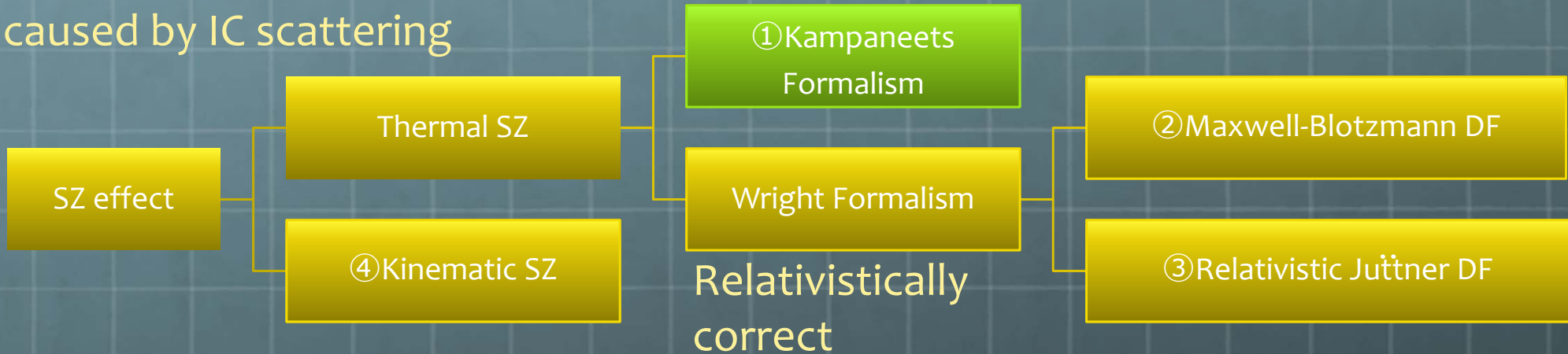


- If $T_e > 30$ keV or narrow line with $T_i \sim T_e \rightarrow 1T$ is plausible
- Fast relaxation processes @ $M=3$
- If $T_e < 25$ keV or broad line with $T_i \gg T_e \rightarrow 2T$ is plausible
- No fast relaxation & Coulomb relaxation?

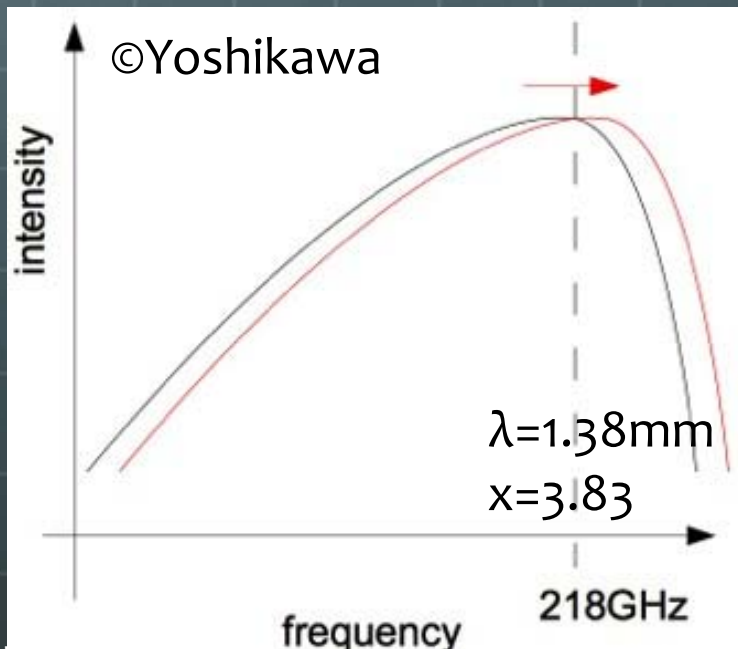
2.3 Sunyaev-Zel'dovich Effects

CMB photon distortion caused by IC scattering

Non-relativistic diffusion approximation



① Thermal SZ (Kampaneets Formalism)



$$\Delta I(x) = I_0 \int g(x) \frac{k_B T_e(l)}{m_e c^2} n_e(l) \sigma_T dl$$

$$x = \frac{h\nu}{k_B T_{\text{CMB}}}$$

$$I_0 = \frac{2(k_B T_{\text{CMB}})^3}{(hc)^2}$$

$$\Delta I(x) = I_0 g(x) y$$

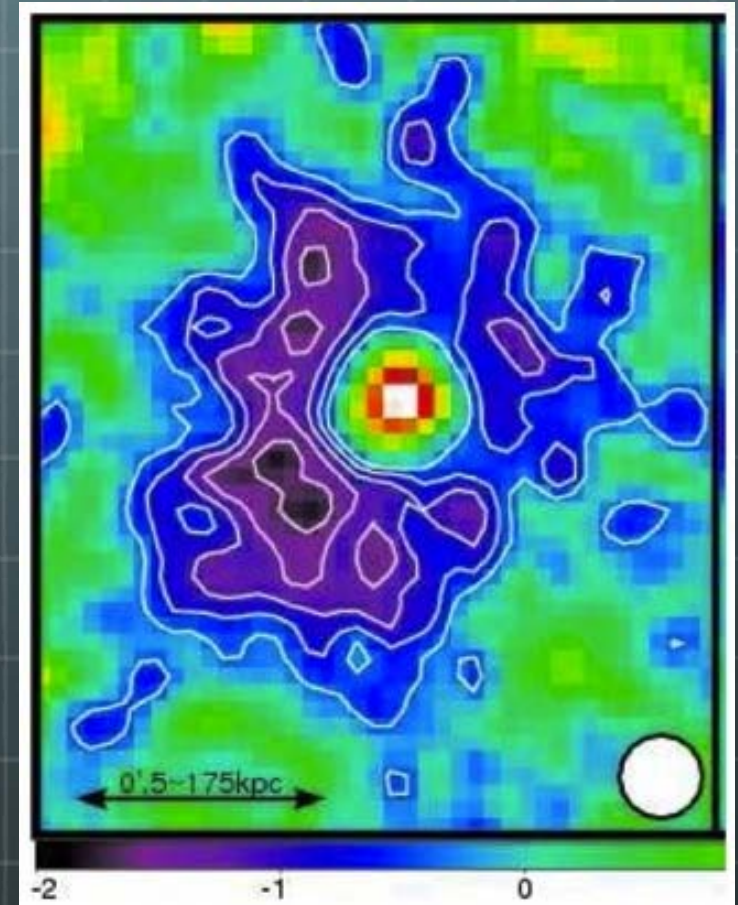
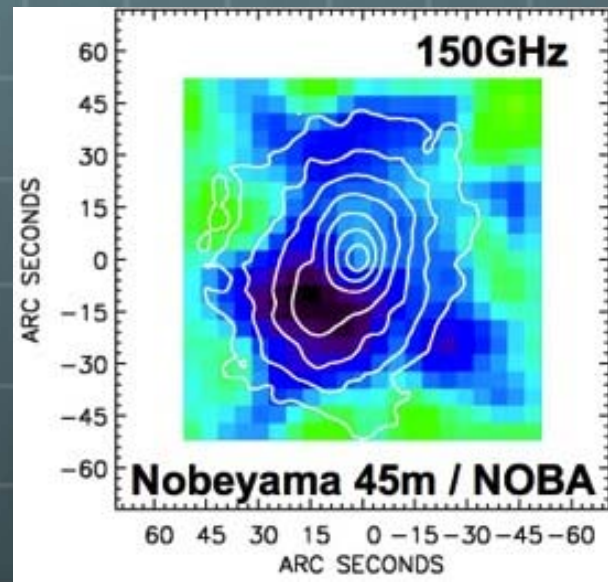
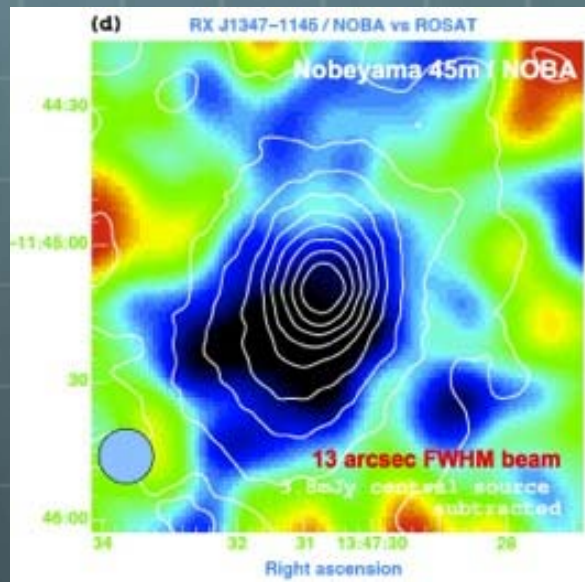
$$y = \int \frac{k_B T_e(l)}{m_e c^2} n_e(l) \sigma_T dl$$

$$g(x) = \frac{x^4 \exp(x)}{[\exp(x) - 1]^2} \left[x \frac{\exp(x) + 1}{\exp(x) - 1} - 4 \right]$$

2.3 Sunyaev-Zel'dovich Effects

RXJ1347-1145

$$\frac{\Delta I}{I_0} \sim 10^{-4} \left(\frac{k_B T_e}{10 \text{ keV}} \right) \left(\frac{n_e}{10^{-3} \text{ cm}^{-3}} \right) \left(\frac{L}{1 \text{ Mpc}} \right)$$



NRO 45m/150GHz
Komatsu+ 01

NRO 45m/150GHz
Kitayama+ 04

M~2 (Kitayama+ 04)

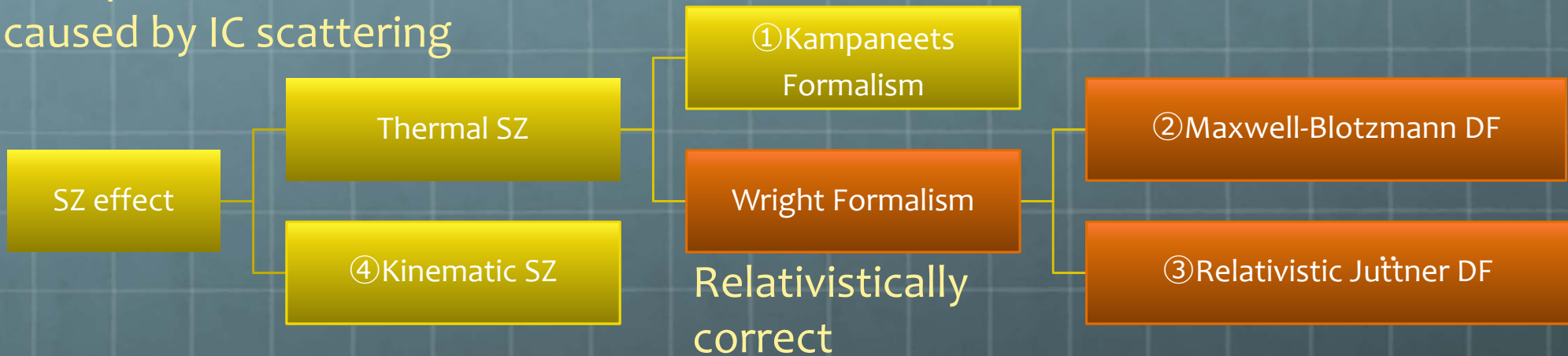
GreenBank 100m/90GHz
Mason+ 10

c.f. $kT = 25.3^{+6.1}_{-4.5}$ keV (Suzaku, Ota+ 08)

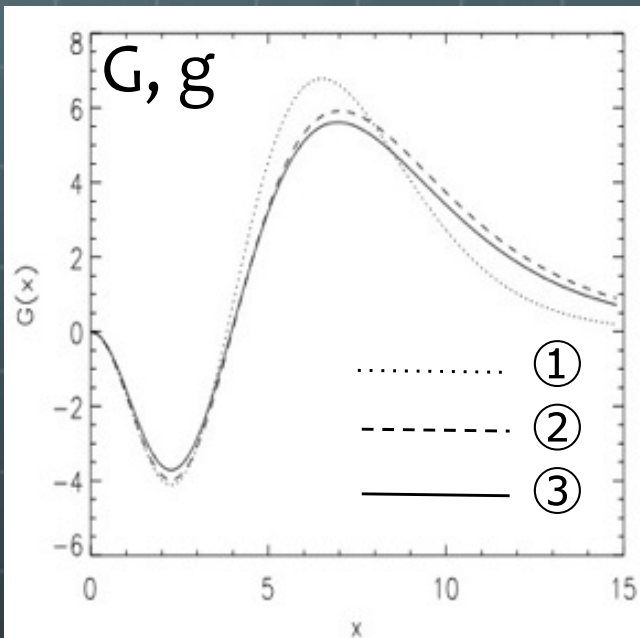
2.3 Sunyaev-Zel'dovich Effects

CMB photon distortion caused by IC scattering

Non-relativistic diffusion approximation



②③ Thermal SZ (Wright Formalism)



$$\Delta I^{\text{rmb}}(x) = I_0 \int G(x, T_e) \frac{k_B T_e(l)}{m_e c^2} n_e(l) \sigma_T dl$$

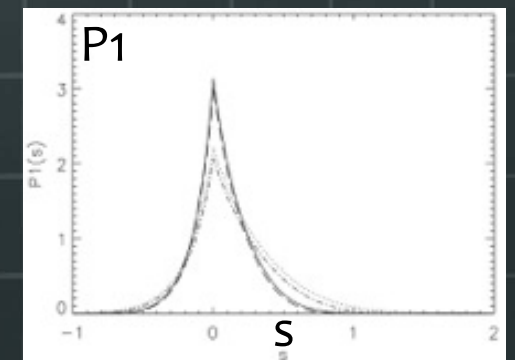
$$x = \frac{h\nu}{k_B T_{\text{CMB}}}$$

$$I_0 = \frac{2(k_B T_{\text{CMB}})^3}{(hc)^2}$$

$$G(x, T_e) = \int \frac{P_1(s, T_e)}{\Theta(T_e)} \left[\frac{x^3 \exp(-3s)}{\exp\{x \exp(-s)\} - 1} - \frac{x^3}{\exp(x) - 1} \right] ds$$

$$\Theta(T_e) = \frac{k_B T_e(l)}{m_e c^2}$$

s the logarithmic frequency shift caused by a scatter, P the scattering kernel (the distribution of frequency shift for single scattering)



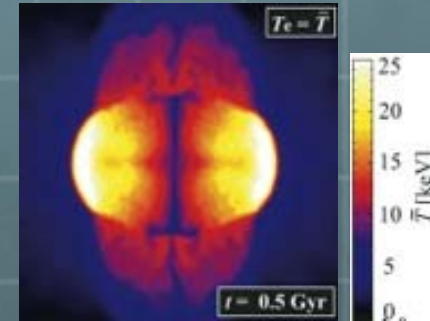
Wright 79; Prokhorov, TA+ 2011abc

2.3 Sunyaev-Zel'dovich Effects

27/53

Kampaneets vs Wright

Wright: I increases @ $T > 10$ keV



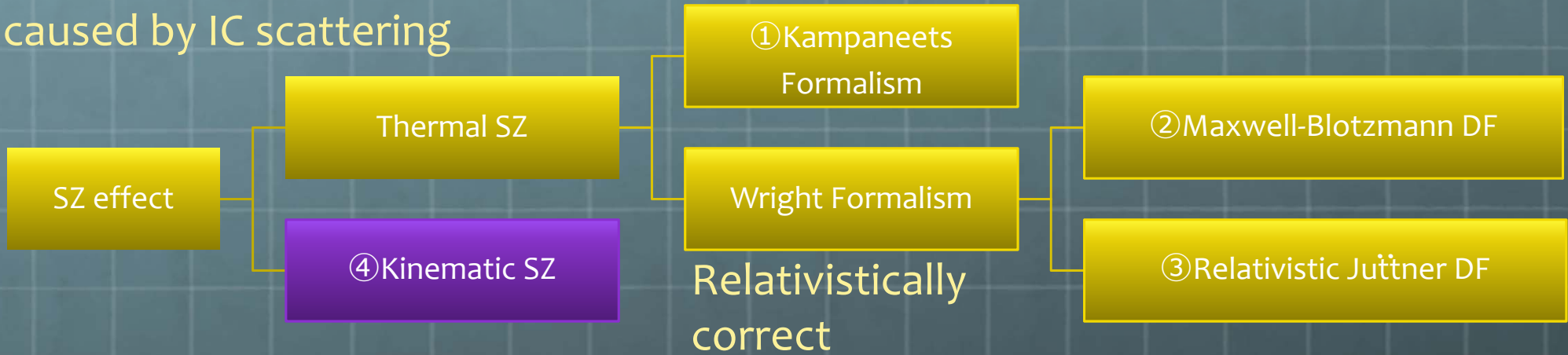
	345GHz	600GHz	857GHz
Kampaneets	Different intensity distortion but same morphology		
Wright			

Different intensity distortion and different morphology

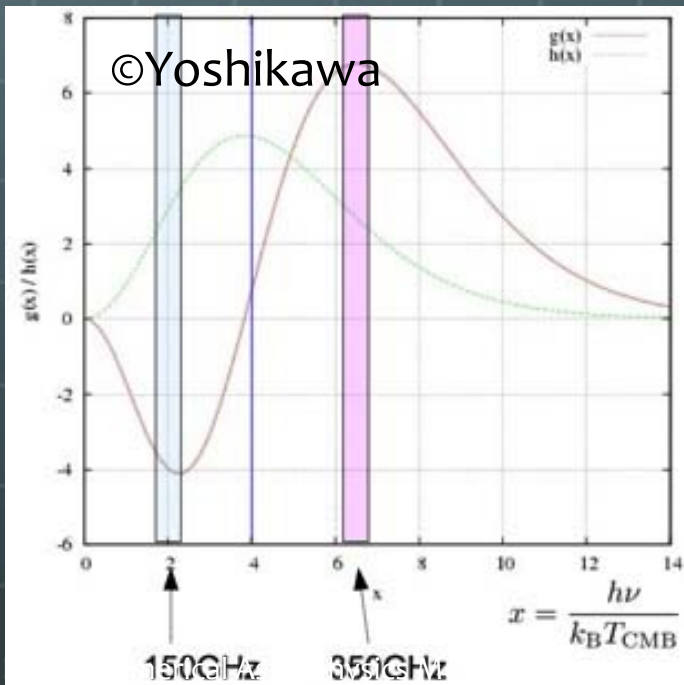
2.3 Sunyaev-Zel'dovich Effects

CMB photon distortion caused by IC scattering

Non-relativistic diffusion approximation



④ Kinematic SZ



$$\Delta I^{\text{kin}}(x) = -I_0 \int h(x) \frac{v_r}{c} n_e(l) \sigma_T dl$$

$$x = \frac{h\nu}{k_B T_{CMB}}$$

$$\Delta I^{\text{kin}}(x) = I_0 h(x) y \quad y^{\text{kin}} = \int \frac{v_r}{c} n_e(l) \sigma_T dl$$

$$I_0 = \frac{2(k_B T_{CMB})^3}{(hc)^2}$$

$$\frac{y^{\text{kin}}}{y} \sim 0.05 \left(\frac{v_r}{300 \text{ km/s}} \right) \left(\frac{k_B T_e}{10 \text{ keV}} \right)^{-1}$$

$$h(x) = \frac{x^4 \exp(x)}{[\exp(x) - 1]^2}$$

Sunyaev & Zel'dovich 72; Challinor, Lasenby 98

Yoshikawa, TA, Kitayama, Komatsu in prep.

2.3 Sunyaev-Zel'dovich Effects

29/53

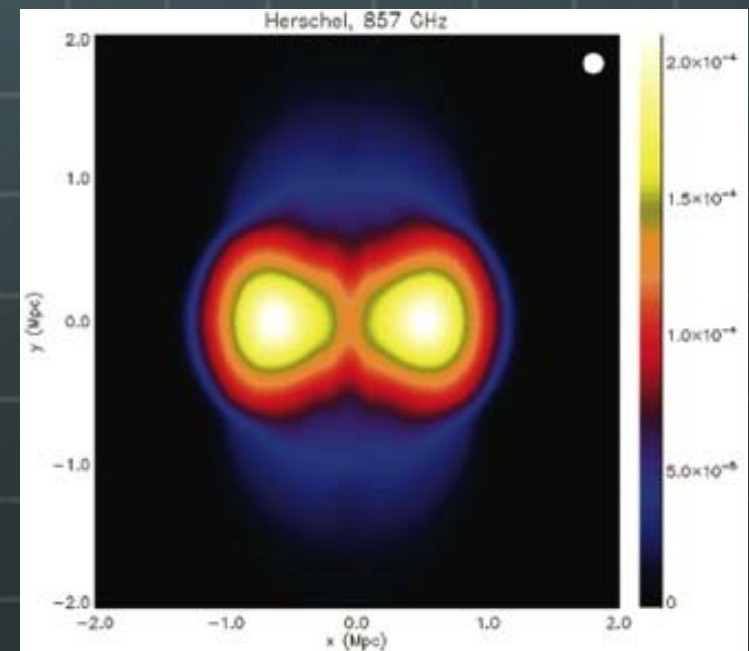
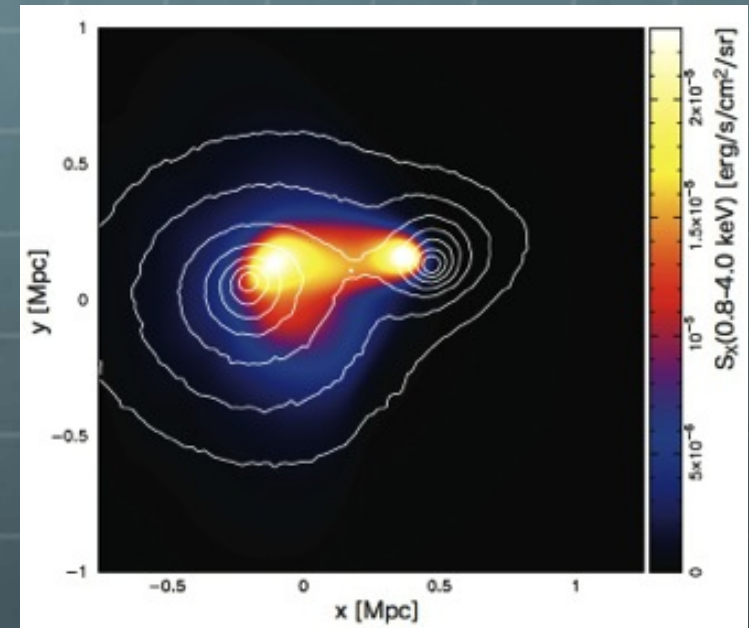
Simulated Bullet cluster

Yoshikawa, TA, Kitayama, Komatsu in prep.

Section 2 Summary

30/53


- 🌐 **Shocks are ubiquitous**
 - 🌐 Mechanism of heating
 - 🌐 Laboratory of plasma
- 🌐 **Non-Equilibrium effects** are significant behind the shocks even in galaxy clusters
- 🌐 **Relativistic correction of SZ effect** is important for very hot ICM heated by the shocks



3. Turbulence

1. As a Driving Mechanism of IGMF
2. Faraday Rotation Measure
3. Galactic Foreground

3.1 As Driving Mechanism of the IGMF 32/53

 **Cosmic Magnetism** – an unresolved problem of astrophysics –

Propagations of...

- UHECRs
- γ -ray halo/echo

Evolutions of...

- Galaxy clusters
- Large-scale structure

Seed Fields of...

- First objects
- Proto-galaxies

IGMF


– Inter-Galactic Magnetic Field –

➤ ICM → *partly known*

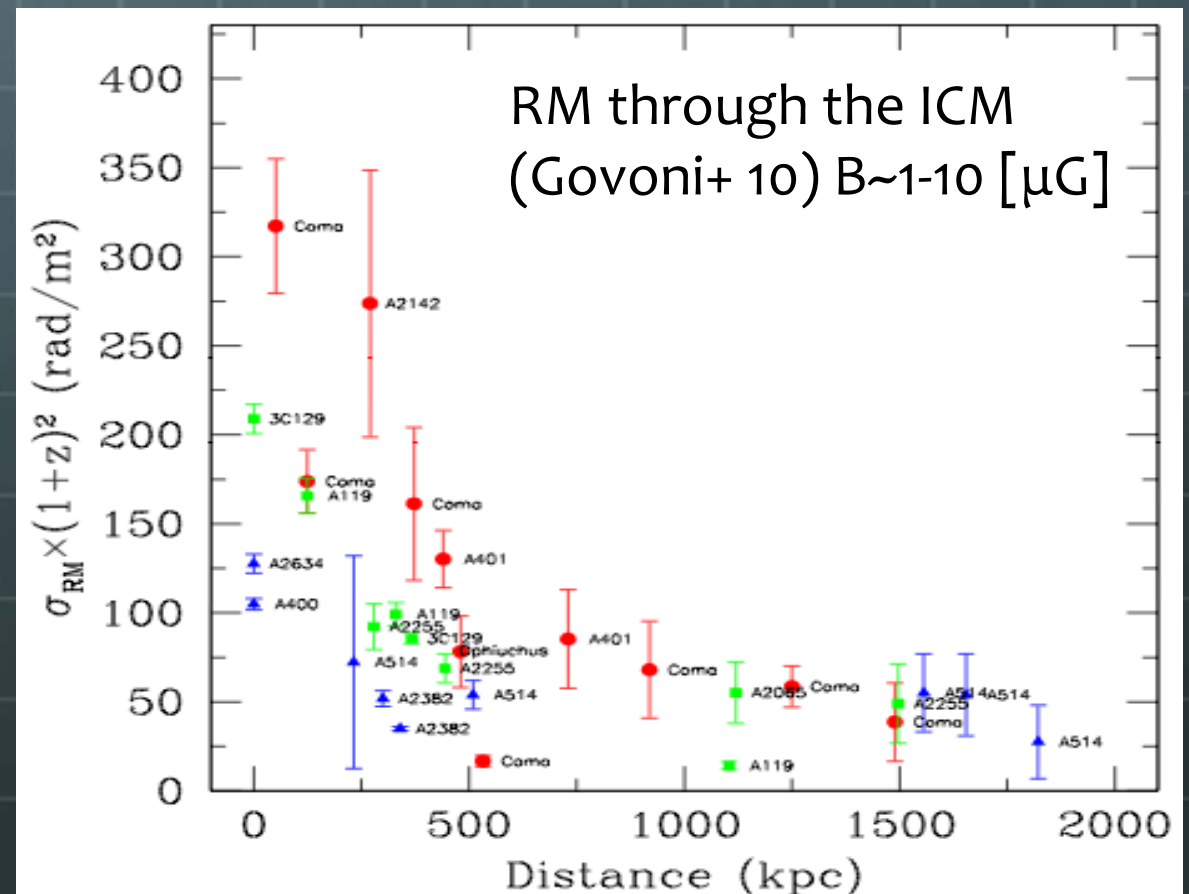
 $|RM| \sim 100$ [rad m⁻²]

 IGMF $\sim 1-10$ [μ G]

➤ WHIM → *unknown*

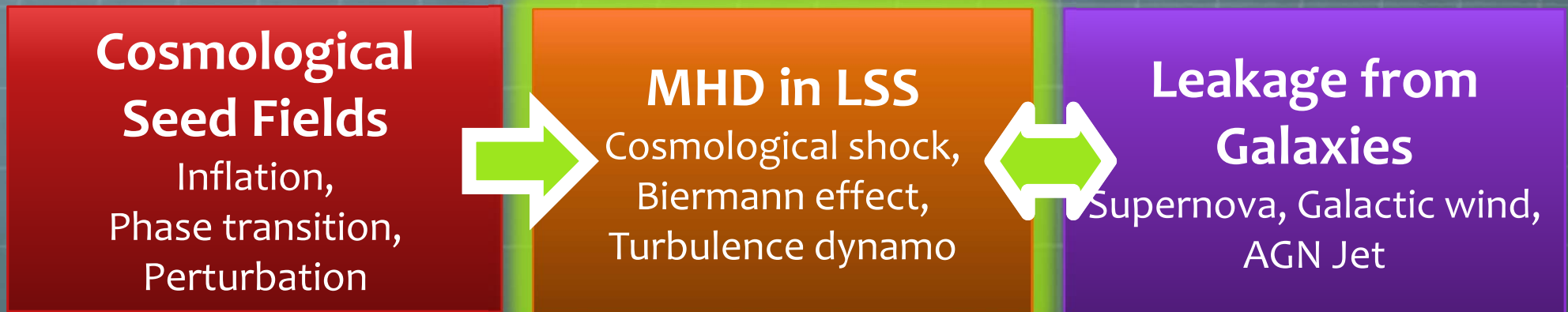
 $|RM| \sim 1??$ [rad m⁻²]

 IGMF $\sim 1-10??$ [nG]

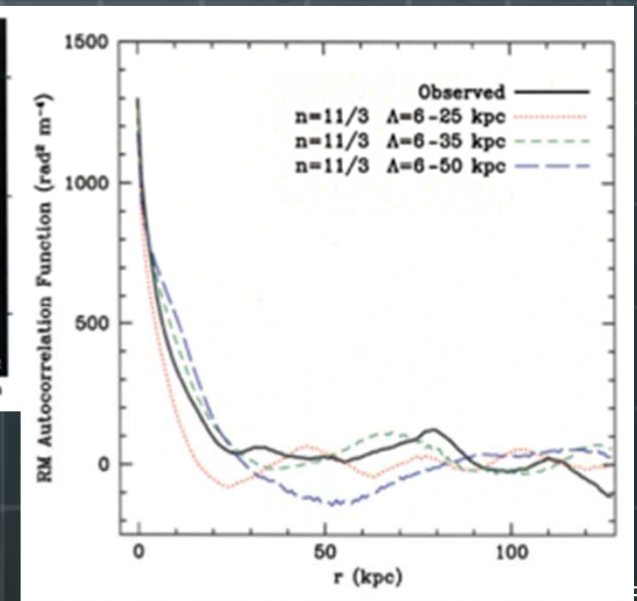
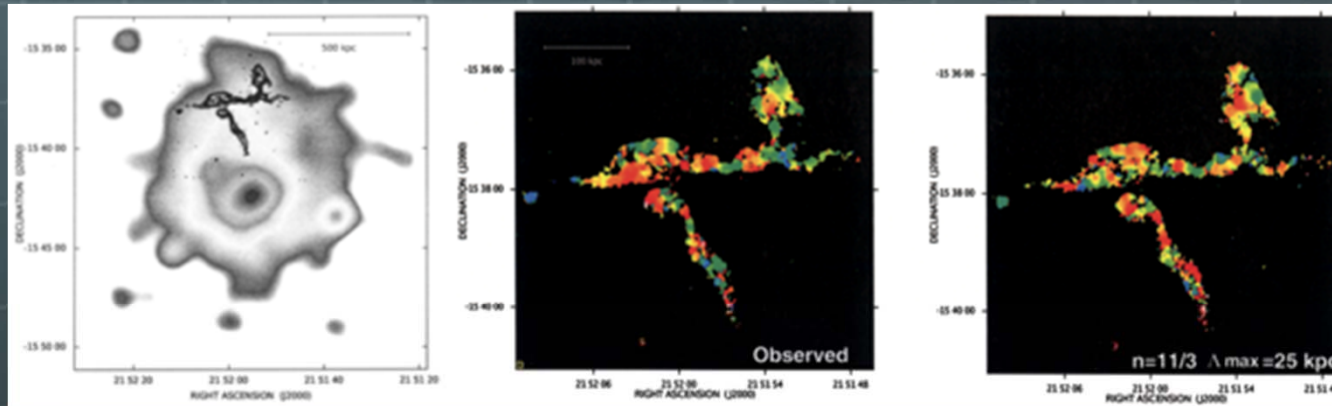


3.1 As Driving Mechanism of the IGMF 33/53

Turbulence Dynamo in the Universe



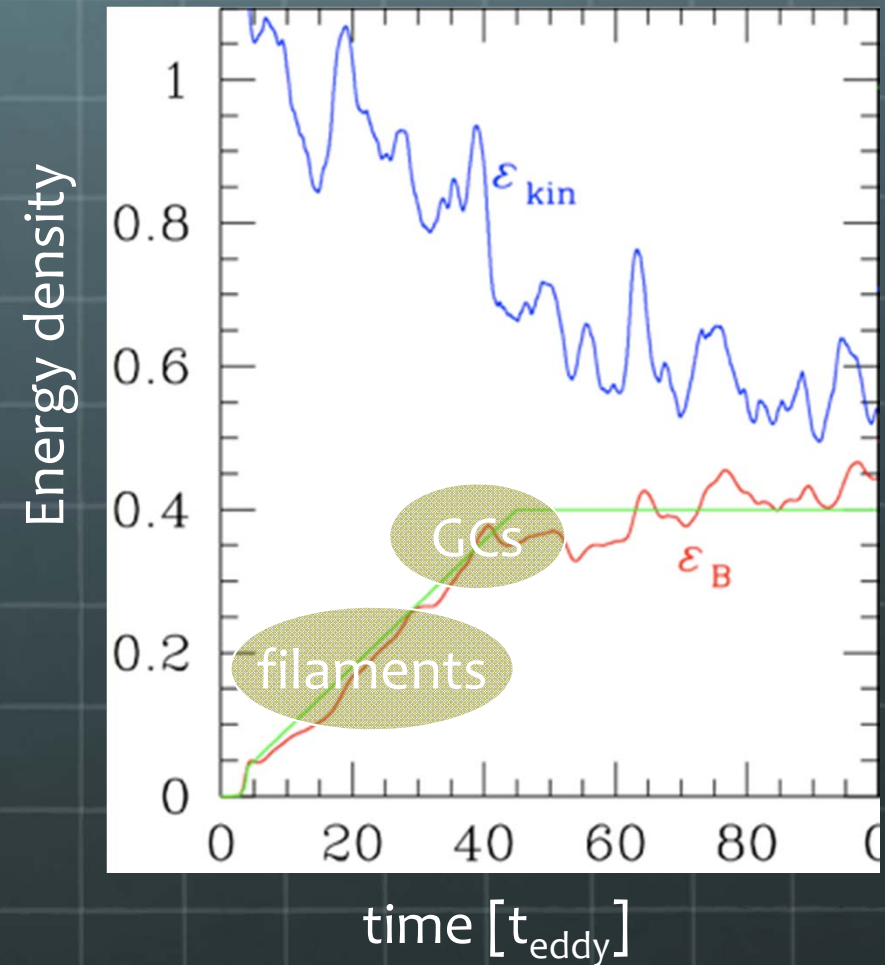
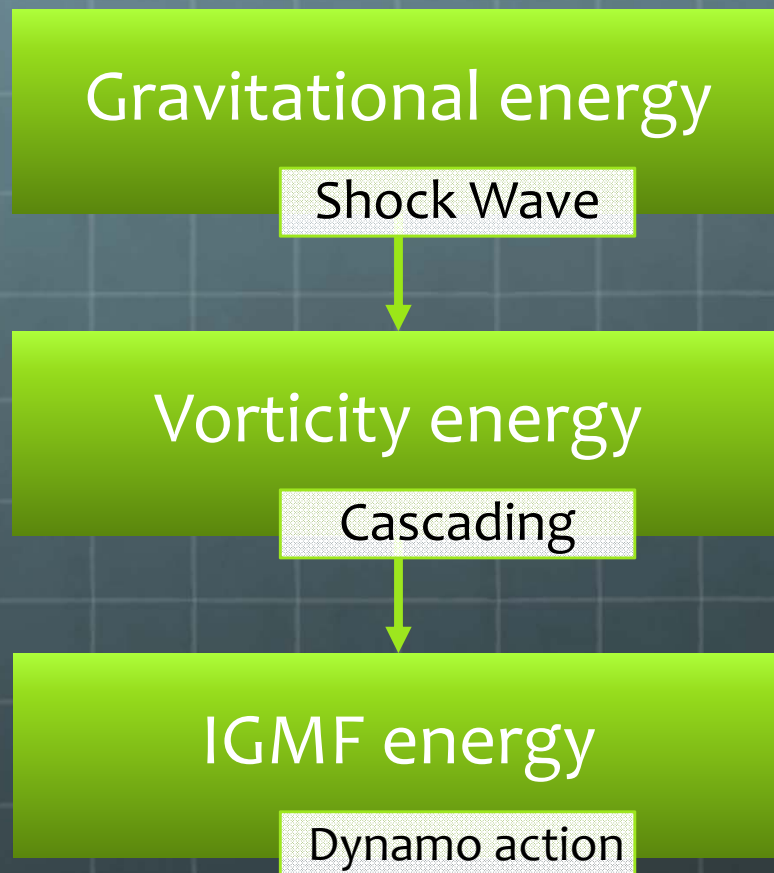
Kolmogorov model can explain the observed RM map → **Existence of turbulence?**



PKS2149-158 & 158C in Abell 2383 (Guidetti+ 08)
ROSAT 0.1-2.4 keV (gray), VLA 4.88 GHz (contour)


3.2 As Driving Mechanism of the IGMF 34/53


Expected turbulence dynamo action

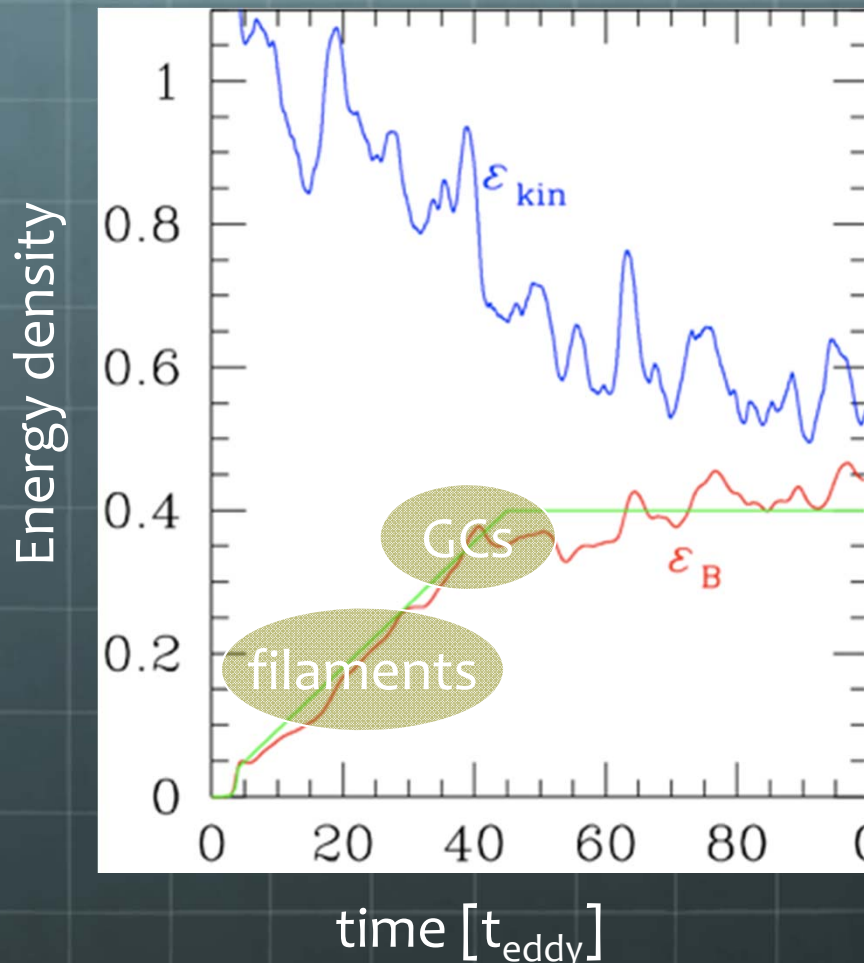


Ryu+ 08

3.2 As Driving Mechanism of the IGMF 35/53

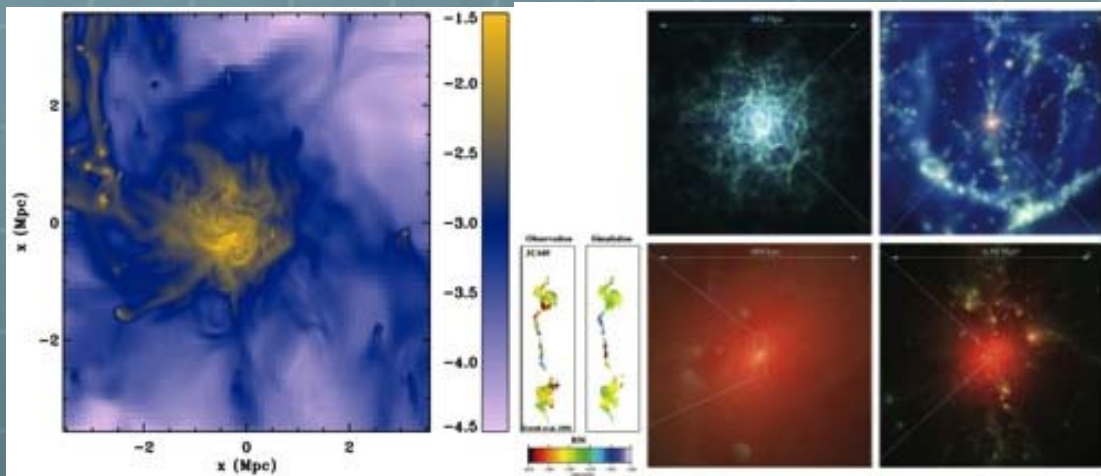
 **Method: Simulation of the cosmological structure formation + turbulence dynamo model (Ryu+ 08)**

 MHD...still hard to treat evolution of turbulence and amplification of the IGMF correctly

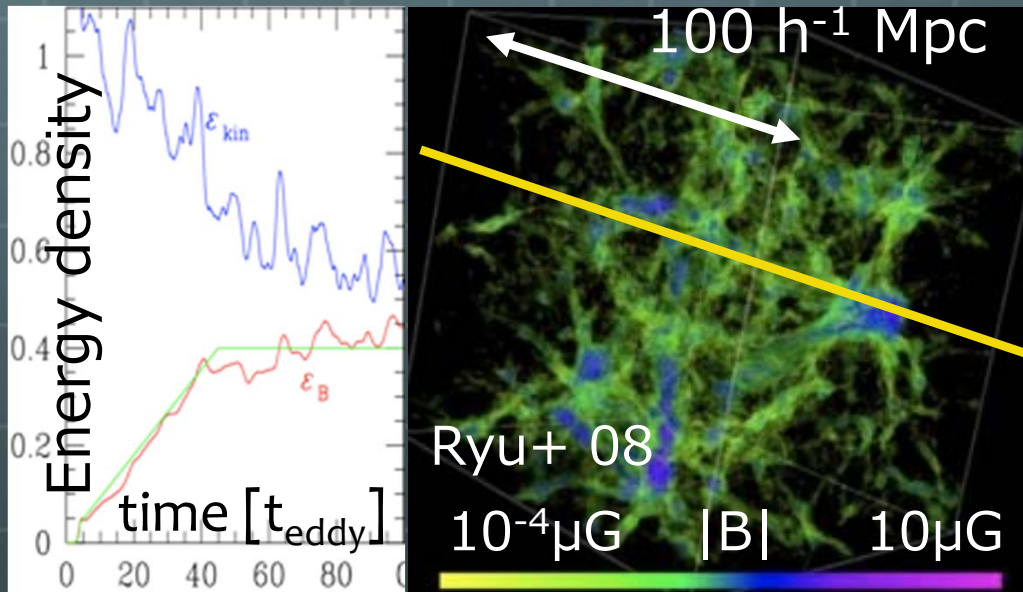


- ① Calculate curl component of flow motion & its energy ϵ_w
- ② Regard ϵ_w as the turbulence energy ϵ_{turb}
- ③ Adopt the growth model $\epsilon_B/\epsilon_{\text{turb}} = f(t/t_{\text{eddy}})$ & $B = (8\pi\epsilon_B)^{1/2}$
- ④ Direction ... passive field

3.2 As Driving Mechanism of the IGMF 36/53



- **Cosmological simulations**
 - AMR-MHD (Dubois, Teyssier 08)
 - SPH-MHD (Dolag, Stasyszyn 09)
 - MHD(passive) + turbulence dynamo model (Ryu, Kang, Cho, Das 08, science)



My Work

Faraday Rotation Measure (RM)
 n_e [cm^{-3}], B_{\parallel} [μG], l [kpc]

$$\text{RM} = 811.9 \int_0^L n_e B_{\parallel} dl \text{ rad m}^{-2}$$

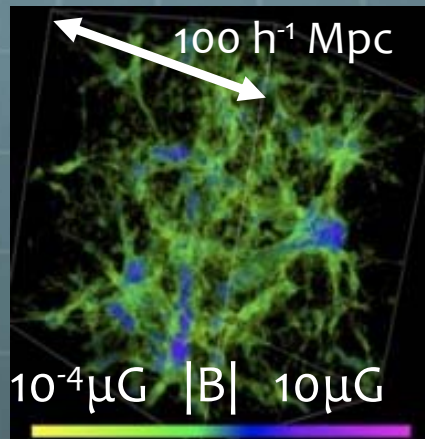
↔ current/future observations

$$\sigma_{RM} \sim 1.5 \left(\frac{\bar{n}_e}{10^{-5} \text{cm}^{-3}} \right) \left(\frac{B_{rms}}{0.3 \mu\text{G}} \right) \left(\frac{L_{int}}{300 \text{kpc}} \frac{L}{5 \text{Mpc}} \right)^{1/2} \text{ rad m}^{-2} \quad \text{Cho, Ryu 09}$$

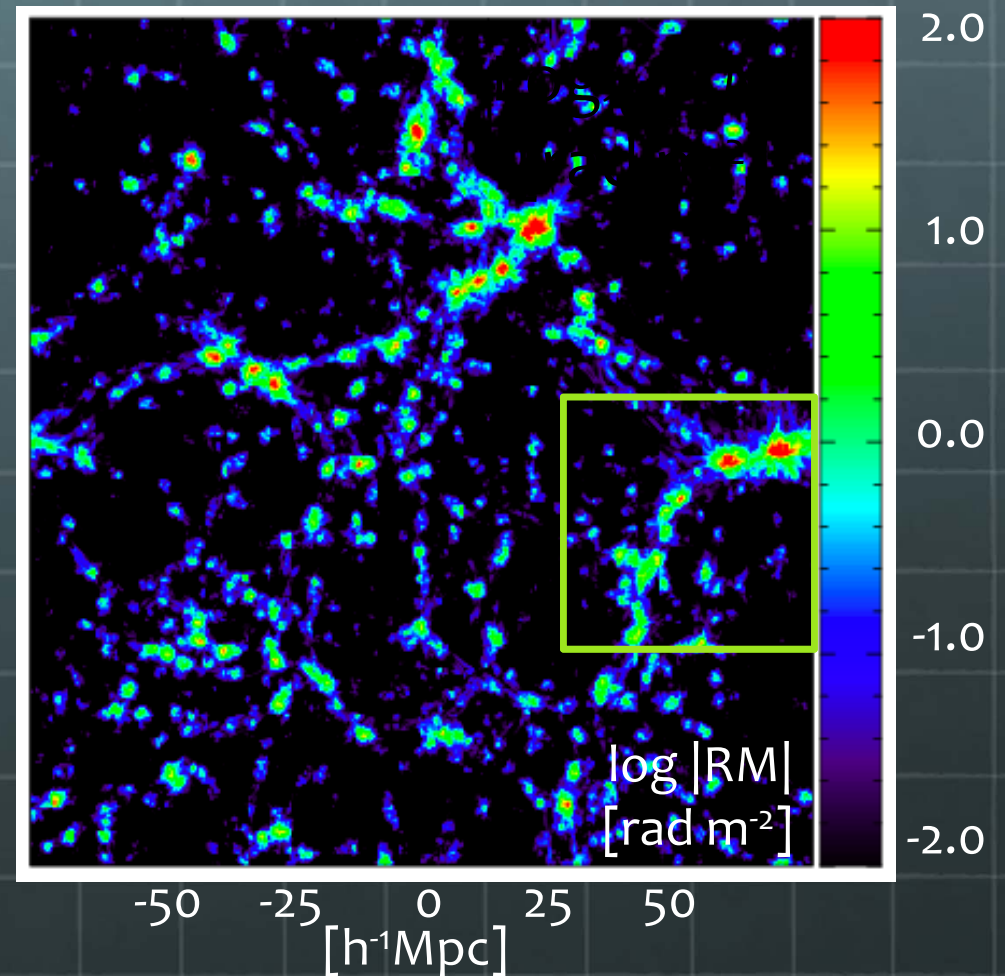
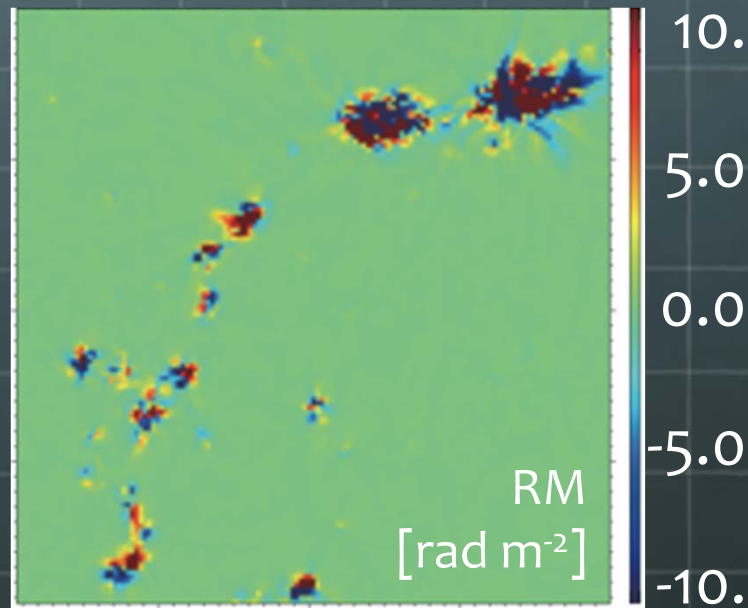
3.2 IGMF RM – Local Universe –

37/53

 RMS of RM through a filament ~ 1 [rad m⁻²]



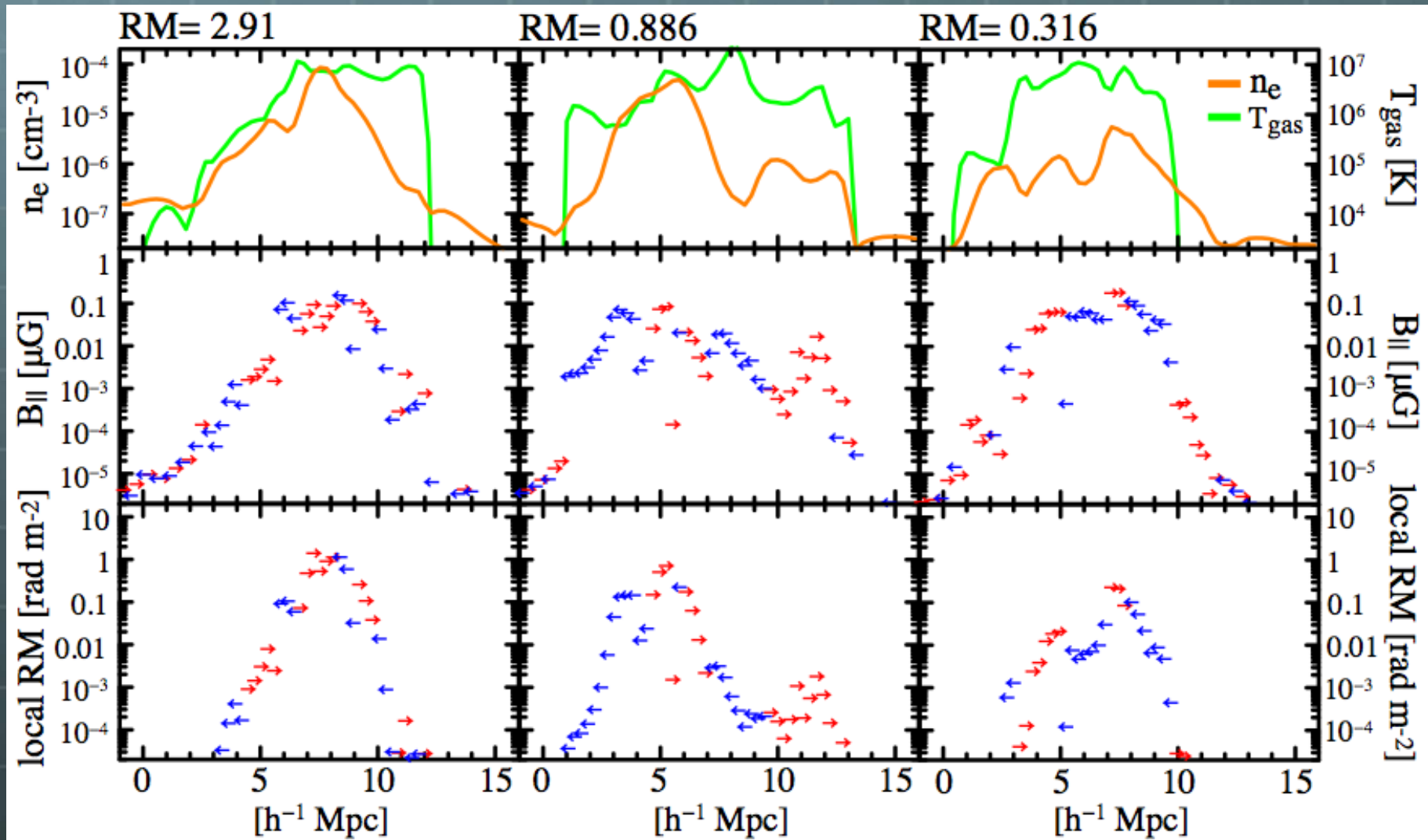
RM ~ 100 (GCs), ~ 10 (Groups), $\sim 0.01-1$ (filaments)



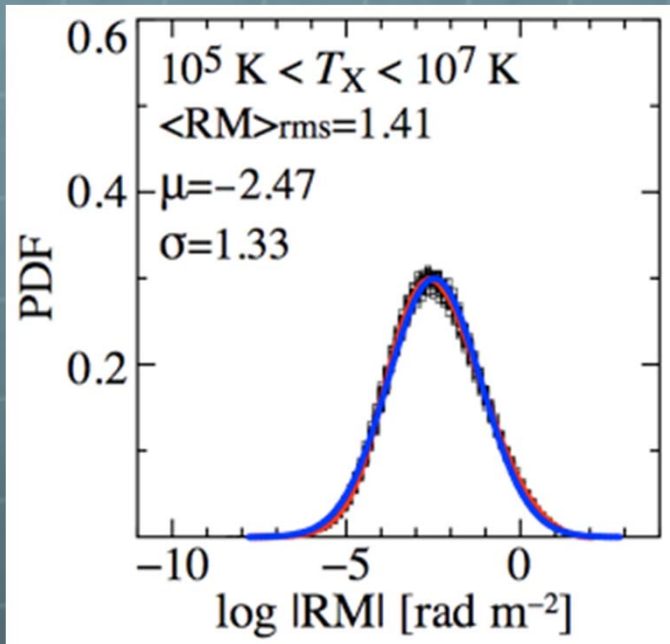
3.2 IGMF RM – Local Universe –

38/53

🌐 Coherence length ~ a few*100 kpc, random walk



3.2 IGMF RM – Local Universe –



PDF of $|RM|$ for WHIM ($10^5 \text{ K} < T_X < 10^7 \text{ K}$)

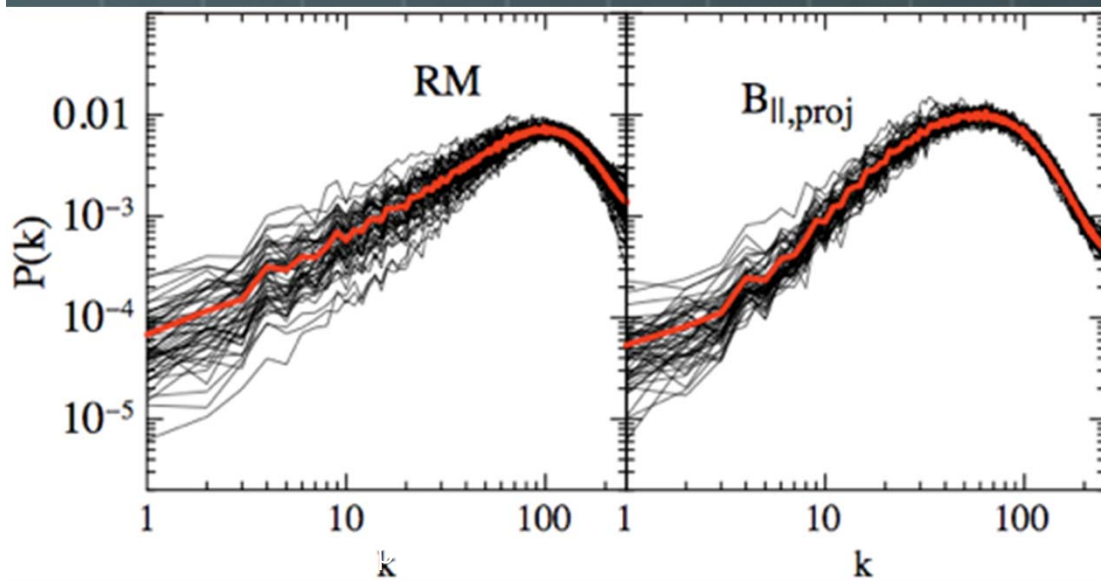
T_X : emissivity weighted temperature.

Black: 3×16 runs, Red: average, Blue: best-fit

$$PDF(\log_{10} |RM|) = \frac{1}{\sqrt{2\pi\sigma^2}} \exp \left[-\frac{(\log_{10} |RM| - \mu)^2}{2\sigma^2} \right]$$

- Lognormal profile of PDF
- rms ~ 1.4 [rad m⁻²] for WHIM

100 h⁻¹ 10 h⁻¹ 1 h⁻¹Mpc 10 h⁻¹ 1 h⁻¹Mpc



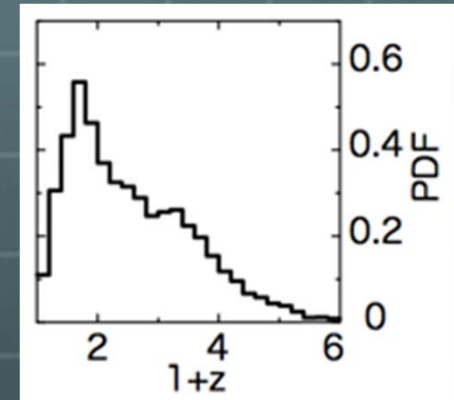
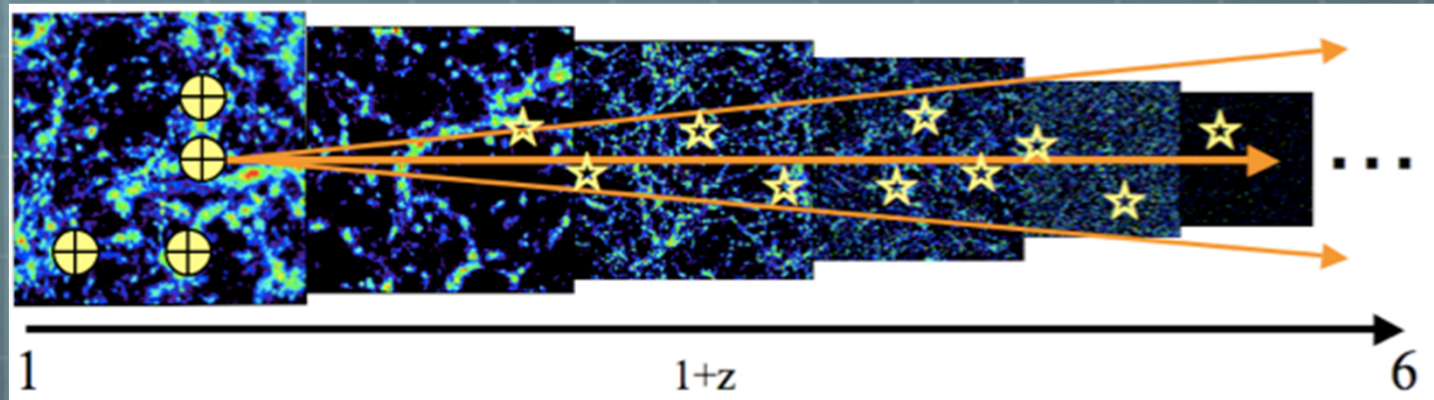
2D power spectra of RM and the projected IGMF

Black: 3×16 runs, Red: average

- Peaked at \sim Mpc scale
- $P^{RM}(k)$ traces $P^{B_{||,proj}}(k)$

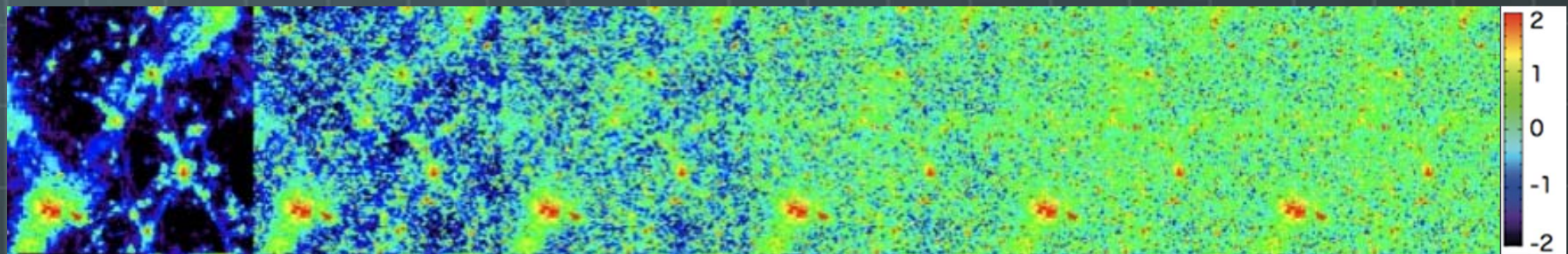
3.2 IGMF RM – Up to z=5 –

Integrating RM up to redshift of 5



$$RM = \frac{e^3}{2\pi m_e^2 c^4} \int_0^{l_s(z_s)} (1+z)^{-2} n_e(z) B_{\parallel}(z) dl(z)$$

Log |RM|
[rad m⁻²]



z=0.1

0.3

0.5

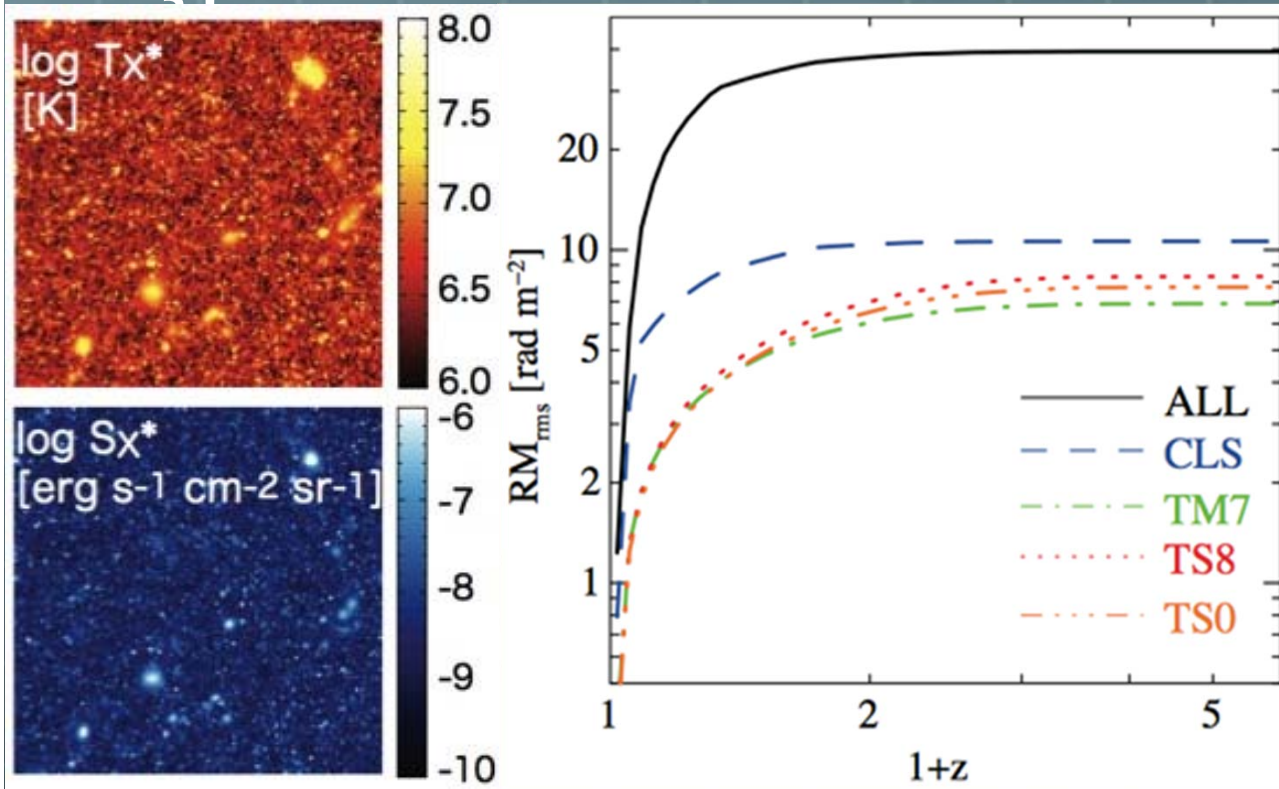
1.0

3.0

5.0

3.2 IGMF RM – Up to $z=5$ –

 RMS of RM through filaments ~several-10 [rad m⁻²]

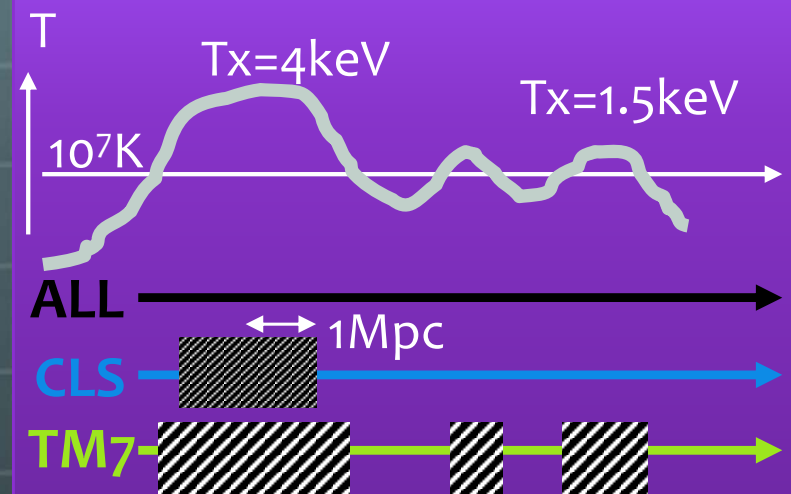


S_x, T_x maps ($z < 5$) 200 deg² FOV

RMS of RM($< z$)


(Ave. of 200 maps = average of 2048*2048*200 pixels)

(I) Subtl. **in** the integration



(II) Subtl. **after** the integration

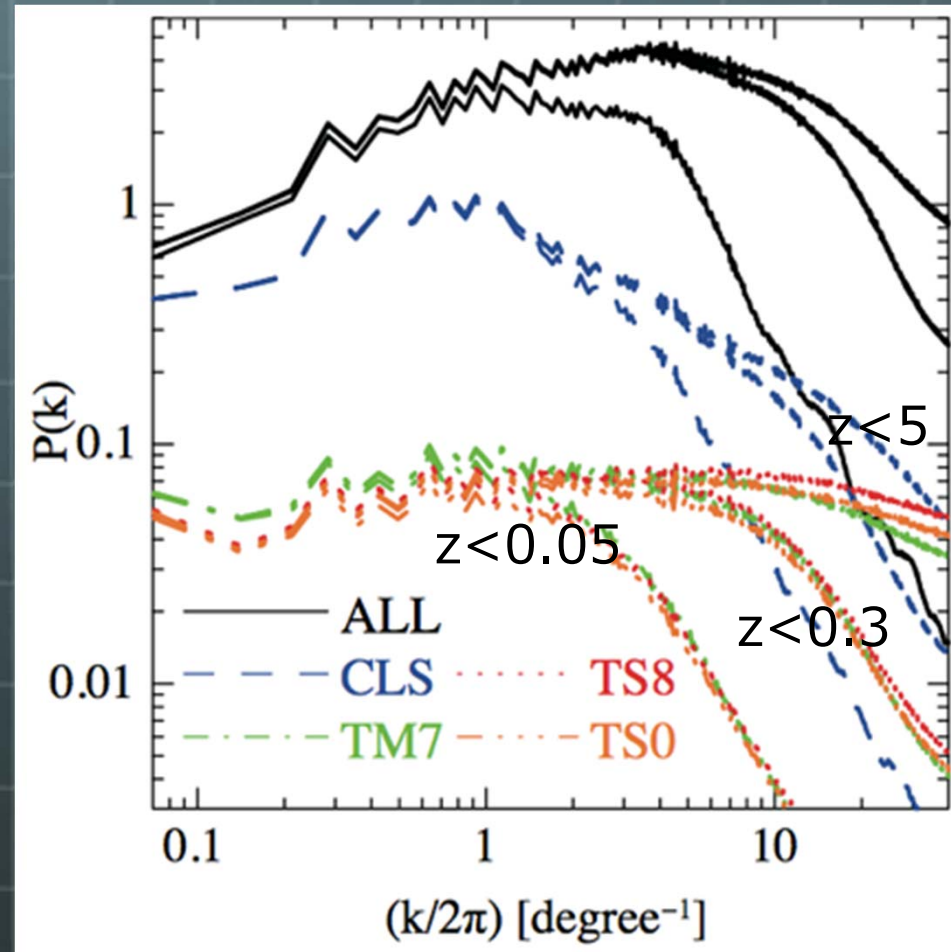
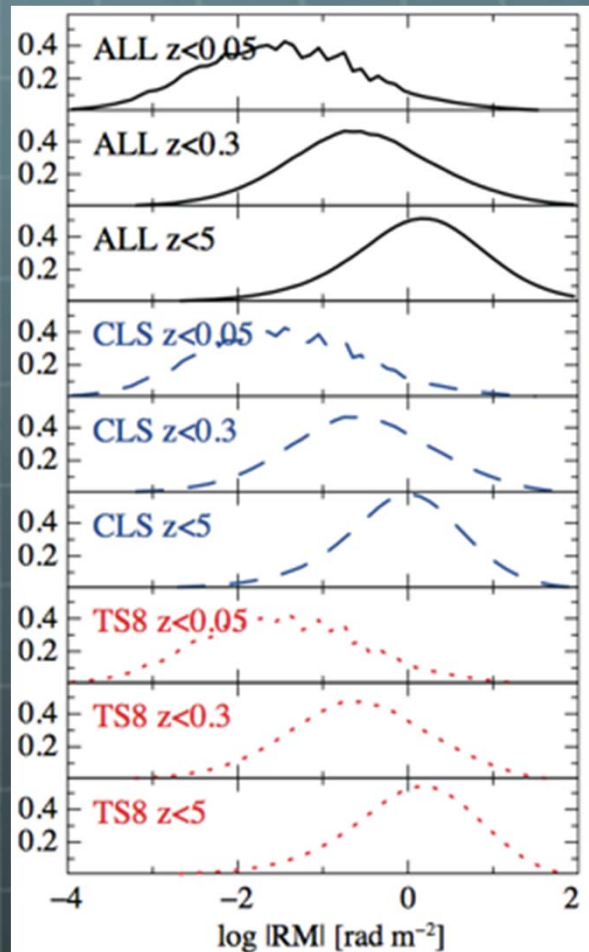
TS8  Pix w $T_x > 10^7 K$ & $S_x > 10^{-8} e/s/cm^2/sr$

TS0  Pix w $T_x > 10^7 K$ & $S_x > 10^{-10} e/s/cm^2/sr$

3.2 IGMF RM – Up to $z=5$ –

42/53

- PDF follows lognormal profile
- Power spectrum peaks at $0.1-0.2^\circ$ scales



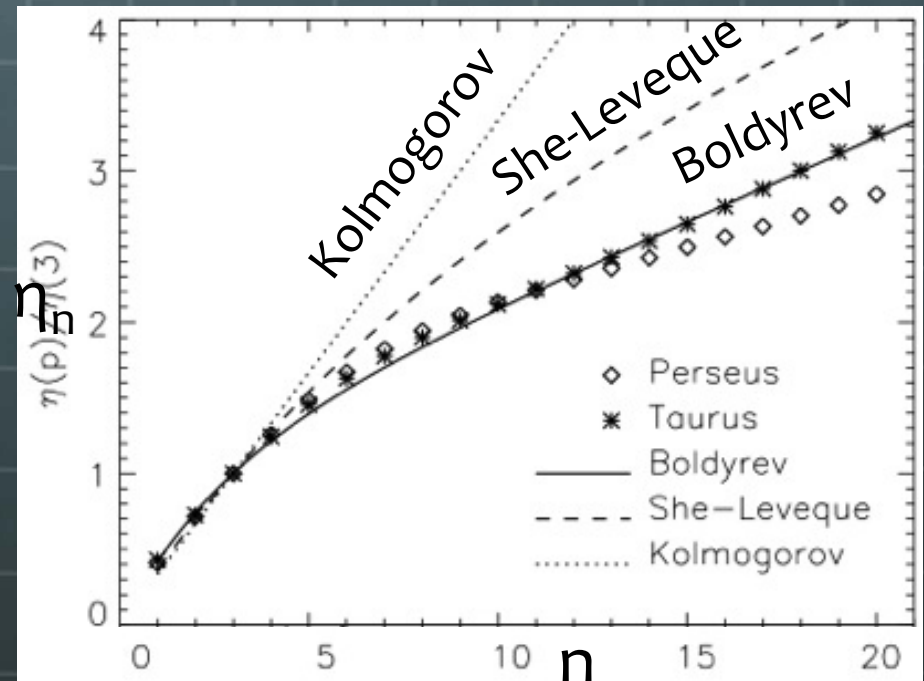
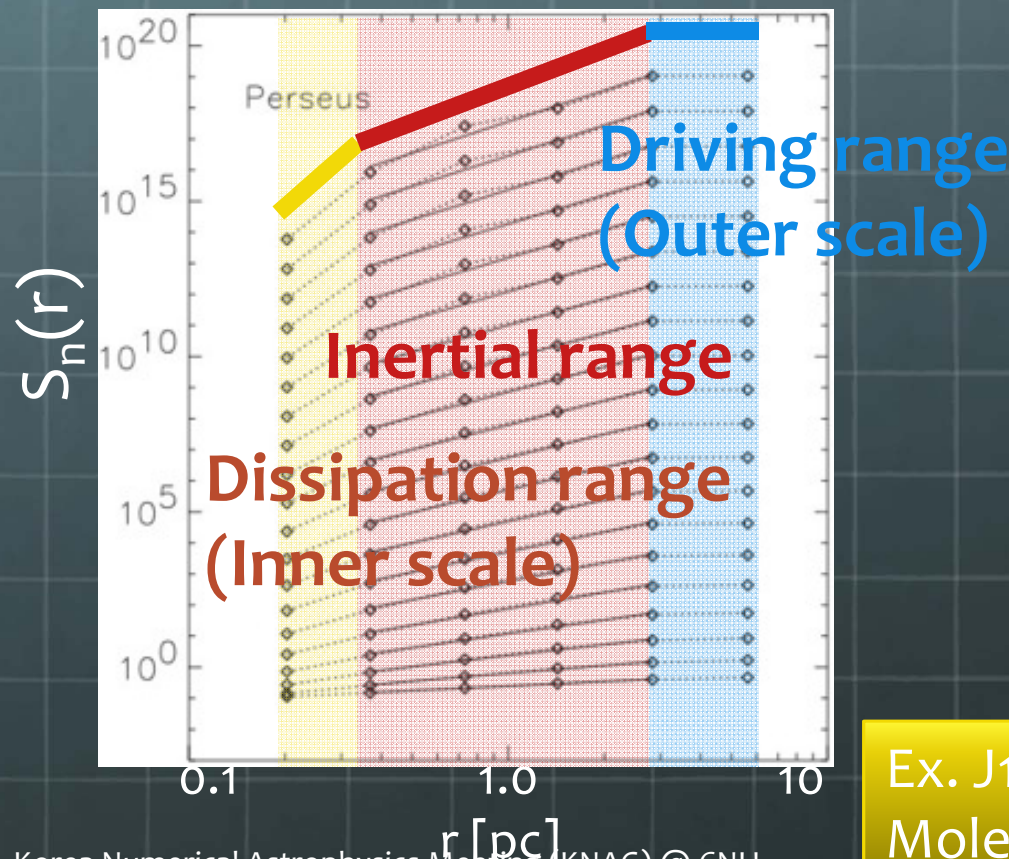
PDFs and Power spectra of RM map (ave. of 200 maps)

3.2 Structure Function (SF) of RM

Structure Function (SF) of Rotation Measure (RM)

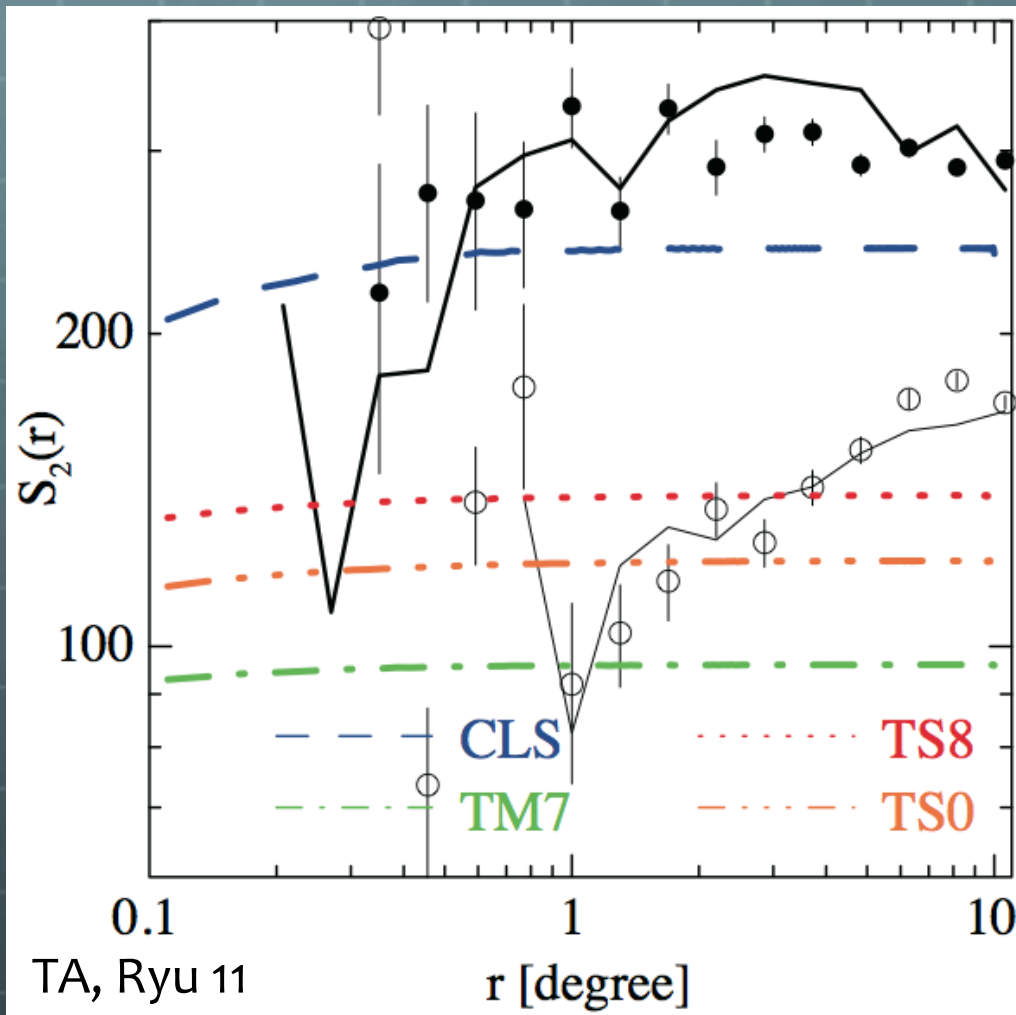
$$S_n(r) = \langle |RM(\vec{x} + \vec{r}) - RM(\vec{x})|^n \rangle_{\vec{x}} \propto r^\eta$$

- Available even for coarse-spacing data without errors
- Shape & Exponents reveal the nature of turbulence



Ex. J1-0 ¹³CO Intensity SF and SF exponents of Molecular Cloud Complexes (Padoan+ 03)

🌐 SFs of RM toward the Galactic Poles (Stil+ 11)



← South Galactic Pole (SGP)
 circles: Mao+ (10) WSRT+ACTA
 lines: Taylor+ (09) NVSS

← North Galactic Pole (NGP)
 circles: Mao+ (10) WSRT+ACTA
 lines: Taylor+ (09) NVSS

← Simulation Results (IGMF)
 colors: Akahori, Ryu (11)


- ✓ Flat @ $r > 0.2^\circ$
- ✓ 100-200 [$\text{rad}^2 \text{m}^{-4}$]

Conclusion

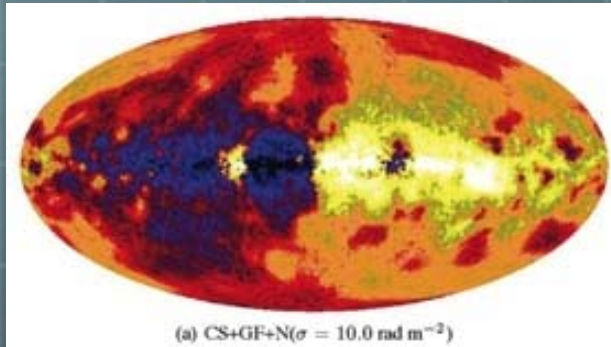
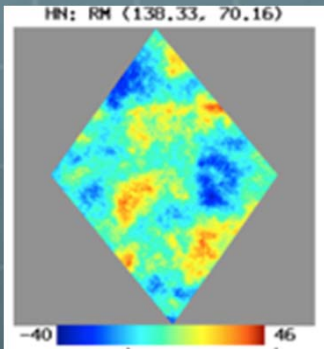
IGMF significantly contributes to the RMs!

3.3 Galactic Foreground RM

45/53

 **GMF** – Galactic Magnetic Field –

 **Analytical model of the Galaxy “HAMMURABI”**



RM map toward $(l,b)=(140,70)$ with $1.5^\circ \times 1.5^\circ$ FOV (Sun, Reich 09)

All-sky RM map (Stasyszyn+ 10) using cosmological SPH-MHD simulation (Dolag+ 09) + HAMMURABI (Waelkens+ 09)

 **But, unsolved issues...**

- ✓ Coupling factor for the thermal electron density fluctuation
- ✓ Suppose uniform $|b| \sim$ a few μG at disk, halo, everywhere
- ✓ Suppose random phase (no sheet/filamentary structures)

Analytic model
for regular
component



Results of MHD
simulations for
random component

My Work

3.3 Galactic Foreground RM

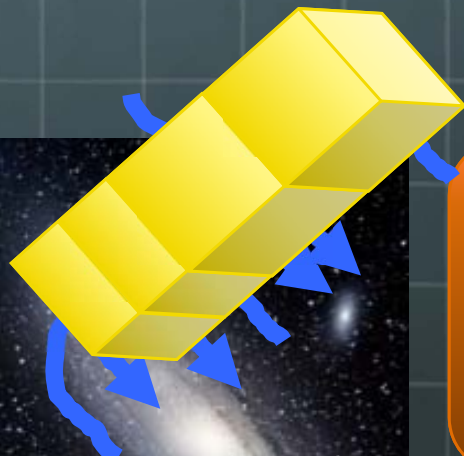
Regular component

- NE2001 (Cordes, Lazio 02;03)
- ASS or BSS, DP or QP, w/o Vertical (Waelkens+09; Sun, Reich 09; 10)

Random component

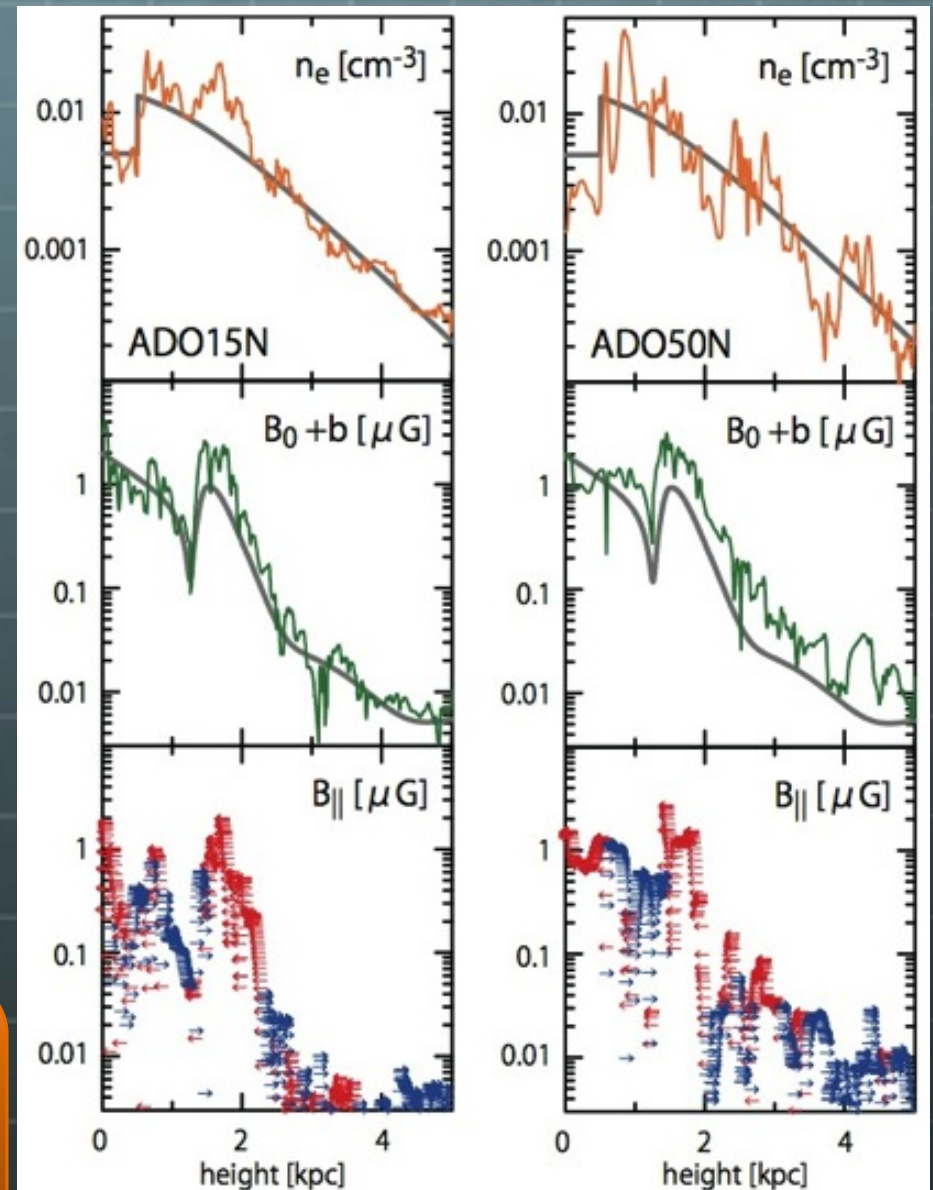
- stack boxes of MHD turbulence simulations (Kim+ 93; Wu+ 09)

Examples of line-of-sight properties toward the NGP



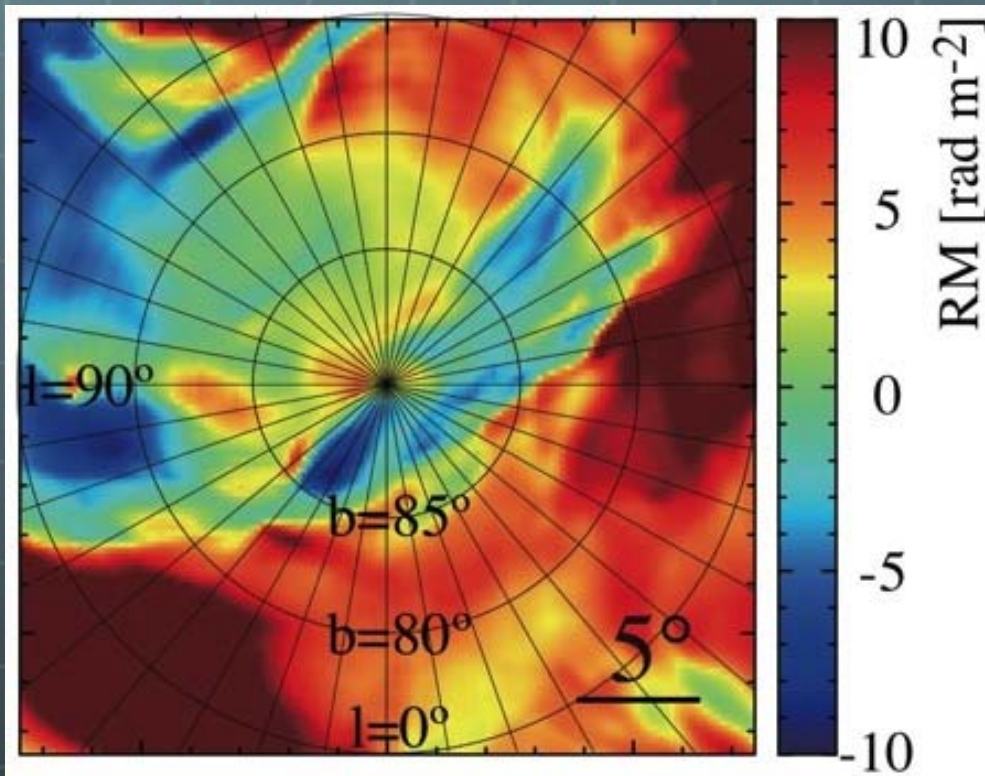
$V_{rms} = 15 - 50 \text{ [km/s]}$
(Tuftte+ 99; Haffner+ 03, 10)

$L_{drive} = 1.67 \text{ [kpc]}$
(Gaensler+ 08 & Wu+ 09)

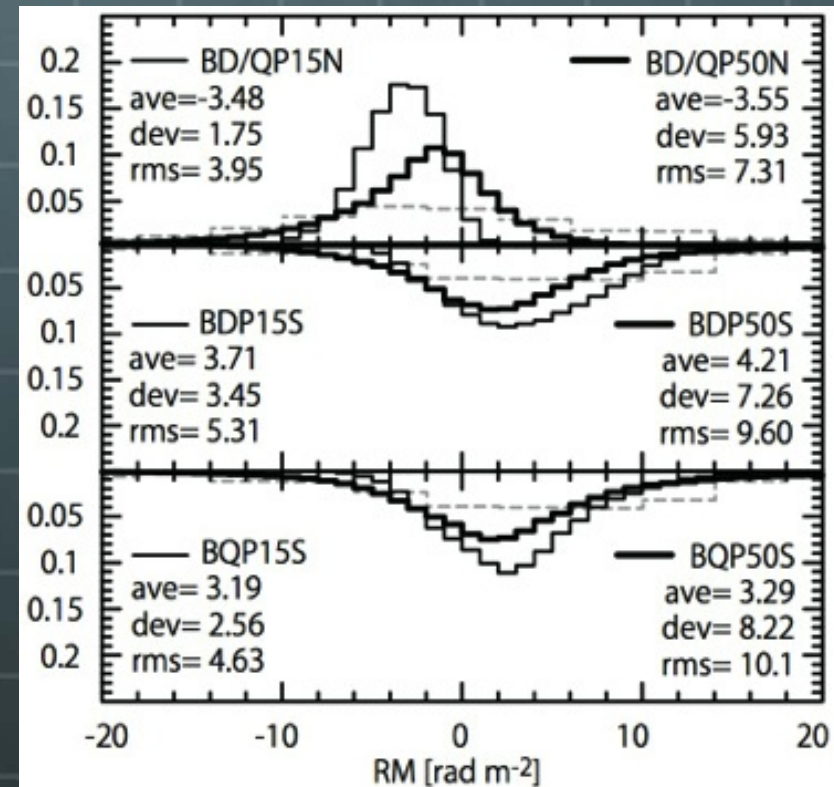


3.3 Galactic Foreground RM

- Regular: Large-scale structure > 10° scales
- Random: Filament/clump structures ~ 1-several° scales
- Ave. ~ ±several [rad m⁻²], std. ~several [rad m⁻²]



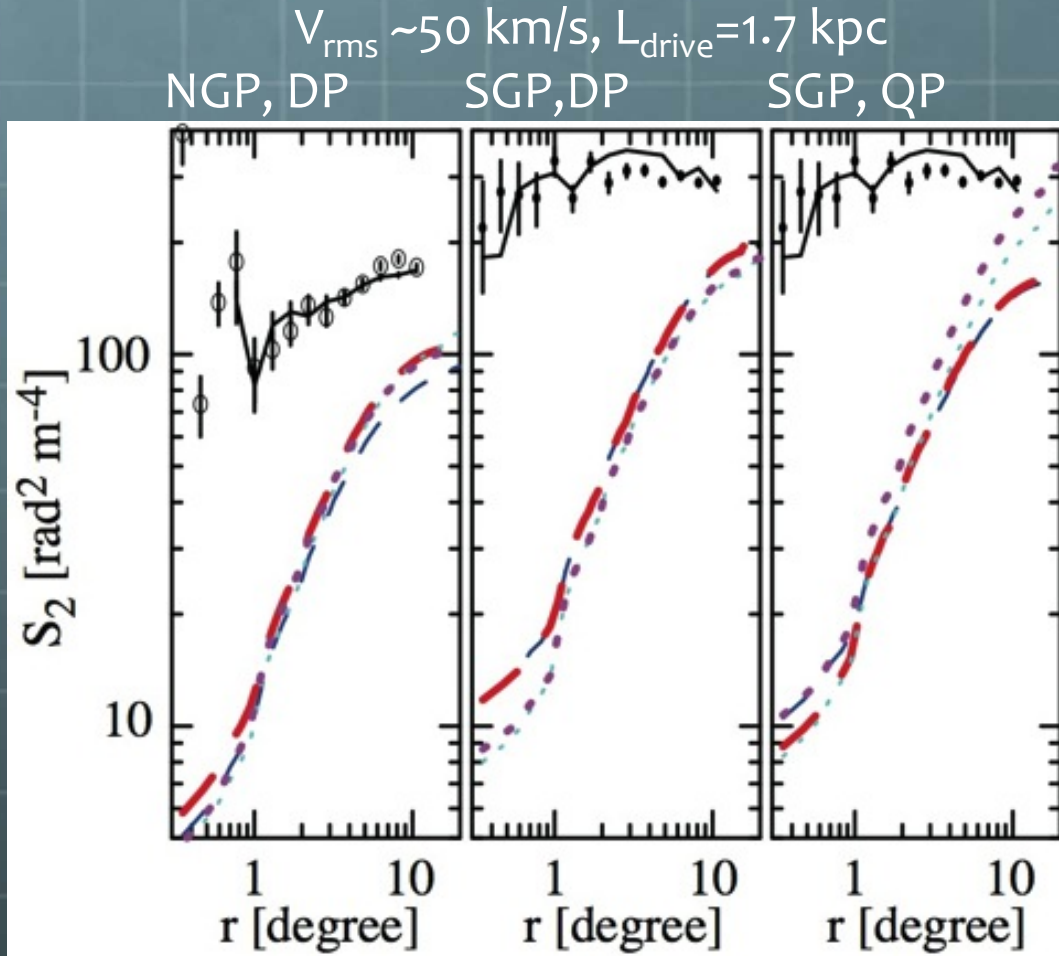
RM map toward NGP



PDF of RMs (Ave. of 200 maps)

3.3 Galactic Foreground RM

SFs of RM toward the Galactic Poles (Stil+ 11)



- ← South Galactic Pole (SGP)
circles: Mao+ (10) WSRT+ACTA
lines: Taylor+ (09) NVSS
- ← North Galactic Pole (NGP)
circles: Mao+ (10) WSRT+ACTA
lines: Taylor+ (09) NVSS
- ← Simulation Results (IGMF)
colors: Akahori+ (11)

✓ Steeper slope
✓ 100-200 [rad² m⁻⁴]

TA, J. Kim, Ryu, Gaensler in prep.

Conclusion

IGMF dominates RMs at small angular scales!

Summary

49/53

🌐 Cosmic Magnetism

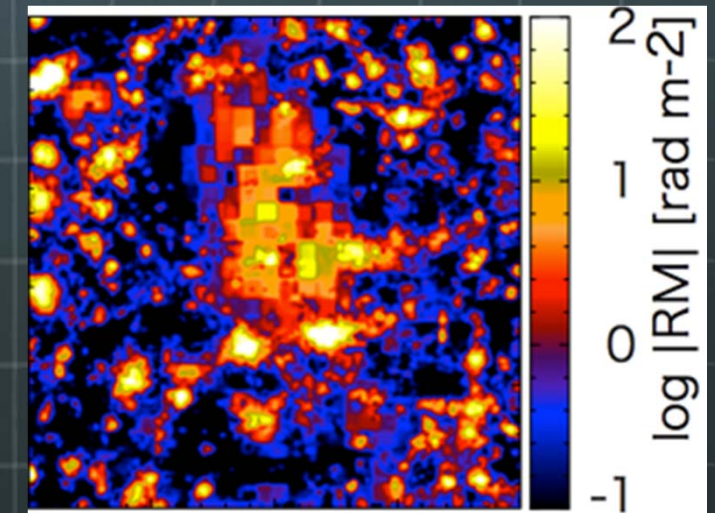
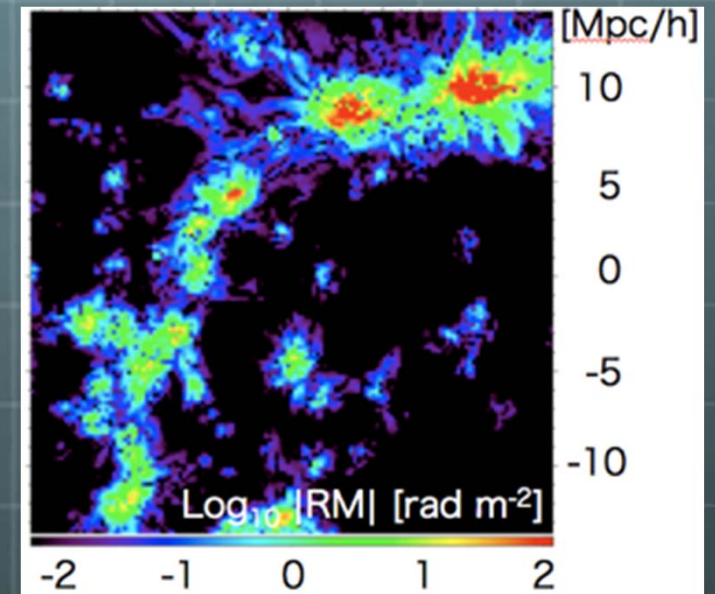
🌐 IGMF-RM

- 🌐 RMS $\sim 1-10$ [rad m⁻²]
- 🌐 SF $\sim 100-200$ [rad² m⁻⁴], flat

🌐 GMF-RM toward Galactic poles

- 🌐 RMS \sim several [rad m⁻²] ($V_{\text{rms}}=50\text{km/s}$)
- 🌐 SF $\sim 100-200$ [rad² m⁻⁴]@10°, slope

🌐 SKA observations



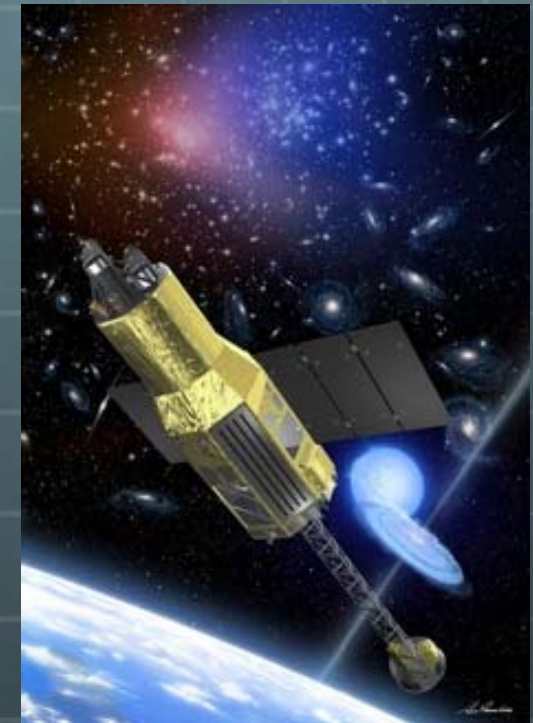
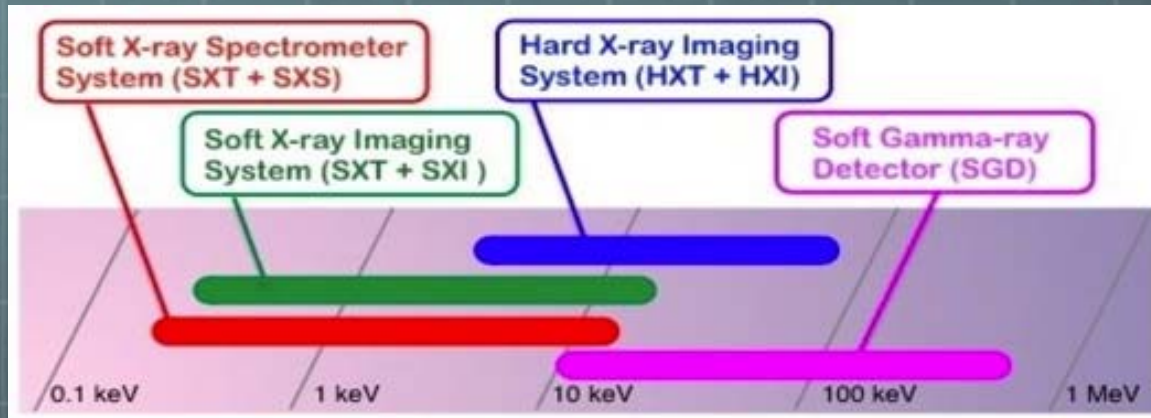
4. Future Observations

1. Astro-H
2. ALMA
2. SKA

4.1 Astro-H

Astro-H (NeXT) 2013-observation

“Revealing the LSS” is one of the key science projects



	SXS	SXI	HXI
FOV (resolution) [arcmin ² , arcmin]	9 (1.3)	1440 (1.3)	81 (1.7)
Energy range [keV]	0.3-12	0.4-12	5-80
Energy resolution in FWHM [eV]	5	150 @6keV	2000 @60keV

We enter the era of observing the LSS!

4.2 ALMA

52/53

- 🌐 ALMA cycle 0 (16) in operation
 - 🌐 25 antennas in observatory
 - 🌐 66 antennas finally
 - 🌐 “SZ effect” may be an important science project (but no proposals are approved in cycle 0...?)



	ALMA
Frequency range [GHz]	80-950
FOV (resolution) @ 900 GHz [arcsec ² ,arcsec]	49 (0.005)
Sensitivity [mJy]	0.005-1

We enter the era of observing the shock!

4.2 ASKAP and SKA

53/53

- 🌐 The Square Kilometer Array (SKA)
 - 🌐 2020- observation (2 trillion won project)
 - 🌐 “Cosmic Magnetism” is one of the five key science projects
- 🌐 Australia SKA Pathfinder (ASKAP)
 - 🌐 2013- observation
 - 🌐 Polarization Sky Survey of the Universe’s Magnetism (POSSUM)



	VLA	ASKAP	SKA
Observational uncertainty [rad m^{-2}]	10	1	0.1
Average separation of sources [degree]	1	0.1	0.01

We enter the era of observing the IGMF!

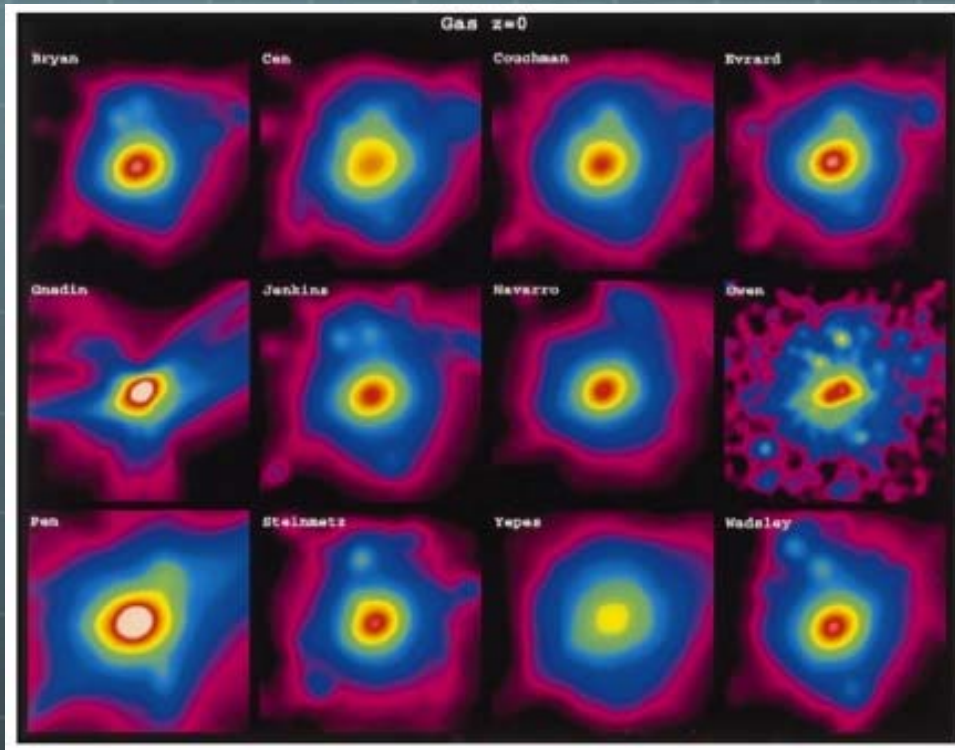
Supporting material

1. Convergence of Simulations

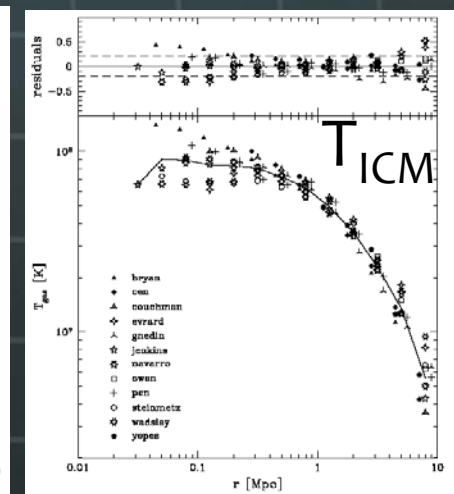
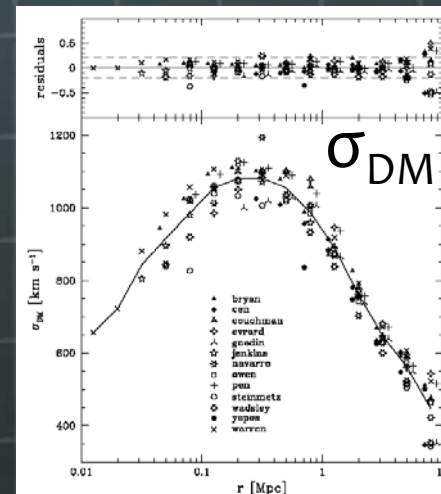
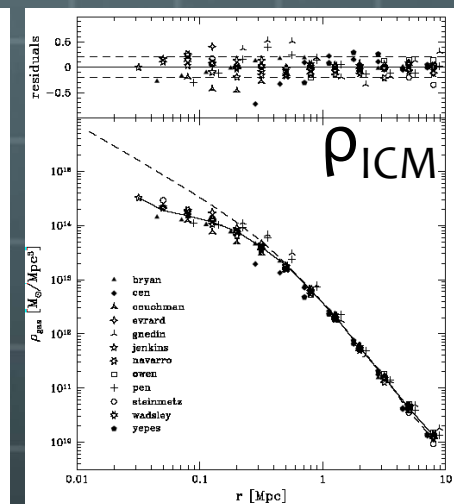
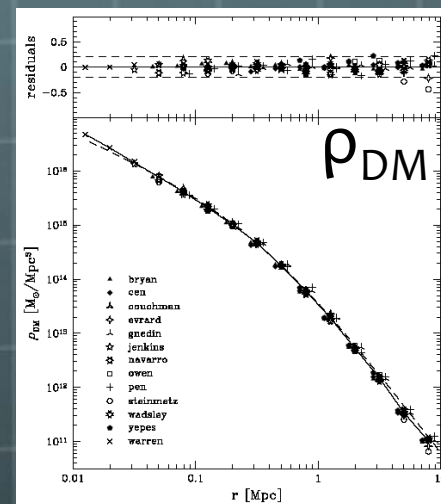
55/53

SBCC Project (Frenk et al. 1999)

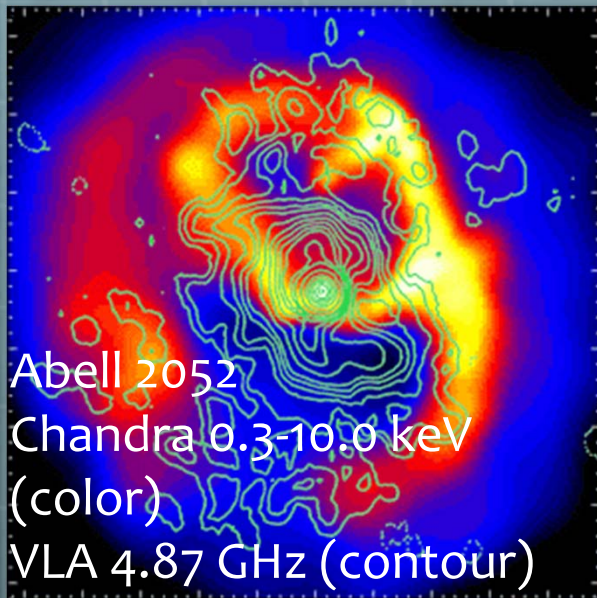
12 different codes on 7 different algorithms from the same Λ CDM



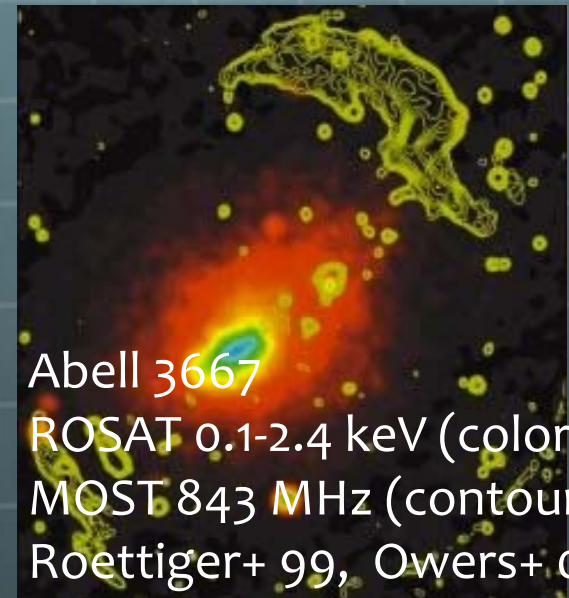
$\rho_{ICM} @ z=0$



2.1 Clues for Shocks (Radio)



Abell 2052
Chandra 0.3-10.0 keV (color)
VLA 4.87 GHz (contour)
Burns 90, Blanton+ 03)



Abell 3667
ROSAT 0.1-2.4 keV (color)
MOST 843 MHz (contour)
Roettiger+ 99, Owers+ 09

- Existence of
- High-energy electrons
 - Magnetic field

Synchrotron emissions

Radio Halo
spherical shape
Close to X-ray peak

Radio Relic
arc shape
Far from X-ray peak
Tend to polarize?

AGN Jet?
Turbulence?

Mini Halo?
Tend to no-polarize?

Halo?
Tend to polarize?

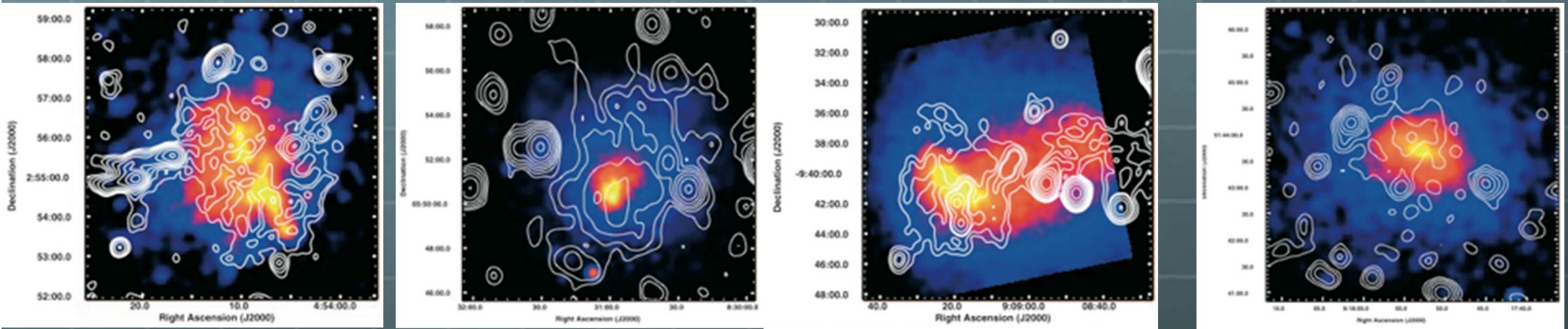
Cosmological shocks?

viewing angle??

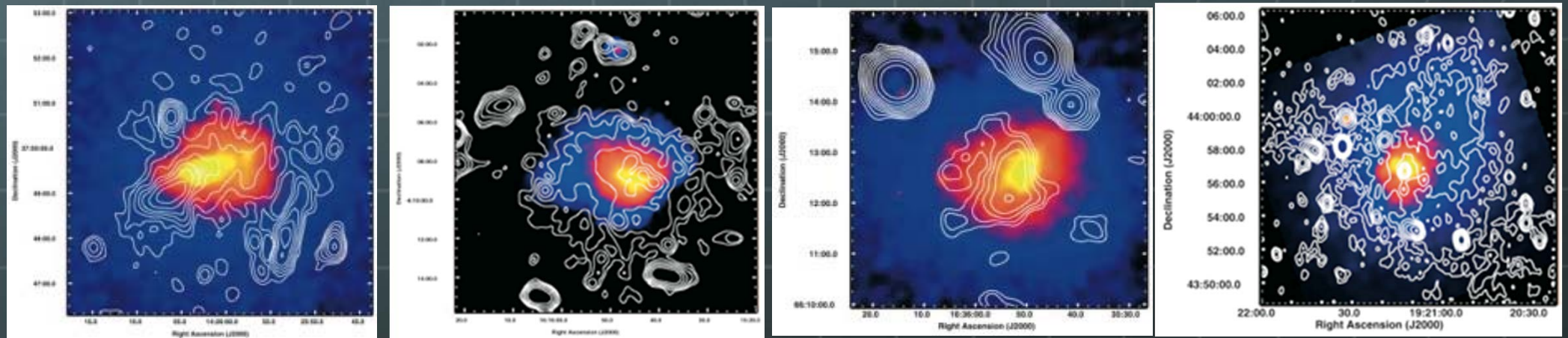
2.1 Radio Halo

57/53

Chandra 0.8-4.0 keV (color) VLA 1.4 GHz (contour) Govoni+ 04



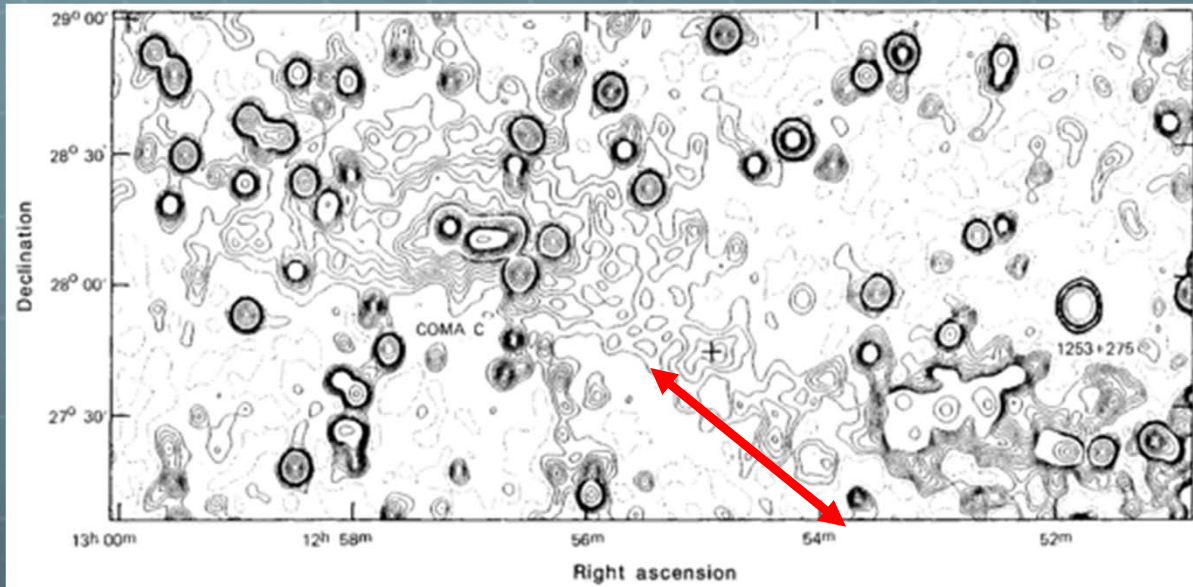
A520, A665, A754, A773



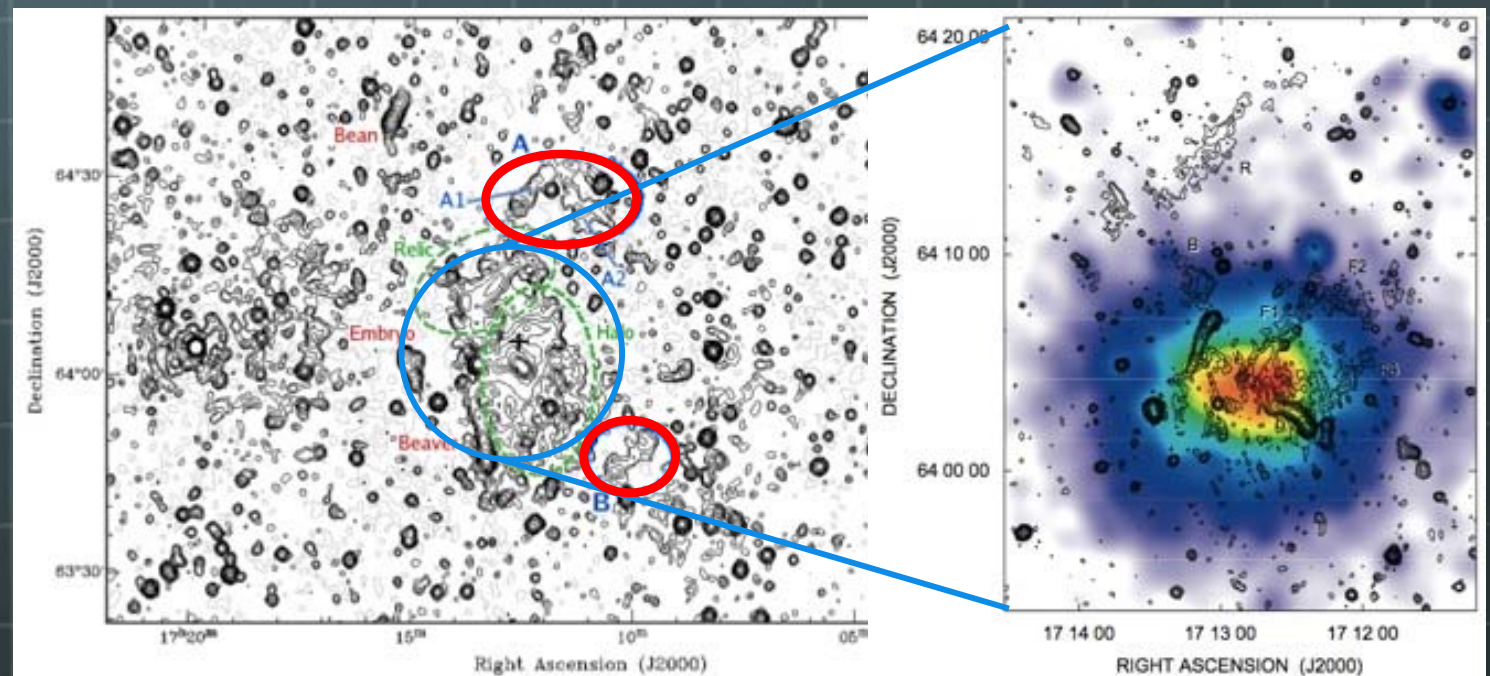
A1914, A2163, A2218, A2319

2.1 Clues for Shocks (Radio)

58/53



Coma cluster
WSRT 324 MHz (contour)
(Kim+ 89)
Extending ~4 Mpc, $B \sim 0.1-0.2 \mu\text{G}$

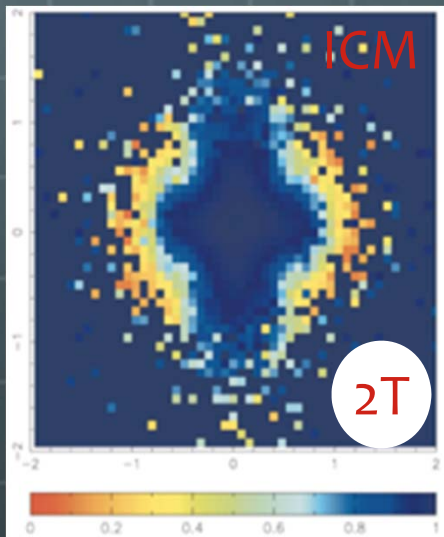


Abell 2255
Radio 85cm (contour)
(Pizzo+ 08)

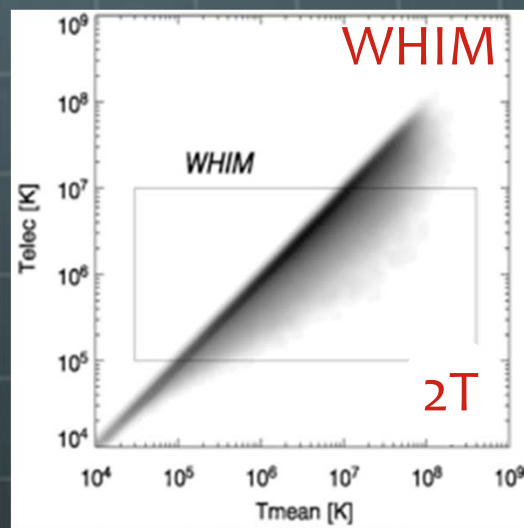
2.2 Non-Equilibrium Plasma

59/53

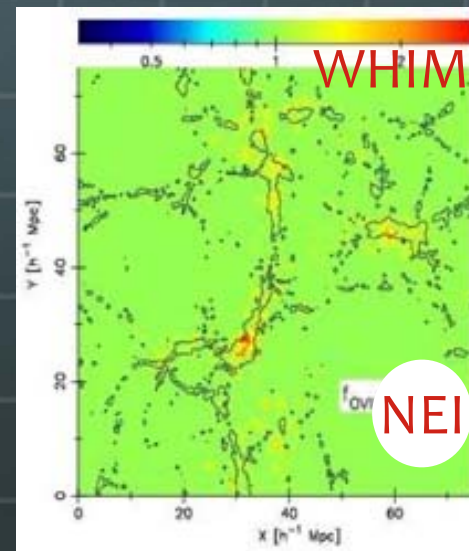
- **NEI and 2T** → the relaxation timescales are longer than the dynamical timescale of the merger
- Timescale of collisional ionization equilibrium (Masai 84)
 - $t_{\text{CIE}} \sim 3 \text{ Gyr} (n_e/10^{-4} \text{ cm}^{-3})^{-1}$
- Timescale of e-i temperature equilibration (Spitzer 56)
 - $t_{e-i} \sim 2 \text{ Gyr} (n_e/10^{-4} \text{ cm}^{-3})^{-1} (T_e/10^8 \text{ K})^{3/2}$



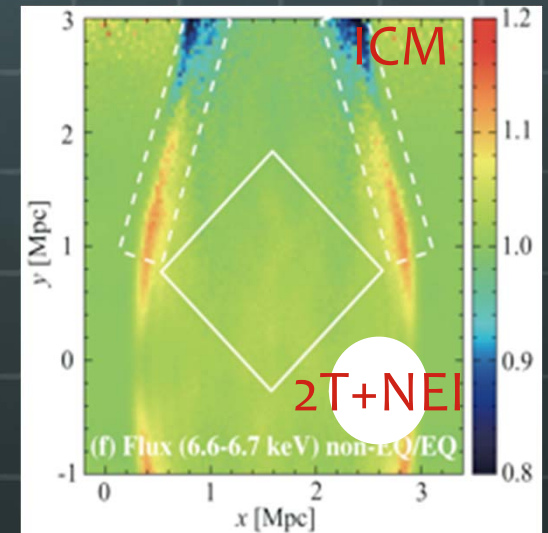
Takizawa 98, 99, 00



Yoshida+ 05



Yoshikawa, Sasaki 06



TA, Yoshikawa 08;10;12

2.2 Thermal Relaxation

60/53

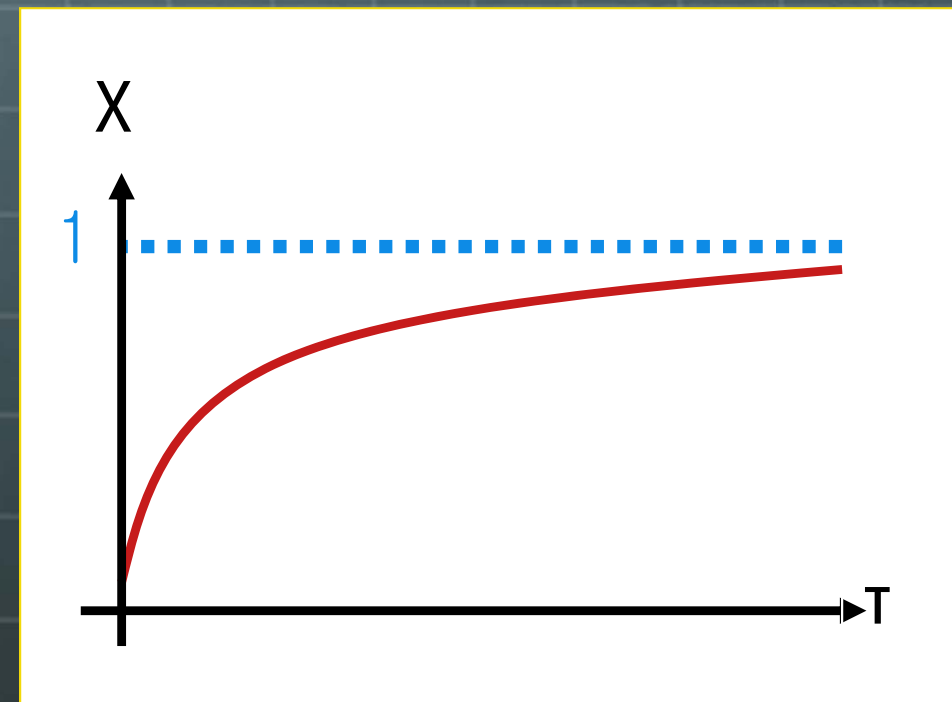
- 🌐 Energy exchange between a field (T_f) and a test particle (T) follows

$$\frac{dT}{dt} = \frac{T_f - T}{t_{\text{eq}}}$$

$$\tau = t/t_{\text{eq}}, \chi = T/T_f$$

$$\frac{d\chi}{d\tau} = 1 - \chi$$

$$\chi = 1 - Ce^{-\tau}$$



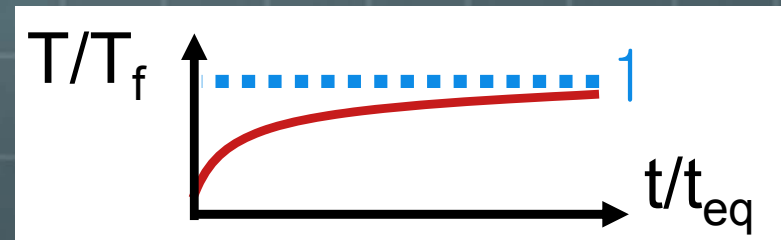
2.2 Thermal Relaxation

61/53

Spitzer thermal relaxation

- Energy exchange between field particles (T_f) and test particles (T) follows

$$\frac{dT}{dt} = \frac{T_f - T}{t_{eq}}$$



- Particle distribution becomes 1T Maxwell-Boltzmann **at most** within the following relaxation time

If there are no any other relaxation processes

$$t_{eq} = \frac{3m^{-1/2}m_f}{8(2\pi)^{1/2}Z^2Z_f^2e^4 \ln \Lambda} \frac{(kT)^{3/2}}{n_f} \left(1 + \frac{m}{m_f} \frac{T_f}{T}\right)^{3/2}$$

$$t_{eq,ep} \sim (m_p/m_e)^{1/2} t_{eq,pp} \sim (m_p/m_e) t_{eq,ee}$$

Spitzer, L., Jr. "Physics of Fully Ionized Gases", 1962, New York: Wiley

Korea Numerical Astrophysics Meeting (KNAG) @ CNU

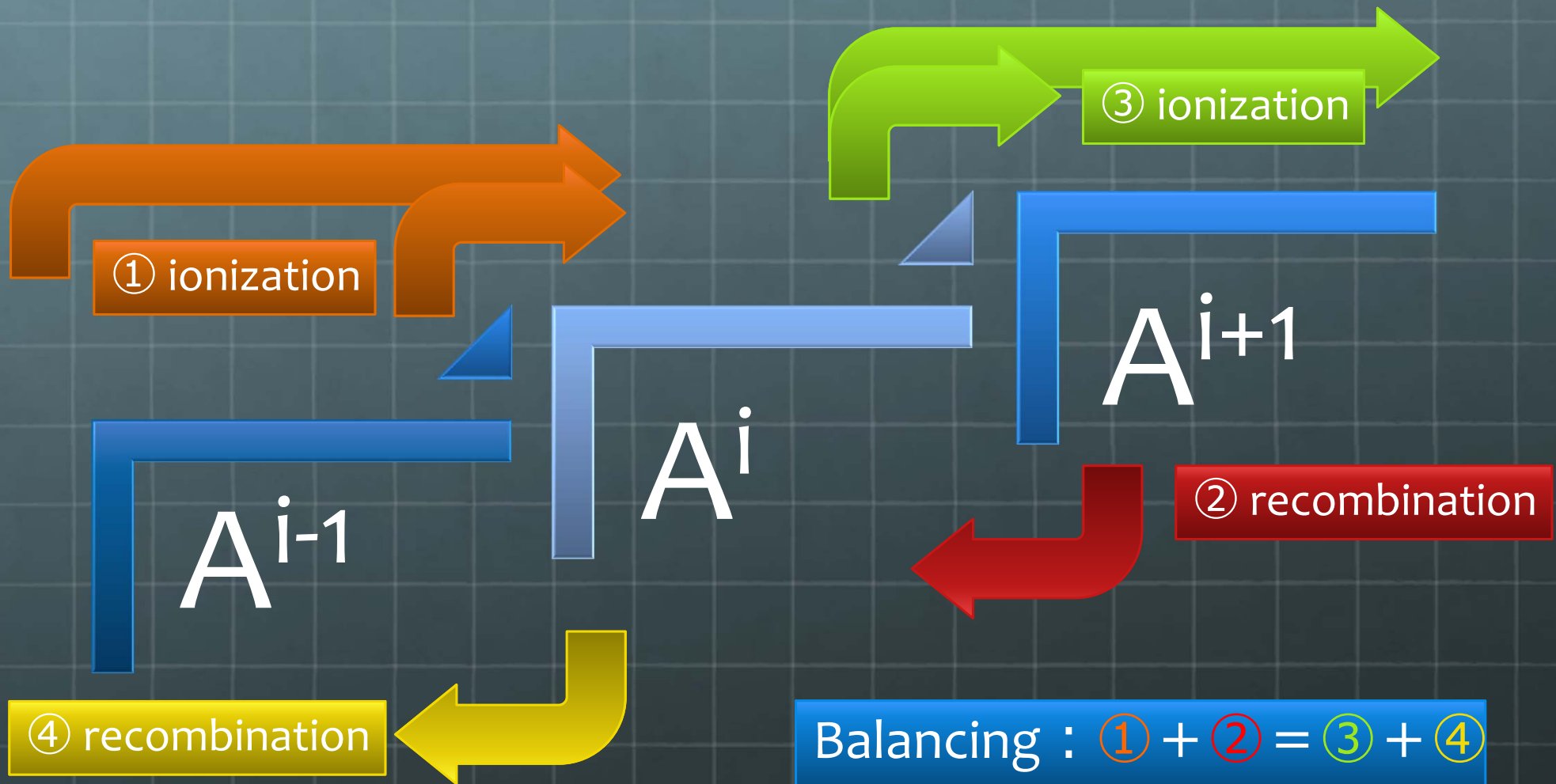
~43

~1830

2.2 Ionization/Recombination Processes

62/53

🌐 For i times ionized ion A

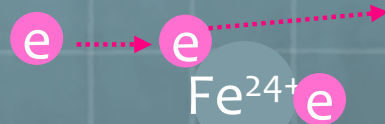


2.2 Ionization/Recombination Processes 63/53



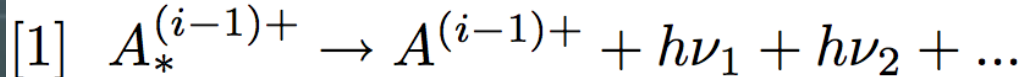
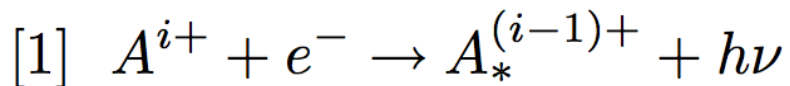
Ionization

- (1) Direct Collisional Ionization
- (2) Excitation-Autoionization
- (3) Auger Effect ionization
- (4) Charge-Exchange ionization
- (5) Photo-Ionizations

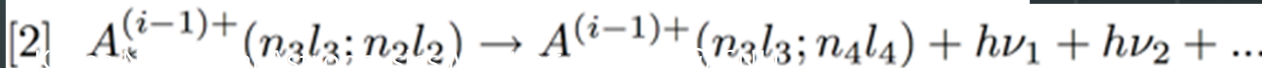
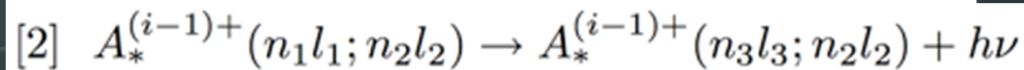
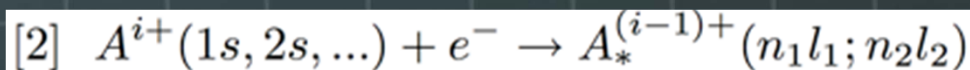


Recombination

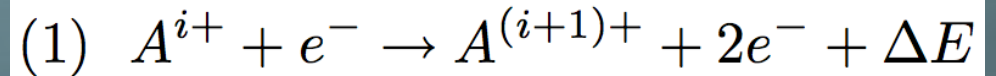
- [1] Radiative recombination
- [2] Dielectric recombination
- [3] C-E recombination



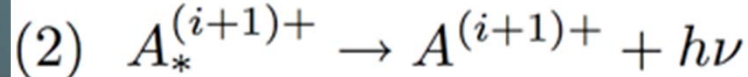
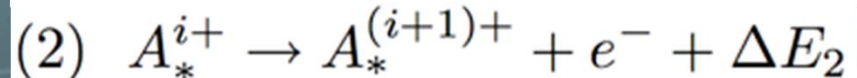
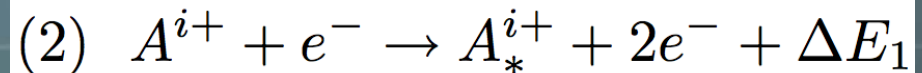
イオンの回りで高い軌道角運動量を持って電子がとっ捕まる。前半は再結合連続線、後半は $\Delta l = \pm 1$ の選択則に従い再結合特定線



束縛電子のひとつを autoionization state にする再結合

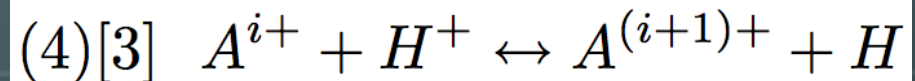


最外殻電子をぶっ叩き Binding energy だけエネルギーを失う

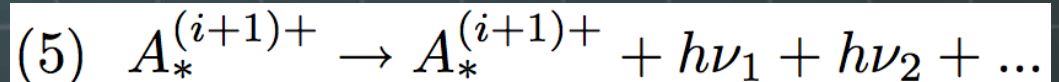
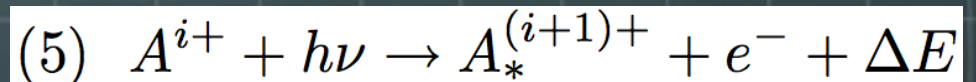


外殻電子がわずかで内殻電子の多い重元素で起こりやすい。

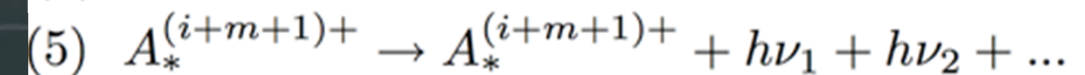
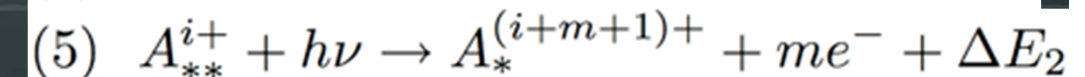
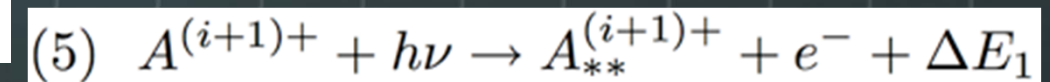
(3) 空乏内殻に対するカスケードの際に、放射が外殻電子にあたって飛び出す



水素がイオンにあたって電子を奪う/与える。ヘリウムの寄与もある。



外殻電子の光電離の場合。光子のエネルギーによっては励起状態を起こす



内殻電子の光電離の場合。Auger ionization がより probable

2.2 Non-Equilibrium Ionization (NEI)

64/53

Collisional Ionization Equilibrium (CIE)

- Balancing between ionization and recombination

$$0 = \frac{dn_{A,i}}{dt} = -n_e n_{A,i} R_{\text{coll}}^{A,i} - n_e n_{A,i} \alpha_{\text{rec}}^{A,i} + \dots$$

$$\tau_{\text{CIE}} \sim n_e^{-1} (R_{\text{coll}}^{A,i} + \alpha_{\text{rec}}^{A,i})^{-1}$$

- Generally, **time evolution of the ionization fraction $f_{A,i}$** for i times ionized ion A is

$$\frac{df_{A,i}}{dt} = \sum_{k=1}^{i-1} S_{i-k,k} f_{A,k} - \sum_{k=i+1}^{z+1} S_{k-i,i} f_{A,i} - \alpha_i f_{A,i} + \alpha_{i+1} f_{A,i+1}$$

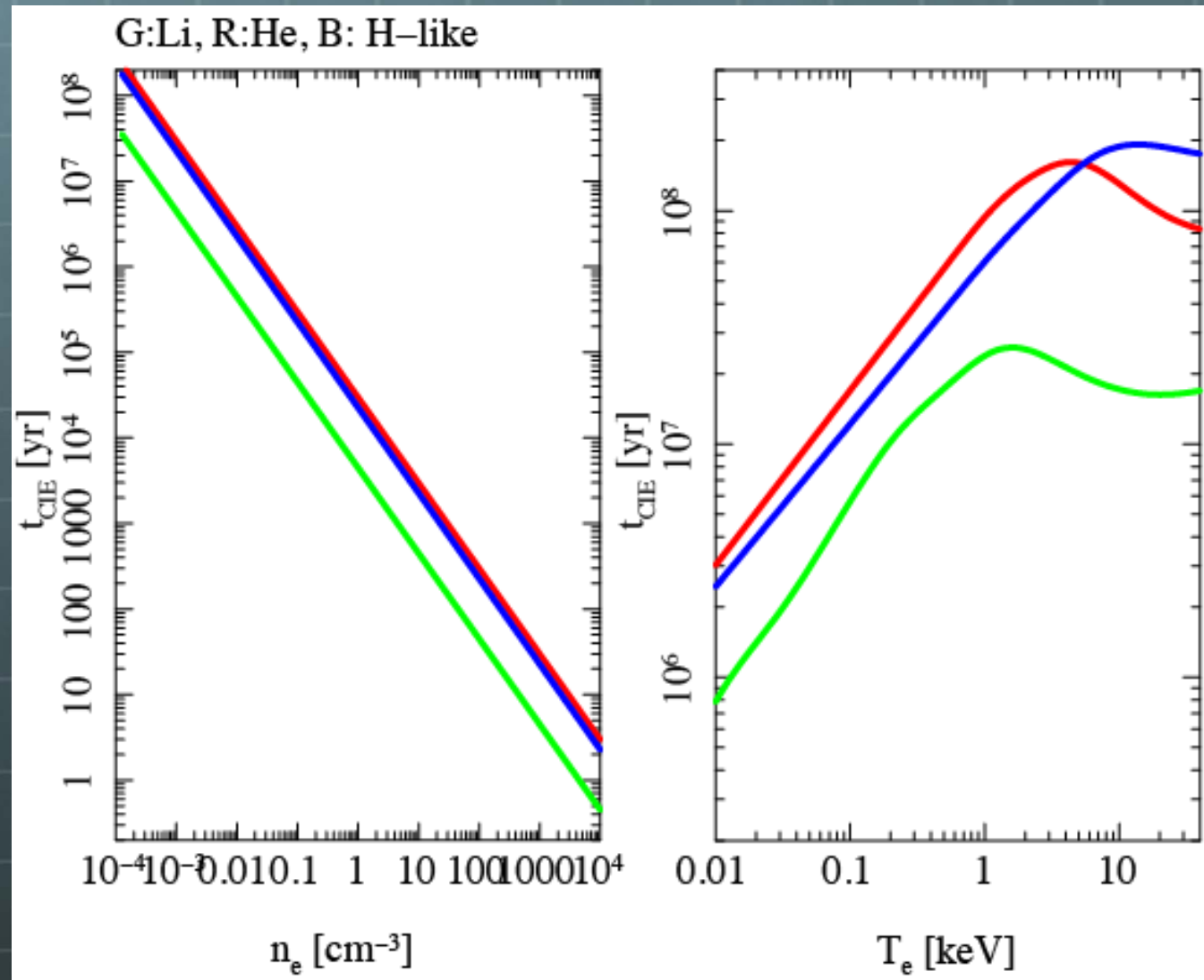
$$\tau_{\text{CIE}} \sim \left(\sum S_{,i} + \alpha_i \right)^{-1}$$

Ref: Dopita, M. A., & Sutherland, R. S. "Astrophysics of the Diffuse Universe", 2003, Springer

2.2 Ionization Equilibrium Timescale

65/53

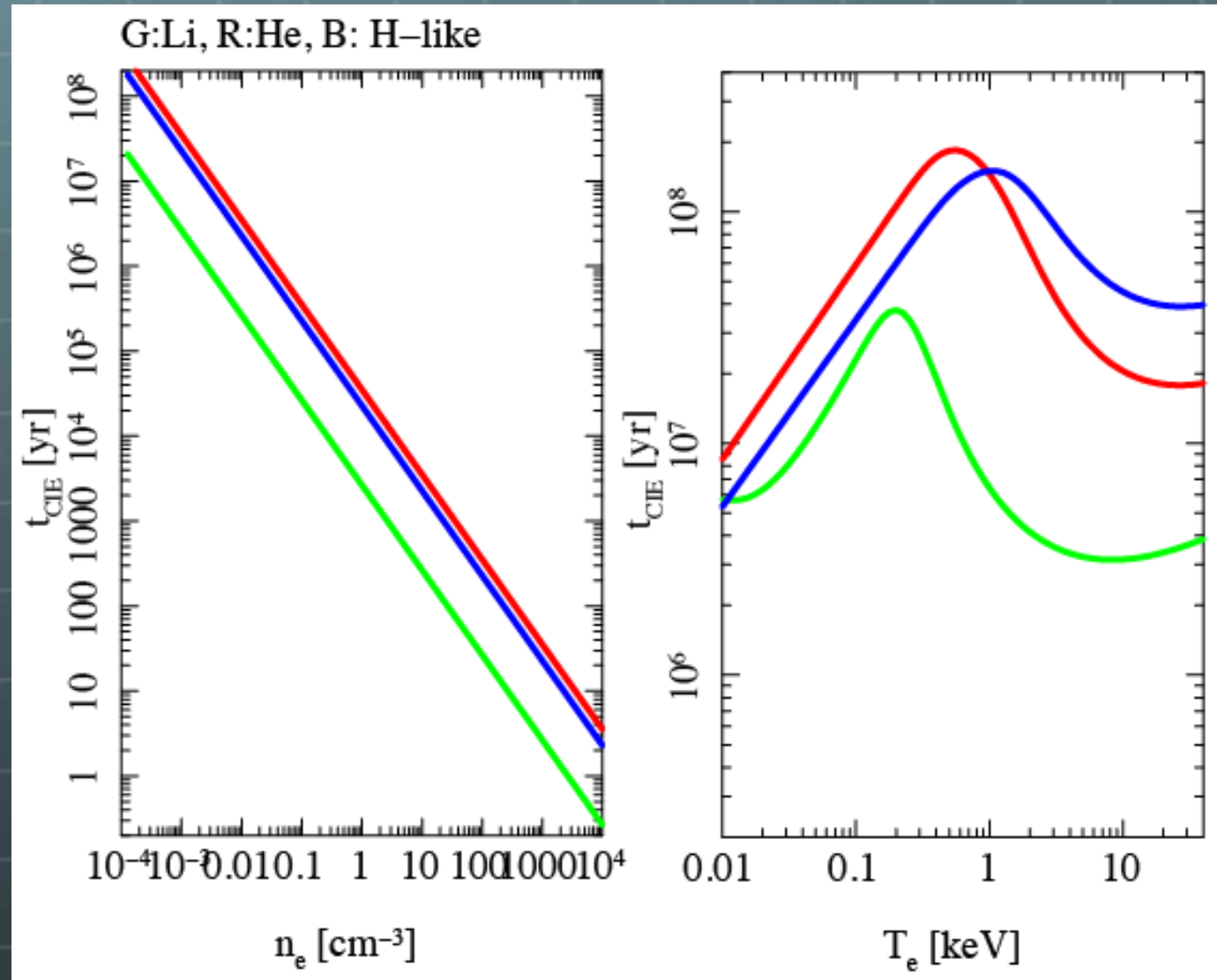
🌐 For Fe, $T_e=3$ keV or $n_e=10^{-4}$ cm $^{-3}$



2.2 Ionization Equilibrium Timescale

66/53

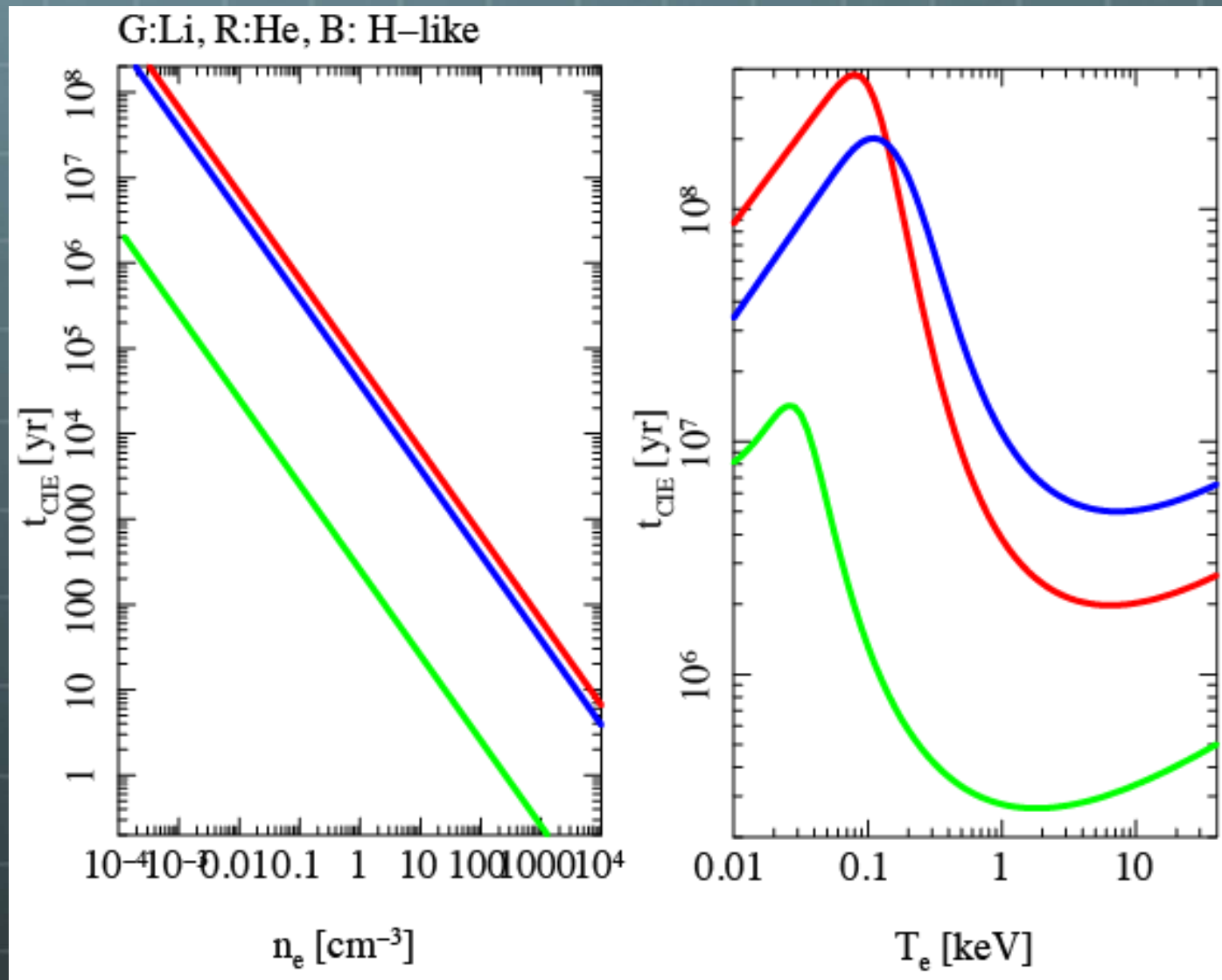
🌐 For S , $T_e = 0.5$ keV or $n_e = 10^{-4}$ cm $^{-3}$



2.2 Ionization Equilibrium Timescale

67/53

🌐 For O, $T_e = 0.1$ keV or $n_e = 10^{-4} \text{ cm}^{-3}$



2.2 The Simulations

68/53

SPH/N-body Calculations

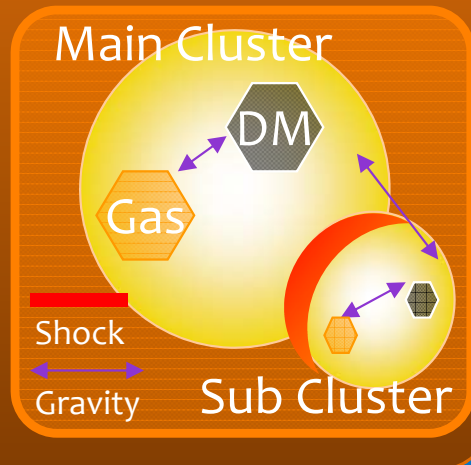
Based on Springel Hernquist 02

Original code optimized for cluster simulations (TA, Masai 05; 06; TA, Yoshikawa 08; 10; 12). MPI/OpenMP hybrid parallel, Burns-Hut Tree (monopole, $\theta=0.4$), artificial viscosity (Monaghan, Gingold 83, Balsara 95) with $\beta=2\alpha$, $\alpha=1$

Initial condition

ICM: β -model (Cavaliere & Fusco-Femiano 76) + hydrostatic temperature profile, or Isothermal + hydrostatic density profile, DM: NFW (Navarro+ 97) profile + Jeans equation

Two clusters contact at virial radius for each other with initial velocity V (free parameter, or Sarazin 02)



Mach Number Calculation

Based on Pflommer+ 06

$$1 + \frac{f_h h}{M_1 c_1 A_1} \frac{dA_1}{dt} = \frac{2\gamma M_1^2 - (\gamma - 1)}{\gamma + 1} \left[\frac{(\gamma - 1)M_1^2 + 2}{(\gamma + 1)M_1^2} \right]^\gamma$$

M: Mach number, c: sound velocity, A: entropic function ($P=A\rho^\gamma$), h: smoothing length of SPH, $f_{h=1}$

NEI/Spectra Calculations

Based on Yoshikawa, Sasaki 06

$$\frac{df_j}{dt} = \sum_{k=1}^{j-1} S_{j-k,k} f_k - \sum_{i=j+1}^{Z+1} S_{i-j,j} f_j - \alpha_j f_j + \alpha_{j+1} f_{j+1}$$

f_j : ionization fraction of ion j (j-1 times ionized ion), $S_{i,j}$: Ionization rate that ion j ejects i electrons, α_j : Recombination rate for ion j

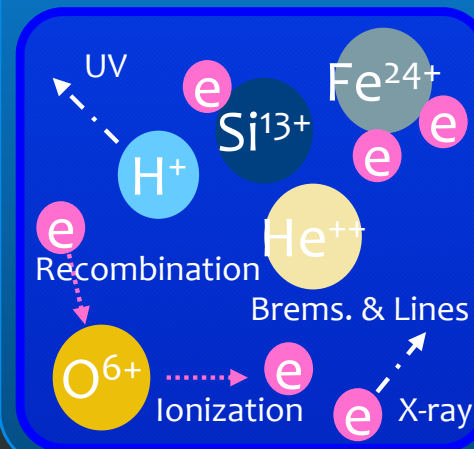
2T Calculation

Based on Takizawa 99

$$\frac{d\tilde{T}_e}{dt} = \frac{\tilde{T}_i - \tilde{T}_e}{t_{ei}} - \frac{\tilde{T}_e}{u} Q_{sh}$$

$$t_{ei} = \frac{3m_e m_i}{8(2\pi)^{1/2} n_i Z_i^2 e^4 \ln \Lambda} \left(\frac{kT_e}{m_e} + \frac{kT_i}{m_i} \right)^{3/2}$$

T_i, T_e : the ion and electron temperatures, \sim : normalized by the gas mean temperature T, u: the internal energy of the gas, Q_{sh} : the shock heating rate, $\mu=0.6$, $\ln \Lambda$: Coulomb logarithm, m_i, m_e : the ion and electron mass



Backward difference formula (sequentially updated in the order of increasing ionization states)
Atomic data/spectra: SPEX ver. 1.10 (<http://www.sron.nl/divisions/hea/speex>)
UV+X background radiation: CUBA code (Haardt, Madau 01)
H, He, C, N, O, Ne, Mg, Si, S, Fe (112 ionization states) for all SPH particles are calculated

2.2 Simulation Details

69/53

Electron-Ion Two Temperature structure

Fox, Loab 97; Takizawa 98

Coulomb two-body relaxation (with T_e and T_i)

$$\rho \frac{du_e}{dt} = -P_e \nabla \cdot v + Q_{\text{rad}} + Q_{\text{ex}}$$

$$\rho \frac{du_i}{dt} = -P_i \nabla \cdot v + Q_{\text{vs}} - Q_{\text{ex}}$$

$$Q_{\text{ex}} = \frac{n_e k}{\gamma - 1} \frac{T_i - T_e}{t_{ei}}$$

$$Q_{\text{sh}} = -\frac{\Pi}{2} \nabla \cdot v$$

$$t_{ei} = 7.97 \times 10^9 \text{ yr} \frac{(T_e/10^8 \text{ K})^{3/2}}{(n_i/10^{-3} \text{ cm}^{-3})} \cdot \frac{1}{\ln \Lambda}$$

We assume that the mean molecular weight μ is constant (H and He are normally fully-ionized).

$$\mu \equiv \frac{m_p n_p + m_{\text{He}} n_{\text{He}} + \dots}{m_p (n_e + n_p + n_{\text{He}} + \dots)}$$

$$\begin{aligned} n_i &= \left(\frac{\rho X}{m_p} + \frac{\rho Y}{m_{\text{He}}} \right) \\ &= \frac{\rho}{m_p} (X + Y/4) \\ &= \mu (X + Y/4) n \\ &\equiv \mu' n \end{aligned}$$

$$n_e = (1 - \mu') n$$

$$nT = n_e T_e + n_i T_i$$

$$T = (n_e T_e + n_i T_i) / (n_e + n_i)$$

$$X_e = T_e / T, \quad X_i = T_i / T$$

$$X_i = \frac{1 - (1 - \mu') X_e}{\mu'}$$

$$\frac{du}{dt} = -\frac{P}{\rho} \nabla \cdot v + \frac{1}{\rho} (Q_{\text{rad}} + Q_{\text{vs}})$$

$$\frac{dX_e}{dt} = \frac{X_e - X_i}{t_{ei}} - \frac{X_e}{\rho u} (Q_{\text{rad}} + Q_{\text{vs}}) + \frac{Q_{\text{rad}}}{(1 - \mu') \rho u}$$

2.2 Simulation Details

Non-Equilibrium Ionization

Yoshikawa, Sasaki 06

SPEX package ver. 1.10

Ionization: collisional, Auger, charge-exchange, photo-ionization

Recombination: radiative, dielectric, charge-transfer

H, He, C, N, O, Ne, Mg, Si, S, Fe

CUBA code

Haardt, Madau 01

UV, X-ray background

Backward difference formula

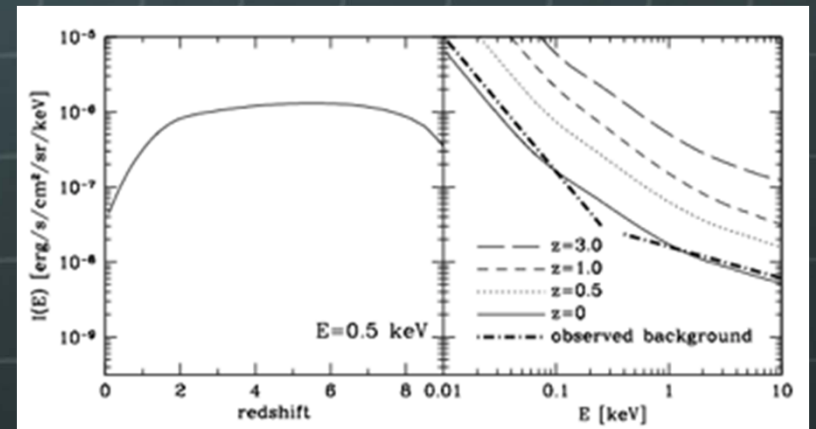
Implicit. Ex. Anninos+ 97

Sequentially updated in the order of increasing ionization states

$$\frac{df_j}{dt} = \sum_{k=1}^{j-1} S_{j-k,k} f_k - \sum_{i=j+1}^{Z+1} S_{i-j,j} f_j - \alpha_j f_j + \alpha_{j+1} f_{j+1}$$

f_j : ionization fraction of j -times ionized ion, Z : atomic number, $S_{i,j}$: Ionization rate that ion j ejects i e, α_j : Recombination rate for ion j

Intensity



redshift

E(keV)


2.2 Simulation Details

71/53

Mach number estimator

Pflommer 06

Entropy increase law

-  Entropic function $A(s)$, 1 and 2 the upstream and downstream

$$\frac{A_2}{A_1} = \frac{A_1 + \Delta A_1}{A_1} = 1 + \frac{f_h h}{M_1 c_1 A_1} \frac{dA_1}{dt}$$

$$P = A(s)\rho^\gamma$$

$$\Delta t = f_h h / v_1$$

$$\Delta A_1 \simeq \Delta t dA_1 / dt$$

$$M_1 = v_1 / c_1$$

$$c_1 = \sqrt{\gamma P_1 / \rho_1}$$

Rankine-Hugoniot law

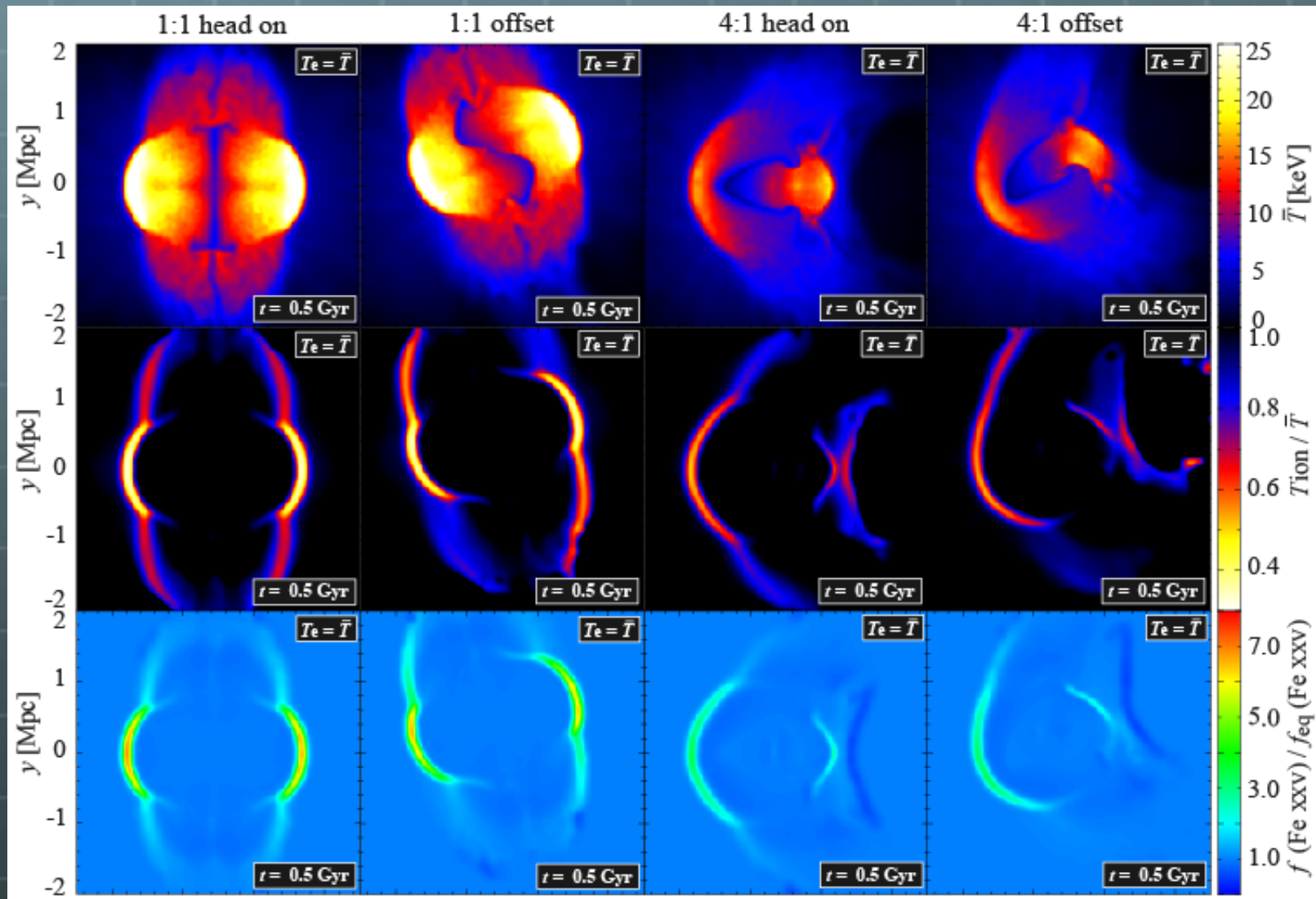
$$\frac{\rho_2}{\rho_1} = \frac{(\gamma + 1)M_1^2}{(\gamma - 1)M_1^2 + 2} \quad \frac{P_2}{P_1} = \frac{2\gamma M_1^2 - (\gamma - 1)}{\gamma + 1} \quad \frac{T_2}{T_1} = \frac{[2\gamma M_1^2 - (\gamma - 1)][(\gamma - 1)M_1^2 + 2]}{(\gamma + 1)^2 M_1^2}$$

$$\frac{A_2}{A_1} = \frac{P_2}{P_1} \left(\frac{\rho_1}{\rho_2} \right)^\gamma = \frac{2\gamma M_1^2 - (\gamma - 1)}{\gamma + 1} \left[\frac{(\gamma - 1)M_1^2 + 2}{(\gamma + 1)M_1^2} \right]^\gamma$$

2.2 Merging Galaxy Clusters

72/53

🌐 Behind the shock layers \rightarrow NEI/2T



2.2 Line Spectrum Width

73/53

Line width δ due to the Doppler shift

Emission of rest-frame wavelength λ_0 ($\omega_0 = 2\pi c/\lambda_0$) at the atom A with forward velocity v

ω at the observer is

$$\omega = \omega_0(1 + v/c)$$

Probability that A with the mass M and temperature T has a velocity within $v - v+dv$ is

Thus, Doppler broadening is

$$\sqrt{\frac{M}{2\pi kT}} \exp\left(-\frac{Mv^2}{2kT}\right) dv$$

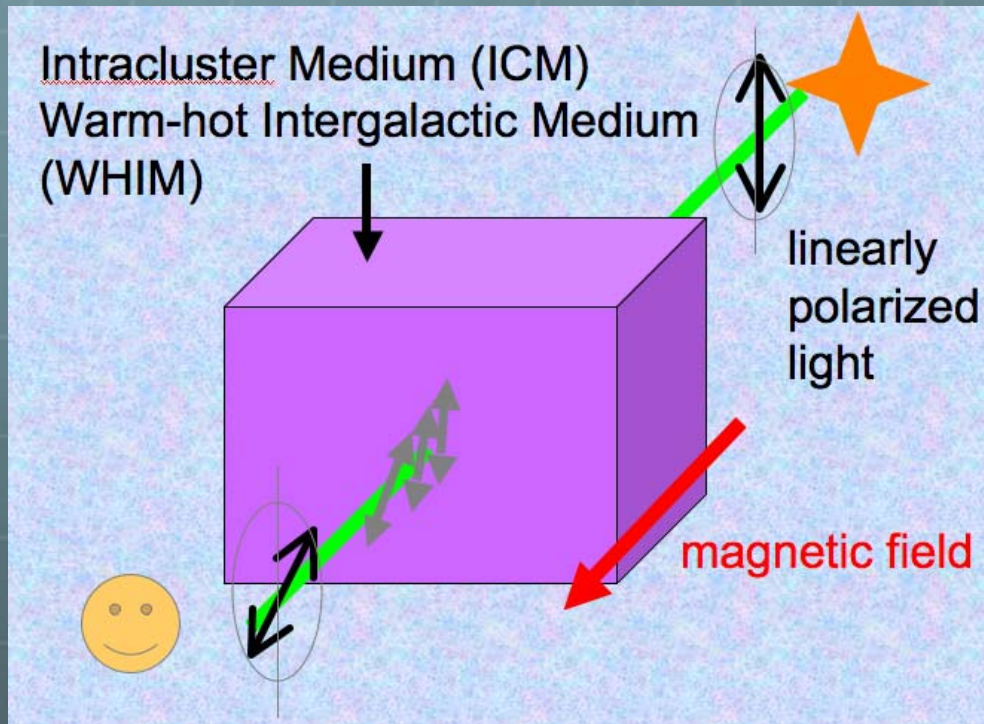
Half width δ is

$$I_D(\omega) d\omega = \sqrt{\frac{Mc^2}{2\pi kT\omega_0^2}} \exp\left[-\frac{Mc^2}{2kT\omega_0^2}(\omega - \omega_0)^2\right] d\omega$$

$$\delta(\omega_0) = 2\omega_0 \sqrt{(2kT/Mc^2) \ln 2} \quad \frac{\delta(\lambda_0)}{\lambda_0} = 7.16 \times 10^{-7} \sqrt{\frac{T}{A}} = 0.967 \times 10^{-3} \sqrt{\left(\frac{T}{10^8 \text{ K}}\right) \left(\frac{56}{A}\right)}$$

3.2 Faraday Rotation Measure

74/53



One of a few methods to explore the intergalactic magnetic field (IGMF)

$$\Phi(\lambda) = \text{RM} \times \lambda^2 + \Phi_0(\lambda)$$

Φ : rotation angle [rad]

Φ_0 : intrinsic rotation angle [rad]

λ : wavelength [m]

Theory

$$\text{RM} = 811.9 \int_0^L n_e B_{\parallel} dl \text{ rad m}^{-2}$$

n_e : thermal electron density [cm^{-3}]

B_{\parallel} : line-of-sight IGMF strength [μG]

L : depth along the line-of-sight [kpc]



Observation



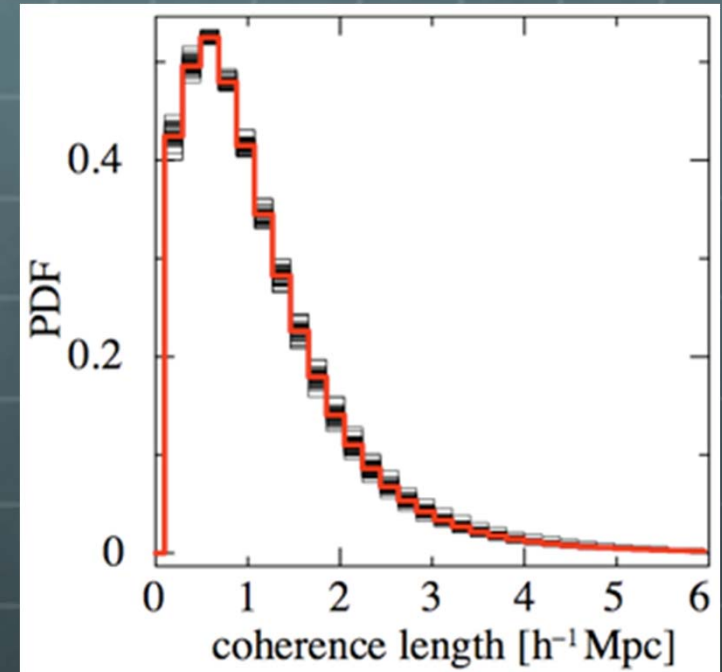
$$\text{RM} = \frac{\Phi(\lambda_1) - \Phi(\lambda_2)}{\lambda_1^2 - \lambda_2^2}$$

3.2 IGMF RM – Local Universe –

75/53

- RM depends on the strength as well as the coherence length of the IGMF
- Check 1: PDF of the length with the same sign of B_{\parallel} along LOSs for WHIM
 $\sim 600 h^{-1} \text{ kpc}$
- Check 2: From “the integral scale”
 $\sim 800 h^{-1} \text{ kpc}$
- Check 3: largest energy containing scale
 $\sim 900 h^{-1} \text{ kpc}$
- Cho & Ryu (09): $\sim a \text{ few } \times 100 h^{-1} \text{ kpc}$
- May be due to the resolution effect
- Although grid size = $200 h^{-1} \text{ kpc} <$ the above coherence length...
- RM is dominantly contributed by the density peak along LOS --> would be not too large to invalidate the results

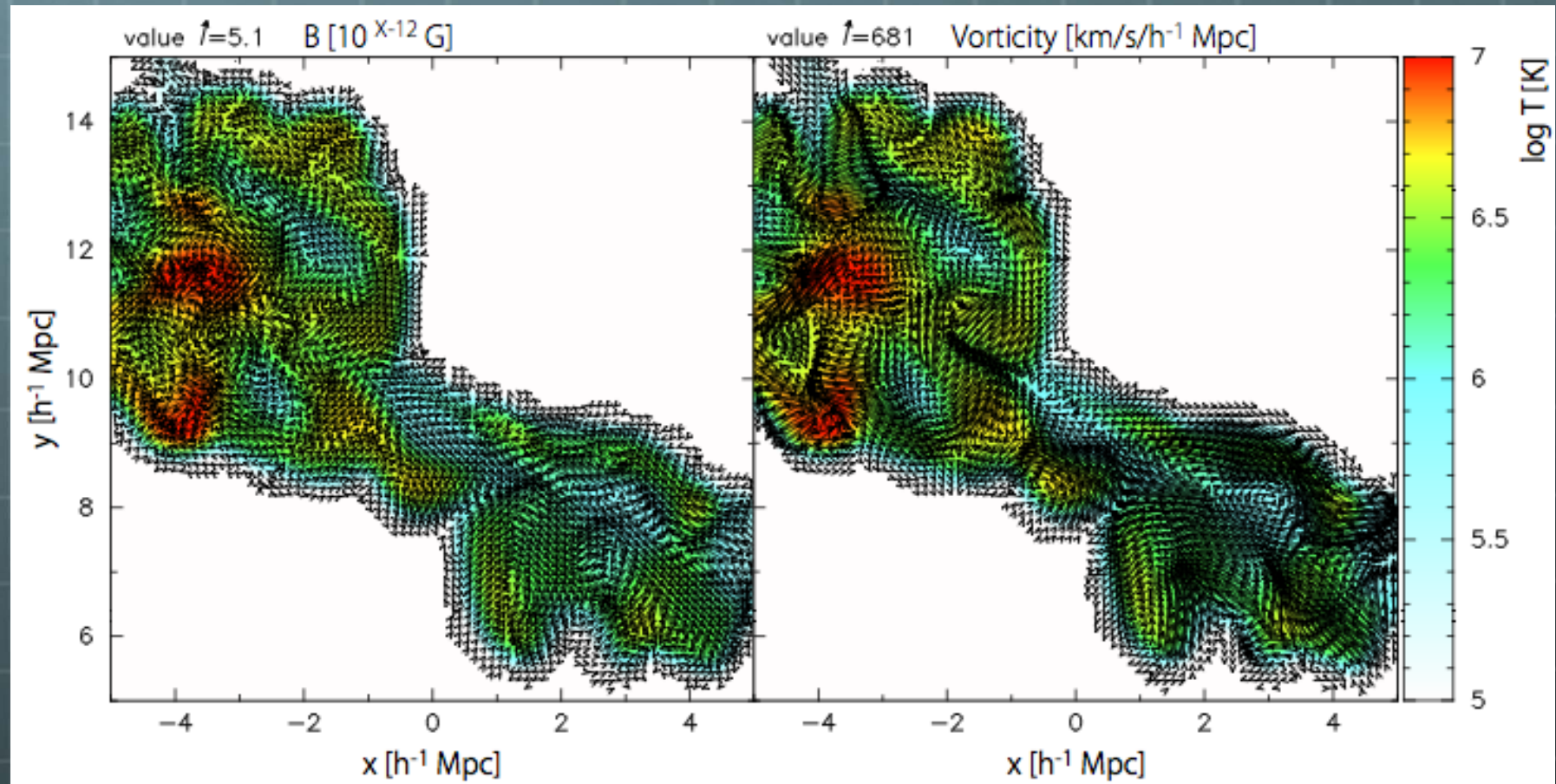
PDF of the coherence length



coherence length of B for

$$\frac{3}{4} \times 2\pi \frac{\int P_B^{3D}(k)/k dk}{\int P_B^{3D}(k) dk}$$

🌐 Passive field and vorticity

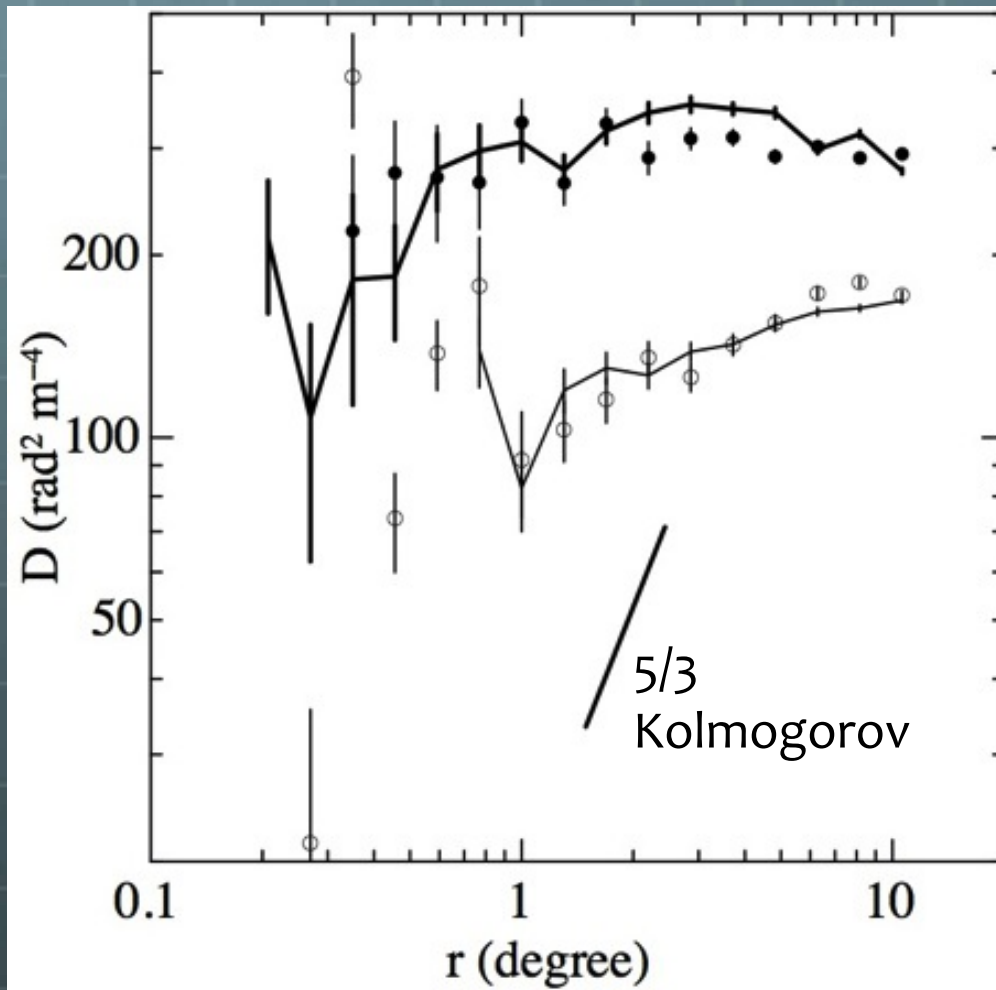


Distributions of IGMF (left) and the vorticity (right) in the 2D slice. The length of arrows for IGMF corresponds to x of 10^{X-12} G. The color shows the gas temperature. The direction of magnetic field correlates with the direction of vorticity in a passive field model.

3.2 Structure Function (SF) of RM

77/53

SFs of RM toward the Galactic Poles (Stil+ 11)



← South Galactic Pole (SGP)
circles: Mao+ (10) WSRT+ACTA
lines: Taylor+ (09) NVSS

← North Galactic Pole (NGP)
circles: Mao+ (10) WSRT+ACTA
lines: Taylor+ (09) NVSS

- ✓ Very flat profile
- ✓ 100-400 [$\text{rad}^2 \text{m}^{-4}$]
- ✓ $SF_{SGP} > 1.5-2 SF_{NGP}$

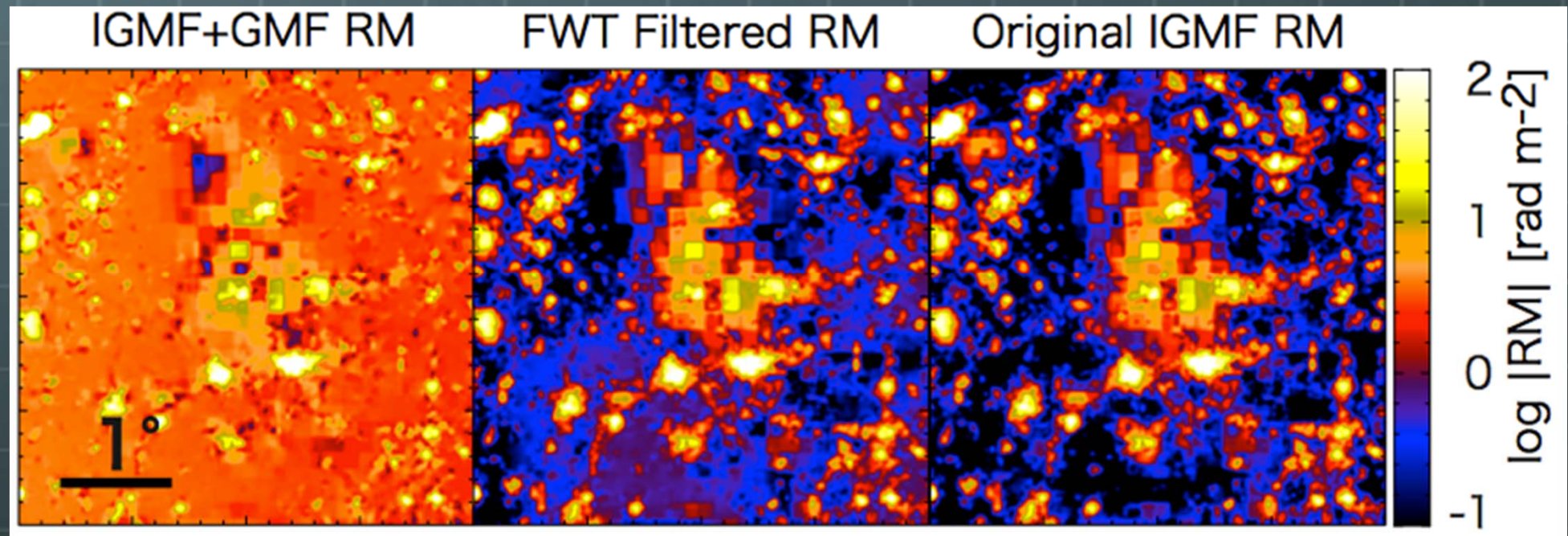
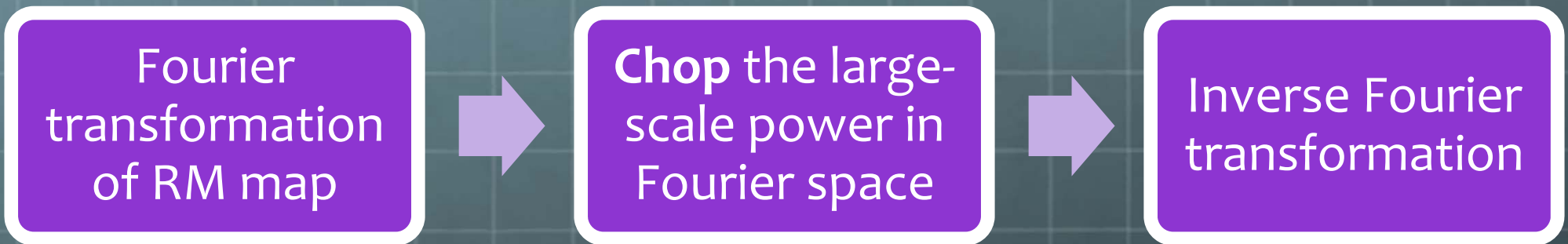
Motivation

How much is the contribution from the IGMF?

Toward ASKAP and SKA

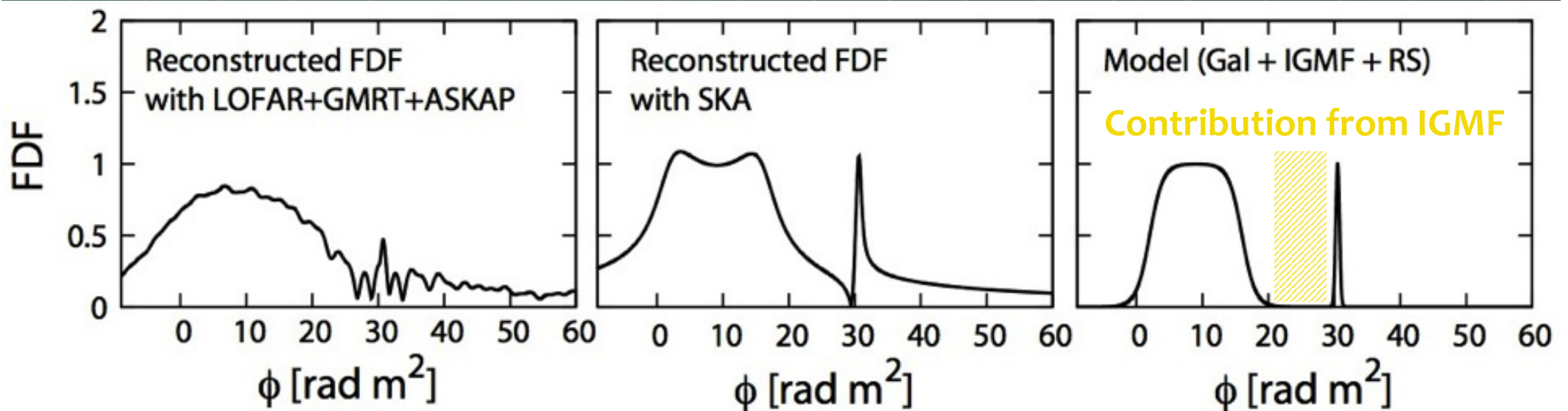
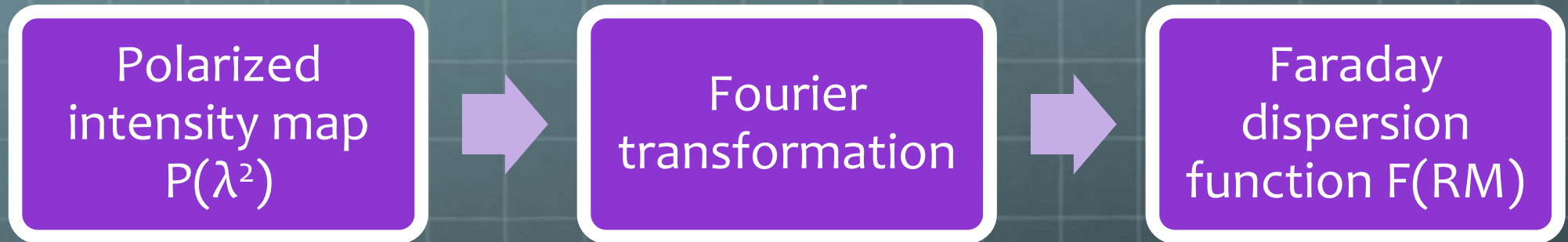
78/53

- Development of Image Processing
 - High-pass filter technique



Development of Image Processing

Faraday RM tomography (e.g., Brentjens, de Bruyn 2005)



Kumazaki, Akahori, Takahashi, Ryu in prep.